NASA CONTRACTOR REPORT

NASA CR-1536

NASA CR-15

AN INVESTIGATION OF THE EFFECTS OF SURROUNDING STRUCTURE ON SONIC FATIGUE

by Thomas F. Nelson

Prepared by
LOCKHEED-GEORGIA COMPANY
Marietta, Ga.
for Langley Research Center

NATIONAL AERONAUTICS AND SPACE ADMINISTRATION • WASHINGTON, D. C. • MAY 1970

~~AN~~ INVESTIGATION OF THE EFFECTS OF SURROUNDING STRUCTURE ON SONIC FATIGUE

By Thomas F. Nelson

Prepared under Contract No. NAS 1-8120 by
LOCKHEED-GEORGIA COMPANY
Marietta, Ga.

for Langley Research Center

NATIONAL AERONAUTICS AND SPACE ADMINISTRATION

For sale by the Clearinghouse for Federal Scientific and Technical Information
Springfield, Virginia 22151 – CFSTI price $3.00

AN INVESTIGATION OF THE EFFECTS OF SURROUNDING STRUCTURE ON SONIC FATIGUE

By Thomas F. Nelson

Lockheed-Georgia Company

SUMMARY

Four different sizes of a basic grid-like skin-stringer structure were tested in sonic fatigue in order to evaluate the effect of specimen complexity on sonic fatigue test data. Specimen size was increased systematically by progressive addition of panel bays, beginning with a single skin bay and adding up to forty-eight similar skin bays around the centrally located reference panel. Random rms strain was the control quanity in conducting the tests and the primary results consisted of twenty-one data points from tests of the four configurations which are plotted in the form of S-N curves. Data points from all four configurations correlate well with a single computed S-N curve for a $K_T = 4$ within a 20% stress deviation band.

Strain and acceleration data are included on specimen frequency and amplitude response to both discrete frequency and random acoustical loading.

INTRODUCTION

One of the basic objectives of structural sonic fatigue testing is to be able to correlate more closely the laboratory test results with actual in-service performance of aircraft.

Usually for reasons of economy, the laboratory tests are run on small portions of the aircraft structure. There is seldom any scaling down or modeling effect, but often the complexity of the actual aircraft structure is drastically reduced.

From a standpoint of obtaining basic sonic fatigue data that could be used by the designer for specific applications, some of the test variables which could affect these data are:

- *surrounding structure*
- temperature
- manner of SPL loading (discrete or random)
- K_T of edge attachments or clamps

Good simulation of all of these variables is desired so that the laboratory tests would accurately predict the time, or cycles, to failure and the mode of failure.

One of the most difficult decisions to make in conducting sonic fatigue design data tests is how extensive should the structural simulation be around the test specimens. In other words, can a single bay of complex structure be taken as the test specimen and bolted to a rigid support frame, or are multiple bays on each side of the test bay required to more realistically simulate the aircraft installation.

This investigation has produced experimental data which assist in answering this question. The general procedure was to obtain fatigue life data from four specimen configurations which differed only in the extent of structure surrounding a central test section.

The structural configurations were typical, flat skin-stringer designs. Extended testing was conducted on four configurations to provide data at two or more strain levels for each configuration. These data are summarized in an S-N plot of strain measured in the failure area; the edge attachment of a skin bay.

The generally high degree of correlation demonstrated by these tests was due in part to uniformity of failure modes where skin cracks occurred around the edge attachments at mid span of the long edge of a skin bay. Symmetry about a central skin bay was maintained in these tests and a verification of these results for assymetrical panel construction should not be assumed on the basis of these tests.

Program monitor for this investigation was Mr. Carl E. Rucker, NASA-Langley. Laboratory testing was done by Mr. J. O. Rasor, assisted by Mr. Ken Smith. Mr. J. R. Carroll was responsible for the analytical design considerations of Appendix A. The latter are Lockheed-Georgia personnel.

SYMBOLS

A	distance from fastener to "heel" of stringer, inches
a	long side of plate, inches
b	short side of plate, inches
B	scan filter effective band width, Hz
c	distance from neutral axis, inches
d	fastener diameter, inches
db	decibels, with a reference of 0.0002 dynes/cm^2
dx	finite area strip of Rayleigh probability density plot
E	Young's modulus of elasticity, psi
e	statistical error
f, f_o	frequency, Hz

$\sqrt{f_o \varphi_o}$ — sound pressure, psi

g — gravitational unit, 386 in/sec^2

H — panel dimension coefficient

Hz — frequency, cycles per second

h — plate thickness, inches

h_f — flange thickness, inches

K — radius of gyration, inches

K_t — stress concentration factor, $\frac{\text{stress at concentration}}{\text{nominal stress}}$

L,l — beam or stringer length, inches

M — bending moment, inch-pounds

N — number of stress cycles to failure (subscripts added in Appendix B)

N_d — number of degrees of freedom

psi — pounds per square inch

p (x) — Rayleigh probability density for ratio of peak-to-rms stress

PSD — power spectral density, (measured quantity) ^{2}/Hz

R — panel dimension coefficient

RC — resistance and capacitance time constant

rms — root mean square

S-N — stress vs cycles to failure

SPL — sound pressure level, db

S — stress, psi

s — fastener spacing, inches

T — data sample length, seconds

w — load density, lb/in

w_o — maximum panel deflection

w (x, y) — mode shape

σ — rms stress, psi, or standard deviation

μ — microinches, inches x 10^{-6}

δ — damping ratio, $\frac{\text{actual damping}}{\text{critical damping}}$

φ_o — sound pressure spectral density, (psi) ^{2}/Hz

TEST SPECIMENS

Basic Design Considerations

To accomplish the purpose of this test program, two extremes in specimen size and complexity were selected. The largest size was a specimen with an area of about 6 ft by 10 ft containing forty-nine bays of the basic test section. The simplest specimen possible, of the same type structure, consisted of one bay of skin riveted to a simple, rigid support fixture. Various other specimen configurations between these two extremes were selected for evaluation.

A typical aircraft skin-stringer type structure was selected. The connecting bays of structure were structurally the same and the same stringer and ring cross section was used in all specimens. The intent was to keep all specimen parameters constant except the extent of specimen structure surrounding, or supporting, a central test section.

Four different configurations of test specimens were selected, each differing only in the extent of similar structure surrounding the central test section. The basic test section was considered to be a flat rectangular skin panel supported by stringers along the two longitudinal edges and heavier rings along the transverse edges. Countersunk rivets attached the skin to the stringers and rings. The particular dimensions, materials and construction details were intended to be typical of aircraft skin-stringer structure subject to sonic fatigue. Each of the four specimen configurations differed in the number of similar skin bays. A particular specimen is identified according to the number of skin bays.

The basic skin panel consisted of a rectangular sheet of 7075-T6 clad aluminum, 0.050 inches thick and measuring 8 inches by 18 inches between attaching rivet lines. The rivets were 5/32 inch diameter, countersunk into the outside surface of the skin. The stringer and ring members were the same for all configurations, except for length which depended on the size of each configuration. Fabrication of the intersection of the stringers and rings at the four corners of each skin panel, or bay, was the same for all supported skin panels in each configuration.

These specimens were designed using the considerations explained in Appendix A. This Appendix contains a typical method for analyzing structure for sonic fatigue. A detail description of each specimen configuration follows.

Single Bay Configuration - Considering that the aircraft structure under consideration is a continuous pattern of skin panels supported by a grid of support structure, the most elementary specimen would be a single bay skin panel attached by the same type of attachments to a rigid test fixture. This configuration retained the aircraft skin panel dimensions and edge attachment stress concentrations, but did not incorporate the edge rigidity of the aircraft support structure. For this purpose, a panel of skin was riveted to a 0.75 inch thick steel plate with a cutout for the skin panel. The same type of rivets were used as for the other configurations. A sketch of the specimen and support fixture is shown in Figure 1.

Nine Bay Configuration - Nine skin bays in a three-by-three arrangement are included, supported by a grid of stringers and rings. This resulted in one basic test section, or one skin bay, isolated from any effects of fixture support by one other skin bay in all directions. This configuration is shown in Figure 2. As for all configurations, the test bay was 8 x 18 inches between attachment lines. The surrounding bays were smaller in order that the response frequency of the surrounding bays be different from that of the center bay. Failure was desired in the center bay, not in the outer edges of the specimen. In addition, the attachments through the skin in the outer bays were not countersunk, to decrease the chance of a skin crack outside the test section. Substructure details are shown in Figure 3.

Twenty-five Bay Configuration - This design contained twenty-five skin bays with the central bay separated from the support fixture by two bays in all directions. The outer bays which tied into the support fixture were smaller than the others, and did not contain countersunk rivets. See Figure 4 for a sketch of this configuration.

Forty-nine Bay Configuration - This was the largest specimen tested measuring about five feet by ten feet and containing forty-nine skin bays. This design had three other bays separating the center bay from the support fixture. A doubler sheet was installed over the outside skin bays to reinforce the skin at the support fixture tie-in. A sketch of this configuration is included as Figure 5.

TEST ARRANGEMENT

Facility and Equipment

A progressive wave type test chamber was used for these tests. The chamber dimensions at the test section were six feet in height, ten feet in length and fourteen inches in width. The flat specimen formed one side of the chamber with plywood panels used to fill in the area around the specimens. The opposite side of the chamber was formed by steel doors. Sound was introduced at one end of the chamber through two rows of six exponential horns from twelve electro-pneumatic noise transducers. At the other end of the wave chamber was a single horn which expanded into a muffler tunnel. A photograph of this test chamber is included as Figure 6. Heavy, movable beams spanning the specimen side of the chamber horizontally and vertically were used to support the smaller specimen support fixtures. Specimens were positioned such that the center was located between about two to five feet downstream from the upstream edge of the test section. A single layer of cloth tape was used to separate all specimens from the surface of the fixtures. This was done to avoid a failure due to friction or corrosion between the aluminum specimen and steel support. A forty-nine bay specimen is shown installed in the test chamber in Figure 7.

The usable frequency range of the wave chamber facility for fatigue testing is from 60 Hz to 1000 Hz. Maximum SPL capacity is 164 db in the range of 100 Hz to 500 Hz. Total acoustical power available is 48,000 watts.

Description of Test Setups

Single Bay Configuration - The support fixture and specimen for this configuration are almost integral and the mounting of the simple sheet specimen has been previously described. The steel plate fixture had two cutouts so that two specimens could be tested at the same time. A sketch of this fixture is shown in Figure 1. The support fixture was bolted at top and bottom to the side of the wave chamber.

Microphones were suspended by bungee cord in front of each specimen and located midway between the specimen and the opposing chamber wall. Between one and four specimens were tested together during this program, therefore, the pattern of microphone locations was changeable. These locations are shown in Figure 8. The microphones were the condenser type with a usable SPL range of from 85 db to 185 db and a frequency range of 10 Hz to 4000 Hz. Overall SPL readout accuracy within ±1.5 db. The microphones were non-directional and were positioned vertically in the wave chamber. Figure 9 is a photograph of the microphones in place for a test of a twenty-five bay specimen.

Strain gage locations were coordinated for all configurations. Since strain was the criteria for setting the sound pressure level (SPL) for each test, gage locations had to be comparable between specimens, if results were to be comparable. The first specimen carried eight gages and the following twelve specimens, at least four each. The particular gages for each specimen are called out in the plots and tables in the test results section of this report. Figures 10 and 11 show the gage locations applicable to any specimen. For this configuration, gage locations 2, 2A and 6 were above the edge of the cutout in the steel plate and locations 3 and 4 were in the center of the bay. The strain gages were the Constantan wire grid type which were bonded with Epoxy adhesive to the specimen.

Nine Bay Configuration - Each specimen panel was fastened to a steel "picture frame" fixture by a double row of screws through the skin and angle clips at the ends of each stringer and ring. All screws were the protruding head type in order to reduce the chance of failure around the outside edge of the specimen. A sketch of the specimen mounted in the support fixture is included as Figure 12.

The support fixture was bolted to the support beams in the side of the wave chamber with the long side of the specimen horizontal.

Microphone locations are shown in Figure 8, and strain gage locations in Figure 10. The gage locations selected for each specimen are listed in the results section of this report. Accelerometer locations are shown in Figure 13. The accelerometers were the piezo-electric type, weighing 2.8 grams and with a usable frequency range of 2 to 5000 Hz.

Twenty-five Bay Configuration - The installation of this specimen in the test chamber was similar to that of the nine bay specimen. A sketch of the support fixture is shown in Figure 14.

Microphone locations were the same as for the nine bay configuration; one microphone in front of each three central skin bays. At least eight of the standard strain gage locations were selected for each specimen, including the primary gage locations of Figure 11. Accelerometers were mounted in the first four standard locations of Figure 13 for a low level random survey.

Forty-nine Bay Configuration - This configuration was considered too large to be supported by a one piece picture frame fixture. Four separate steel members were bolted to the four sides of the test chamber and the specimen then attached to the support members. Figures 8 and 15 show the test setup.

Four microphones were positioned as shown in Figure 8. The first specimen carried eighteen gage locations and the remaining two specimens, eight gage locations.

Six accelerometers were mounted on the specimens to record response to random loading. The locations are shown in Figure 13.

INITIAL SURVEYS

Outline of Surveys

Before starting the life test (fatigue test to failure) of a specimen, a number of frequency response surveys were conducted. Since the life test was conducted by concentrating the available acoustical power around the desired specimen response frequency, it was necessary to determine these resonant frequencies and define the corresponding modes of deflection.

The order of these surveys was as follows:

- sinusoidal frequency response
- mode shape survey
- accelerometer survey - random excitation

Sinusoidal frequency survey - This survey was conducted by slowly sweeping the frequency of the SPL from about 70 Hz to 500 Hz. The SPL is held fairly constant during this sweep in order to determine the relative magnitude of each specimen resonance. The frequency of the SPL increased at the rate of twice per octave. The output of all of the microphones were rectified to a direct current signal, averaged together, and used as the feedback in the closed-loop SPL control circuit. The two plots of SPL vs frequency in Figure 16 are typical of the acoustical loading during this type of survey.

The SPL was selected to be high enough to fully excite each specimen, but not to apply significant damage.

Strain and SPL were recorded on magnetic tape. The frequency of the SPL function generator was also recorded for later use as the driving signal of the frequency axis of an X-Y plotter. An initial voltage calibration signal was recorded before each sweep for calibration of the plot ordinate.

Mode Shape Survey - The deflection patterns of each specimen, at significant resonant frequencies, were visually observed. The specimens were installed in the test chamber and discrete frequency acoustical loading was used to excite the specimens. A strobe light, synchronized by the SPL function generator, was used in the darkened room to observe the deflection modes.

Since observers with ear protectors were in the room near the wave chamber, the SPL was usually kept down to about 130 db.

Accelerometer survey under random loading - This survey produced specimen deflection data under random excitation which could not be observed visually. Accelerometers were glued to the skin surface with a brittle, quick drying, cement for easy removal after the survey.

With the results of the frequency response and mode shape surveys, the spectrum shape of the random acoustical loading for the life test could be determined. The specimen was then excited under life test conditions except that the SPL was reduced to keep the accelerometers on the specimen.

This survey lasted only long enough to record the output from the accelerometers on magnetic tape.

Since this data was random in amplitude, presentation is in the form of power spectral density (PSD) plots. The narrow band spectrum level reduction process is further explained in the Life Test Results section of this report.

TEST RESULTS

Initial Surveys

Single Bay Configuration - Typical plots of frequency response to sinusoidal excitation are included in Figure 17. Two gages on the first of thirteen specimens of this configuration were selected for presentation. The first bending mode produced significantly higher strains in the transverse gages.

The first five bending modes occurred at 167, 220, 285, 383 and 506 Hz. All had mode lines parallel to rings running across the transverse direction of the skin panel. The definition of these panel modes was much clearer than for the multi-bay specimens.

Accelerometers were not used on this configuration since there were no supporting stringers or adjacent skin bays. The deflection survey under random excitation was intended primarily for multi-bay specimens.

Nine Bay Configuration - Frequency response at four selected gages locations are presented for this configuration. These plots are Figures 18 and 19. This one also exhibited only one significant strain response. The mode shape for this response is shown in Figure 20 and labeled as the life test mode. Torsion of the stringers was very noticeable, however, the heavier rings had very little motion at any resonance.

Accelerometer PSD plots are included as Figure 21. These plots indicate very little motion at the stringer-ring intersection as compared with that at one-third the stringer span along the center skin bay.

Twenty-five Bay Configuration - Six strain gage plots of specimen frequency response are presented as Figure 22 and 23. This configuration exhibited the first evidence of a number of predominate strain responses. The peak strains of the gages measuring transverse strain were almost the same in amplitude. Stringer bending strains were significant in this configuration (gage location 16), with peak strains of 170 μ in/in at 170 Hz.

The predominate mode shapes detectable with a strobe light are shown in Figure 24. The life test mode with the center bays in phase produced the highest strain at the edges of the skin bays. The second bending mode of the center bay was within 20 Hz of that for the preceeding configurations.

Figures 25 and 26 are PSD plots of accelerometer outputs under random excitation. The deflections at the stringer-ring intersections of the center skin bay were greater than for the preceeding nine bay configuration. Probability density analysis of acceleration signals indicate good approximation of Gaussian random characteristics.

Forty-nine Bay Configuration - Strain response to a discrete frequency sweep is shown in Figures 27 through 29. Multiple peaks of strain response are more evident than for previous configurations. A larger number of bays result in more combinations of intra-bay resonances.

The mode shapes determined by strobe light, sketched in Figure 30, indicate a number of overall panel deflection modes at low frequencies. The frequencies which induced individual skin panel deflection were selected for the life test to be consistant with the life test conditions of previous configurations. The higher modes which involved individual bays were very difficult to define on a panel of this size. Phasing of deflection changed with only a slight change of frequency (above 100 Hz) indicating numerous combinations of skin bay motion, or phasing.

Accelerometer data are shown in Figures 31 through 33. Plots of probability density indicated good randomness (Gaussian).

Life Test Results

Following the initial strain and deflection mode surveys, each specimen was fatigue tested to failure. (Several single bay specimens were removed without failure after a reasonable length of time). Life testing was done using random acoustical loading. A relatively flat spectrum level, about 100 Hz wide, was centered about the major response frequency of each specimen. This allowed a concentration of available acoustical power to obtain a high strain level in the specimen.

The specimens were inspected for failure using dye penetrant to detect cracks. The inspection schedule was once every half hour, up to three hours, then once every hour.

Data recorded were output voltages from microphones and strain gages. This data was recorded on magnetic tape and read using true rms meters. The tape recording was made at the start of the life test. Meter readings were made throughout the duration of the test. Primary signal amplifiers were direct current, differential type with a frequency range of 0 to 75 KHz. The magnetic tape recorder was operated at a tape speed resulting in a cut-off frequency of 5000 Hz.

Random Data Reduction - Reduction of the taped data consisted of narrow-band, spectrum level PSD plots of strain and SPL and Gaussian probability plots of selected strain and SPL signals.

The PSD plots were made using a constant band width analog type analyzer with a linear scan filter sweep rate. A sample of data was recorded on a tape loop, which is the data sample mentioned below. The purpose of the plots is primarily to define the shape of the response spectrum. The cycles to failure for each specimen was computed using the frequency of specimen strain response obtained from the strain PSD plots. The square root of the area under the PSD plots should approximate the rms meter readings.

The following data reduction constants were employed:

data sample = 5 seconds

analyzer time constant (RC) = 5 seconds

scan filter effective bandwidth = 6 Hz

scan rate = 0.25 Hz/sec

Using the standard expression of $N_d = 2BT$ for statistical degrees of freedom, where:

N_d = number of degrees of freedom

B = effective bandwidth of scan filter

T = data sample length

$N_d = 2(6)(5) = 60$

The statistical error, e, of the PSD plot reading from the true value (with infinite analyzing time) is expressed by:

$$e^2 = \frac{2}{N_d} = \frac{1}{BT} \quad \text{(reference 1, chapter 6)}$$

$$e = \frac{1}{\sqrt{(6)(5)}} = 18.3\%$$

The above expression means that the PSD plots are accurate within ±18.3%, with a confidence level of 67%. The fact that RC averaging is used will increase the above value of e to some degree (about 4%), however the continuous plot resulting from RC averaging is usually more readable than a series of points resulting from true averaging.

The probability density plots were made with a scan time of 32 minutes, from -4σ to $+4\sigma$, where σ = rms value of the overall random signal. The analyzer time constant was 3.6 seconds. Each plot was calibrated using the known density shape of a sinusoidal signal.

Single Bay Configuration - Nine specimens were tested to failure and four were removed without failure. Acoustical loading was adjusted until the desired strain level was read on the most sensitive strain gage near the edge of the panel. Since the maximum strains would be expected along the edge of the long side and since this is the area where failure would be expected, a gage was used in this area for the control strain.

A typical spectrum plot of the acoustical loading applied during any life test (except for spectrum level) of this program is shown in Figure 34.

Four strain PSD plots are included to show the typical random strain response of this configuration. These plots are Figures 35 and 36.

The randomness of this strain signal is indicated by probability density plots. Strain gage no. 2 signal indicated positive Kurtosis (peakedness) with a peak at about 0.6 and gage no. 3, a flattened peak at about 0.36. The bell-shaped curve for a pure random Gaussian signal has a peak at 0.4 on the density scale (reference 1, chapter 4).

The overall random strain levels for the life test of each specimen are listed in Table I. The maximum edge strain read on each specimen was considered the test strain level in plotting the results on an S-N plot (stress vs number of cycles). Results for the S-N data points are shown in Table II. The relationship of stress to strain is assumed to be:

Stress = E x Strain;

where E = Young's modulus, or 10^7 psi for aluminum

and Strain = inches per inch x 10^{-6}

TABLE I

SINGLE BAY CONFIGURATION - LIFE TEST STRAIN LEVELS

Specimen Number	SPL *	Strain at Gage Location Number μ in/in rms								
		1	2	2A	3	4	5	6	7	8
1	138 db	332	483		382	123	418	345	259	248
2	132	255	350		284	80		260		
3	132	272	361		297	95		297		
4	131	392	231		314	83		392		
5	131	342	416		371	95				
6	134		179		246	66		353		
7	133		315		282			360		
8	127	214	261	206	247			189		
9	127		307	366	282			316		
10	126	161	247	360	276			313		
11	126		176	272	182			190		
12	134	200	232	423	287			350		
13	133		349	462	334			423		

* Spectrum level

TABLE II

SINGLE BAY CONFIGURATION - S-N DATA

Specimen	Strain μ in/in rms	Time To Failure-Hr.	Cycles To First Crack
1	483	1	0.65×10^6
2	350	5	3.60
3	361	7	4.67
4	392	1.5	1.27
5	416	6	4.32
6	353	1	0.79
7	360	3	2.27
8	261	14	9.07
9	366	19	No Failure
10	360	18	No Failure
11	272	18	No Failure
12	423	12	No Failure
13	462	12	9.07

Therefore, stress is computed as ten times the measured strain for plotting purposes.

Number of cycles to failure, N, as shown on an S-N plot was computed as follows:

$$N = (\text{test time to failure}) \times (\text{life test strain response frequency})$$

A typical failure was a crack near the mid-span of one of the longitudinal edges and near, or through, an attachment hole. All of the unfailed specimens were tested two at a time while all failed specimens were tested either one, two or four at a time.

Nine Bay Configuration - Three specimens were tested to failure using the strain reading from gage location 2 to adjust the acoustical loading. A table of the life test strain readings follows with the eight gages on each specimen listed.

TABLE III

NINE BAY CONFIGURATION - LIFE TEST STRAIN LEVELS

Specimen Number	SPL*	Strain at Gage Location Number μ in/in rms									
		1	2	3	4	5	6	11	12	16	17
1	142 db	382	431	328		359		309	304	336	480
2	139	361	369	340	103	309	209			286	347
3	139	308	360	315	96	298	153			259	333

* Spectrum level

TABLE IV

NINE BAY CONFIGURATION, S-N DATA

Specimen Number	Strain μ in/in, rms	Time to Failure-hr	Cycles To First Crack
1	431	1	0.78×10^6
2	369	2	1.44
3	360	1	0.76

Power spectral density plots of strain signals from specimen no. 2 are shown in Figures 37 and 38. As the rms overall strains listed in Table III indicate, the spectrum level of gages 1, 2 and 3 are similar in magnitude. This was the first configuration to have stringers spanning more than one skin bay. The bending strains in the stringers were noticeable, compared to skin strains. However, failure occurred in the skin at the rivet attachment stress concentration.

Initial failures in all three specimens consisted of skin cracks in the same area as for the single bay configuration; through, or near, attachment holes in the mid-span area of the long edge of the skin bay. Skin cracks after extensive testing are shown in the photograph of Figure 39.

Twenty-five Bay Configuration - Two specimens of this configuration were tested with the same procedure as for previous configurations. Life test strain readings are listed in Table V and test results, in Table VI.

TABLE V

TWENTY-FIVE BAY CONFIGURATION - LIFE TEST STRAIN LEVELS

Specimen Number	SPL*	Strain at Gage Location Number μ in/in rms											
		1	2	2A	3	5	6	10	11	13	16	17	21
1	133 db		431		307	332	246	290	328	226	345		
2	132	314	329	360	248		258				296	275	268

* Spectrum level

TABLE VI

TWENTY-FIVE BAY CONFIGURATION, S-N DATA

Specimen Number	Strain μ in/in, rms	Time to Failure-hrs	Cycles to First Crack
1	431	0.5	0.27×10^6
2	360	4	2.45

Figures 40 and 41 contain PSD plots of four strain gage outputs. These gage locations are the same as for some previous configurations. The strain response under the 100 Hz wide acoustical loading spectrum tended to be similar to that of a single degree-of-freedom specimen. The probability density plots of two strain gage signals indicated a resonable degree of randomness.

Initial failures (skin cracks) occurred near the skin attachments within the central four skin bays of these two specimens.

Forty-Nine Bay Configuration - Life test strain data from three specimens of this configuration are listed in Table VII and the life test results in Table VIII.

TABLE VII

FORTY-NINE BAY CONFIGURATION - LIFE TEST STRAIN LEVELS

Specimen Number	SPL*	Strain at Gage Location Number μ in/in rms												
		1	2	2A	3	6	9	11	13	16	17	18	20	21
1	142db		426		227		204	257	212	720		320	317	
2	137	245	360	329	247	177				329	400			462
3	135	298	356	370	233	179				378		369		391

* Spectrum level

TABLE VIII

FORTY-NINE BAY CONFIGURATION, S-N DATA

Specimen Number	Strain μ in/in, rms	Time to Failure-hrs	Cycles to First Crack
1	426	2	1.00×10^6
2	360	5	2.52
3	370	4	2.16

Plots of PSD strain of six strain gage locations are included as Figures 42 through 44. This was the first configuration to exhibit a strong multiple peak strain response under life test loading. The large number of skin bays surrounding the center bay produce a large number of resonant peaks within a small frequency bandwidth. The S-N data in Table VIII are computed from an average frequency of the strain response peaks. Stringer bending strain was significant compared to skin strain. The probability density plots of Figure 45 indicate reasonable randomness in the strain response even though the acoustical loading plot is distorted from the Gaussian shape.

This configuration exhibited the only stringer failure. The first of three specimens incurred a failure in the outstanding flange of a stringer spanning the center bay. Cracks in the skin along the rivet lines were discovered at the same time. The other two specimens incurred skin cracks near, or through, the line of attachments at the edge of the central skin bays.

Summary of Test Results - Test results are presented as S-N data in Figure 46, along with a random $K_t = 4$ curve (see Appendix B). This curve, computed from existing fatigue data, is shown for reference in comparing the data from all four configurations. Scatter about this selected curve is reasonable, or generally within a 20% deviation band in stress level.

For a presentation of results in terms of SPL vs cycles to failure, Figure 47 has been included. The accompaning curve was developed using the prediction method of Appendix A. For these tests, spectrum level SPL is 20 db below octave band level.

CONCLUSIONS

The sample size considered in this experiment is quite small, but the uniform results point to the conclusion that there is virtually no advantage to testing a panel consisting of more than nine bays for sonic fatigue evaluation.

The S-N data from these tests lends support to the selection of a $K_t = 4$ for prediction of stress due to skin bending across countersunk rivet lines.

APPENDIX A

Basic Design Considerations

To evaluate the resistance of a structural configuration to sonic fatigue damage it is necessary to make basic assumptions as regards structural response, resulting stress levels, and fatigue damage. For this analysis, the following are postulated:

1. Stresses which contribute to sonic fatigue damage are significant only in the primary structural resonant modes.

2. Lightly damped structure will respond significantly in only one mode when exposed to random excitation and the structural response can therefore be expressed by Miles' theory, Reference 2, as

$$\sigma^2 = \frac{\pi f_o \varphi_o}{4\delta} (\sigma_o^2)$$

3. For single mode response the sound pressure correlation is unity; i.e., the pressure everywhere on the surface under the random pressure load is in phase.

4. Fatigue damage is accumulated at a linear rate.

5. The random pressure can be defined statistically as the probability of occurrence of instantaneous pressures with the probability distribution being Gaussian. The response to this pressure has a frequency equivalent to that of the significant mode and whose amplitude has a random variation with a Rayleigh peak probability distribution.

Structural Response - Applying the above to the various test configurations, estimates of response frequency, resulting stress, and cycles to failure are made.

For analysis it is assumed that the specimen skin bays have all boundaries fully fixed such that the fundamental response frequency is obtained from

$$f = (2.16 \times 10^5) \frac{h}{b^2} \left[1 + 2/3 \left(\frac{b}{a}\right)^2 + \left(\frac{b}{a}\right)^4 \right]^{\frac{1}{2}} \qquad \text{eq. (1)}$$

where

f = resonant frequency ~ Hz

h = plate thickness ~ in.

a = panel long side dimension ~ in.

b = panel short side dimension ~ in.

The assumed mode shape is given by,

$$w(x,y) = \frac{w_o}{4}\left(1 - \cos\frac{2\pi x}{b}\right)\left(1 - \cos\frac{2\pi y}{a}\right) \qquad \text{eq. (2)}$$

For the 8.0" x 18.0" x 0.050" panel bays considered here,

$$f = (2.16 \times 10^5)\,\frac{.050}{(8.0)^2}\left(1 + \frac{2}{3}\left(\frac{8}{18}\right)^2 + \left(\frac{8}{18}\right)^4\right)^{1/2}$$

$$f = 193 \text{ Hz}$$

For convenience, equation (1) is plotted in Figures 48 and 49, where the aspect ratio correction factor is to be multiplied times the frequency found in Figure 49 as appropriate.

There are several analytical expressions available for determining rms stresses in skin panels subjected to random acoustic pressures. Most are based on Miles' single degree of freedom system expressed as,

$$\sigma^2 = \frac{\pi f_o \varphi_o}{4\delta}\sigma_o^2 \qquad \text{eq. (3)}$$

where

σ = rms random stress ~ psi
δ = damping ratio
f_o = response frequency ~ Hz
φ_o = spectral density of the pressure at the response frequency $(psi)^2/Hz$
σ_o = ratio of static stress to unit pressure load at location of interest

Basically, the analytical methods available differ only in the definition of σ_o. For example, the expression for clamped edge stress at the center of the long side from Reference 3, page 221, is

$$\sigma_o = 25E\left(\frac{h}{b}\right)^2 = 9750 \qquad \text{eq. (4)}$$

Substituting into eq. (3) above

$$\sigma^2 = \frac{\pi f_o \varphi_o}{4\delta}(9750)^2$$

Where it is assumed for this example,

$$\delta = .015$$

$$\sqrt{f_o \varphi_o} = 1.22 \times \text{octave band SPL for 150 db} = .110 \text{ psi}$$

For the 8" x 18" x .050" panel,

$$\sigma = 7780 \text{ psi}$$

For the same panel, clamped on all edges, Reference 4 suggests,

$$\sigma = \left(\frac{\pi}{4\delta} f_o \varphi_o\right)^{1/2} \left(\frac{.8519\left(\frac{b}{h}\right)^2}{H}\right) \qquad \text{eq. (5)}$$

$$\text{where } H = 1.442 + 1.442\left(\frac{b}{a}\right)^4 + 0.8737\left(\frac{b}{a}\right)^2$$

Using eq. (5) and the same panel size, noise level, and damping ratio as previously.

$$\sigma = 10{,}480 \text{ psi}$$

For a configuration similar to the one bay specimens, it is assumed that all edges are rigidly clamped and the edge stress can be approximated by equations (4) or (5). As noted, however, there is considerable difference in stress magnitude and there appears to be no exact analytical technique for predicting rms stresses.

The support flexibility for actual aircraft structure is for the most part rather difficult to analyze and the dynamics engineer has design charts and nomographs available for usage. The actual aircraft structure will be something between the clamped and simply supported edge cases; maximum moment for clamped edges and zero moment for simple supports. The design nomograph shown in Figure 50 has been developed from measured data from full scale structure and is used to calculate the rms edge stress for all except the single bay configuration.

From Figure 50, for the 8" x 18" x 0.050" panel,

$$\sigma = 4500 \text{ psi}$$

again for octave band SPL = 150 db.

As noted in Figure 50, the rms stress is for a panel aspect ratio of 1.0. To account for varying aspect ratio, the Δdb correction is added to the octave band sound pressure levels before determining rms stress.

From the above and Equation (5), for example

$$(\text{actual})\sigma = 0.42\ (\text{calculated})\sigma$$

In all cases, measured stress data at the panel edges is in good agreement with the rms stress from Figure 50 and is considerably less than that calculated using Equations (4) or (5). Also Figure 47 shows good agreement between this test data and the design nomograph.

From Figure 51, ($K_t = 4$) the number of cycles to failure, using 4500 psi rms, is approximately 10^6 cycles which is in good agreement with test data.

Another area subject to sonic fatigue damage is the flange of the stringer adjacent to the skin panel. For this area,

$$\sigma_f \propto \frac{bA}{h_f}$$

where,

σ_f = rms flange stress ~ psi
b = panel short side dimension ~ in
A = distance from fastener to "heel" of the stringer ~ in
h_f = flange thickness ~ in

Also, it has been shown empirically that the rms stress in the stringer is

$$\sigma_f = \frac{C_1 bA\sqrt{f_o \varphi_o}}{h_f^2} \qquad \text{eq. (6)}$$

C_1 = 42.5 for single flange

For the nine, twenty-five and forty-nine bay panels,

$$\sigma_f = \frac{(42.5)(8)(.402)(.110)}{(.063)^2} = 3780 \text{ psi}$$

To determine cycles to failure, enter Figure 51 ($K_t = 2$) with the 3780 psi above.

To determine the stress in the stringers at each end and at the midspan; consider the stringer as a fixed-ended beam 18" long and an effective skin width twice the stringer flange width.

$$\sigma = \sqrt{\frac{\pi f_o \varphi_o}{4\delta}} \left(\frac{Mc}{I}\right)$$

where,

M = bending moment ~ lb-in
c = distance from neutral axis ~ in
I = moment of inertia ~ in^4
M = 1/12 wl^2 at ends
M = 1/24 wl^2 at center

For $\delta = 0.015$ and SPL = 150 dB

σ = 983 psi at ends
σ = 492 psi at center

From Reference (5) the stringer response frequency is

$$f = \frac{C_1 K}{L^2} = 1012 \text{ Hz}$$

where,

C_1 = constant = 71.95
K = radius of gyration ~ in
L = beam length ~ in

As can be seen, the stringer response frequency is very high as compared to the panel response frequency and the stress levels are low. From a fatigue damage standpoint, stresses developed with the stringer responding as a beam should be insignificant.

For the fastener spacing for skin to stringer attachment (Reference 6)

$$s \propto \frac{d^2 b}{h^2}$$

where,

s = fastener spacing ~ in
d = fastener diameter ~ in
b = stringer spacing ~ in
h = skin thickness ~ in

For these test specimens and the 5/32" rivet diameter,

$$s = 1.40''$$

APPENDIX B

Computation of Random S-N Curve

An S-N curve for random loading can be computed from a reference S-N curve for periodic, constant amplitude loading by using a probability curve which relates the occurrence of various levels of peak stresses for a given random rms stress level. The resulting random S-N curve is for the same K_t value, mean stress and material as the reference S-N curve.

An arbitrary random rms stress level is selected and a cycles to failure quantity, N_r, is computed. This coordinate is one point of the random S-N curve. The procedure is repeated for each point until the random S-N curve can be defined.

The equation below expresses the computation procedure.

$$N_r = \frac{1}{\int_0^\infty \frac{p(x)dx}{N_x}}$$

where

N_r = cycles to failure for random loading

N_x = cycles to failure for periodic, constant amplitude loading

$p(x)$ = Rayleigh probability density of a given peak-to-rms stress occurrence

dx = finite range of peak-to-rms stress values

In the above equation, the term $p(x)dx$ is the probable occurrence of a particular peak stress, so that the denominator of the above equation is in the form of Miner's expression of linear cumulative damage;

$$\sum \frac{n}{N}$$

The quantity N_x is obtained from the reference periodic, constant amplitude S-N curve for each peak stress probably applied. Each peak stress value is determined by the dx strip being integrated, and the probability of that peak value occurring is the product, $p(x)dx$.

Principal references for the above procedure are references 2 and 6. The following sketches illustrate the curves employed in the above procedure.

The reference periodic, constant amplitude S-N curve for Figure 46 was obtained from reference 7, page 32 (mean stress equal zero).

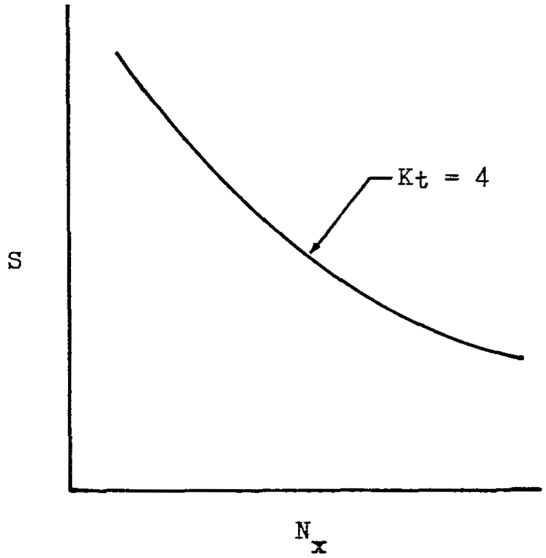

Reference S-N Curve

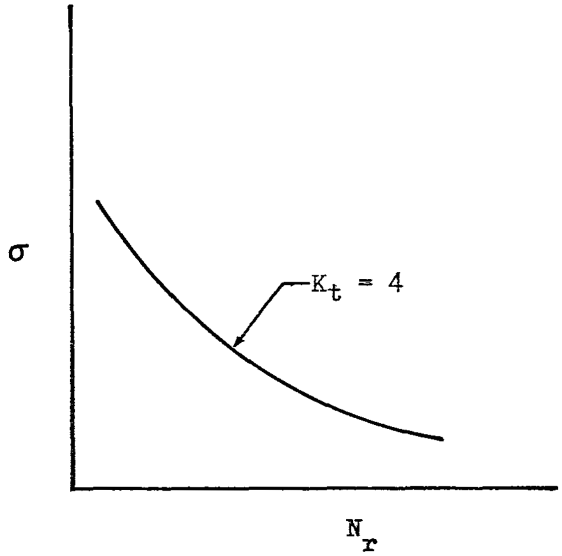

Computed Random S-N Curve

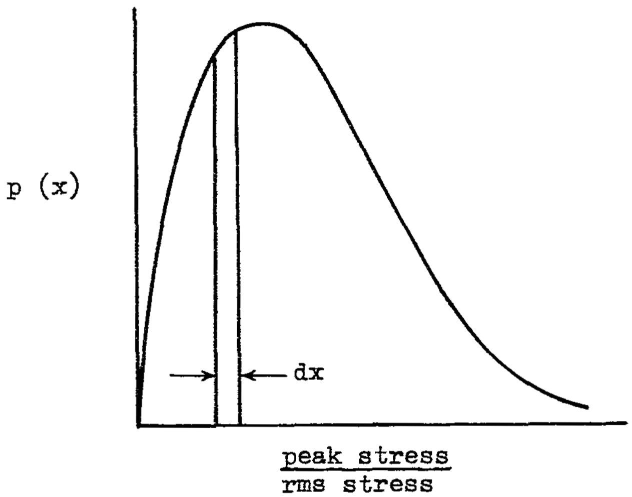

Rayleigh Probability Density Curve

REFERENCES

1. Bendat, Julius S. and Piersol, Allan G.: Measurement and Analysis of Random Data, John Wiley and Sons, Inc., 1966.

2. Miles, John W.: On Structural Fatigue Under Random Loading, Journal of the Aeronautical Sciences, Vol 21, No. 11 pages 753-762, November 1954.

3. Roark, Raymond J.: Formulas for Stress and Strain. McGraw-Hill Book Company, Inc., 1954.

4. Arcas, Noe: Prediction of Stress and Fatigue Life of Acoustically Excited Aircraft Structures, The Shock and Vibration Bulletin, No. 39 Part 3, January 1969.

5. MacDuff, N.N. and Felgar, R.P.: Vibration Frequency Charts, Machine Design, February 1957.

6. McGowan, P.R., et al: Structural Design for Acoustic Fatigue, ASD-TDR-63-820, 1963.

7. Illg, Walter: Fatigue Tests on Notched and Unnotched Sheet Specimens of 2024-T3 and 7075-T6 Aluminum Alloys and of SAE 4130 Steel with Special Consideration of the Life Range from 2 to 10,000 cycles. NACA TN 3866, 1956.

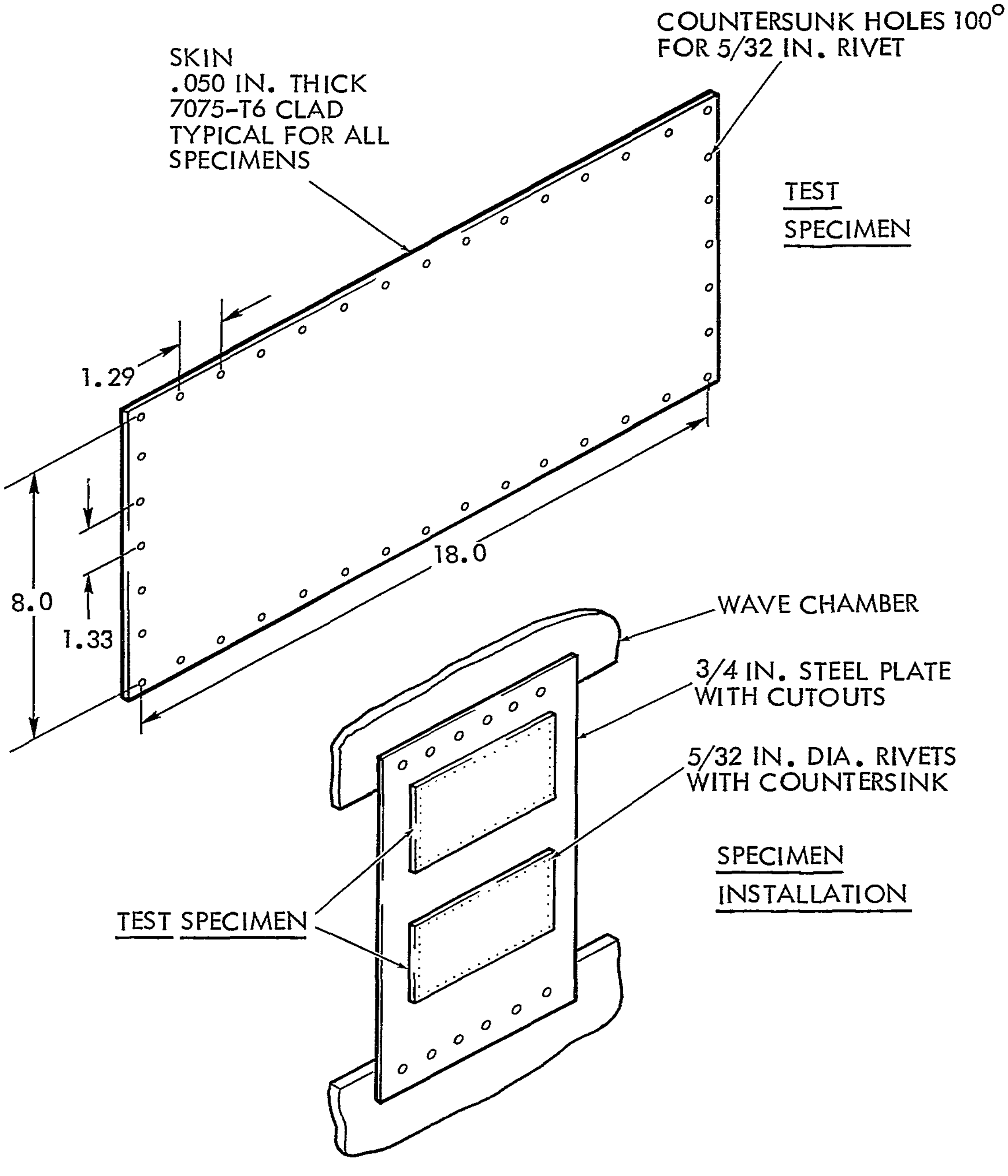

Figure 1 - Single Bay Configuration and Test Setup.

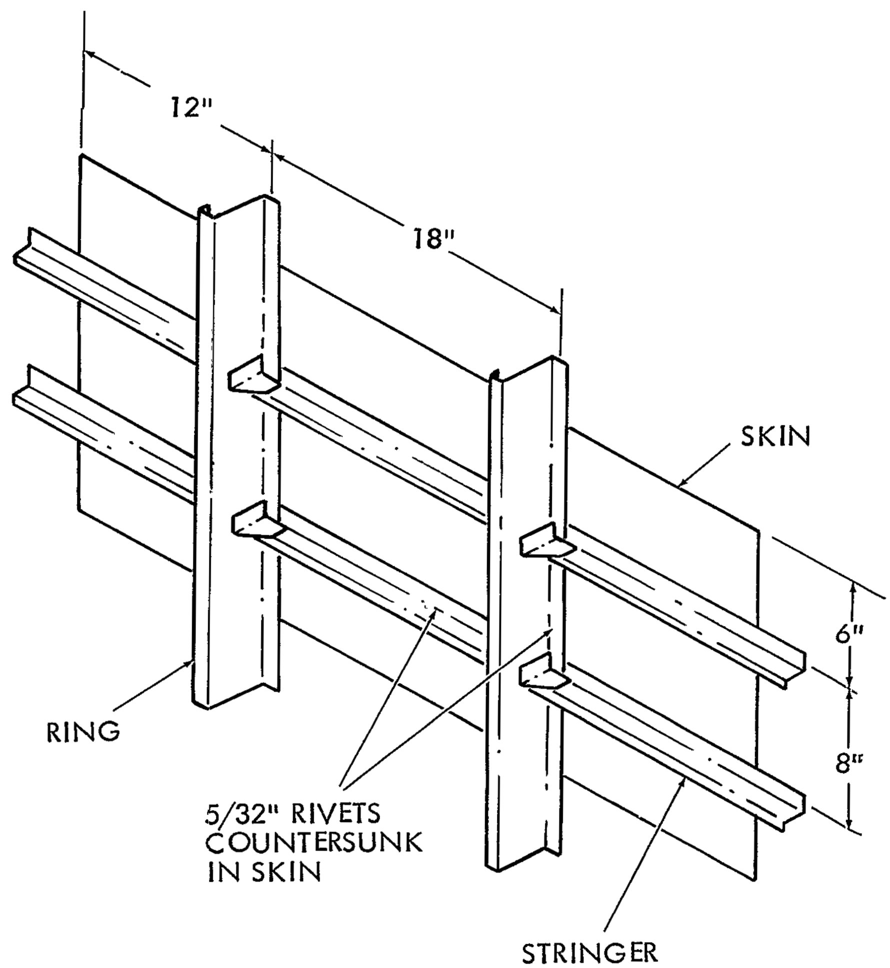

Figure 2 – Test Specimen; Nine Bay Configuration

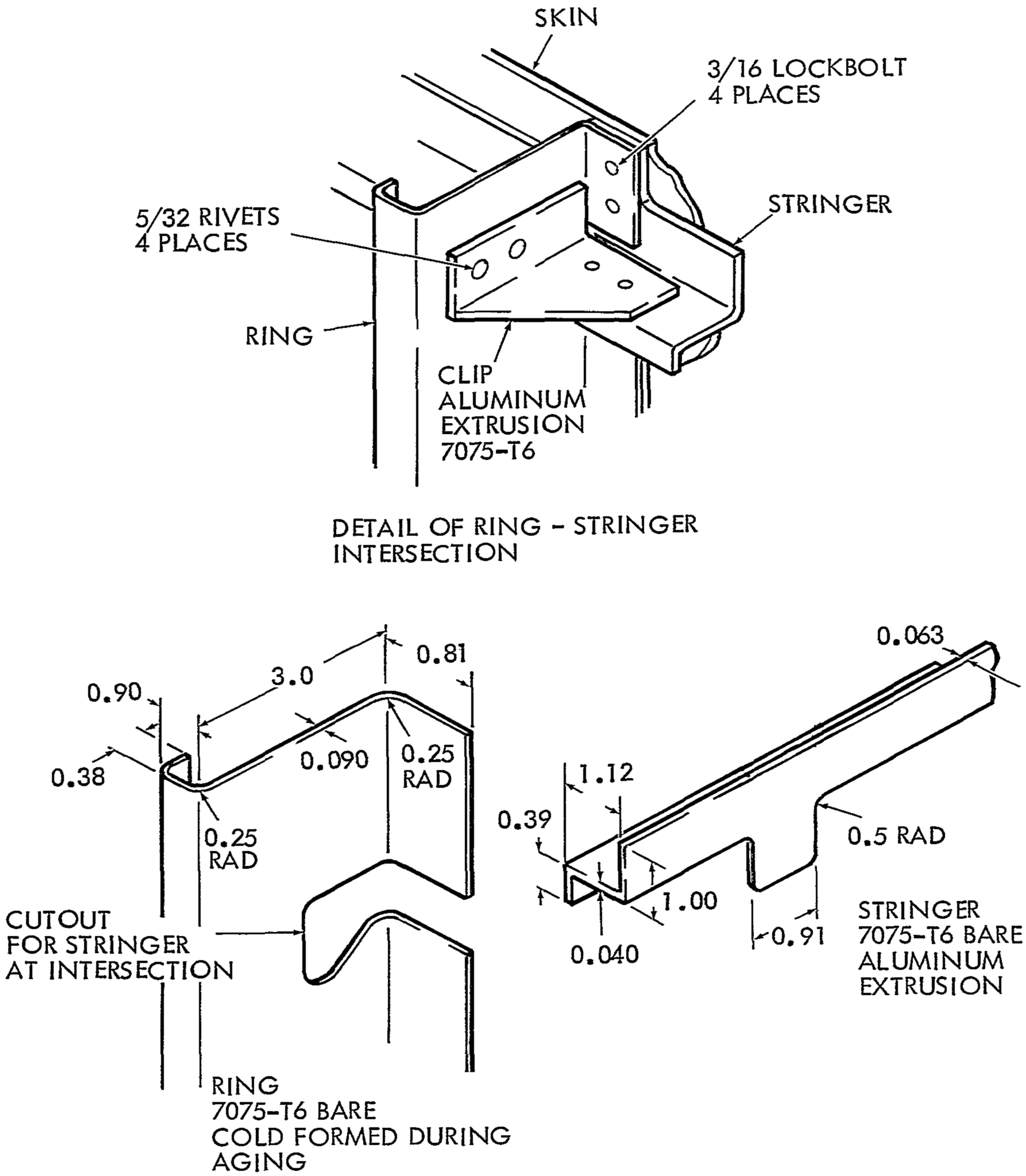

Figure 3 - Stringer and Ring Sections for All Multi-Bay Specimens.

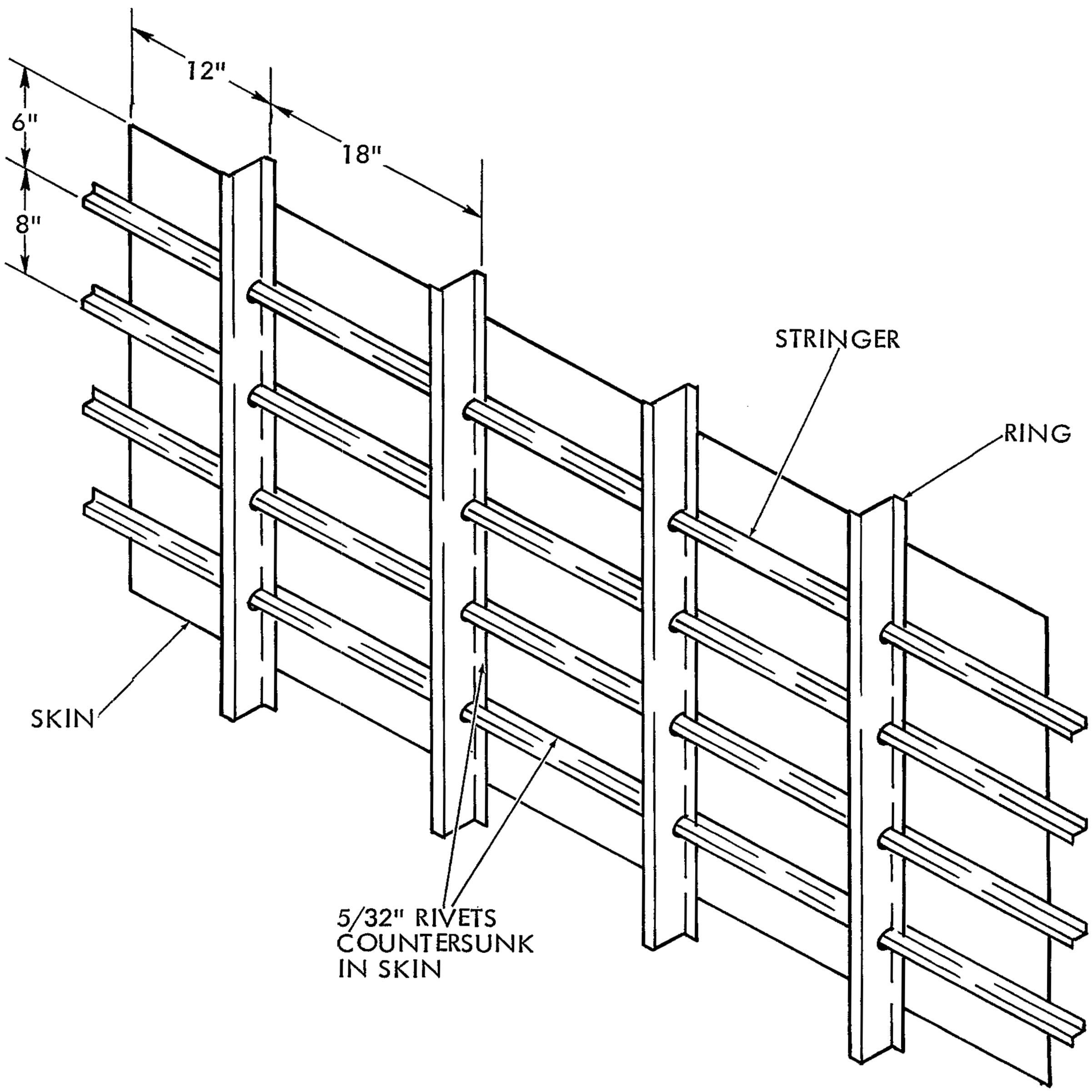

Figure 4 – Test Specimen; Twenty-Five Bay Configuration

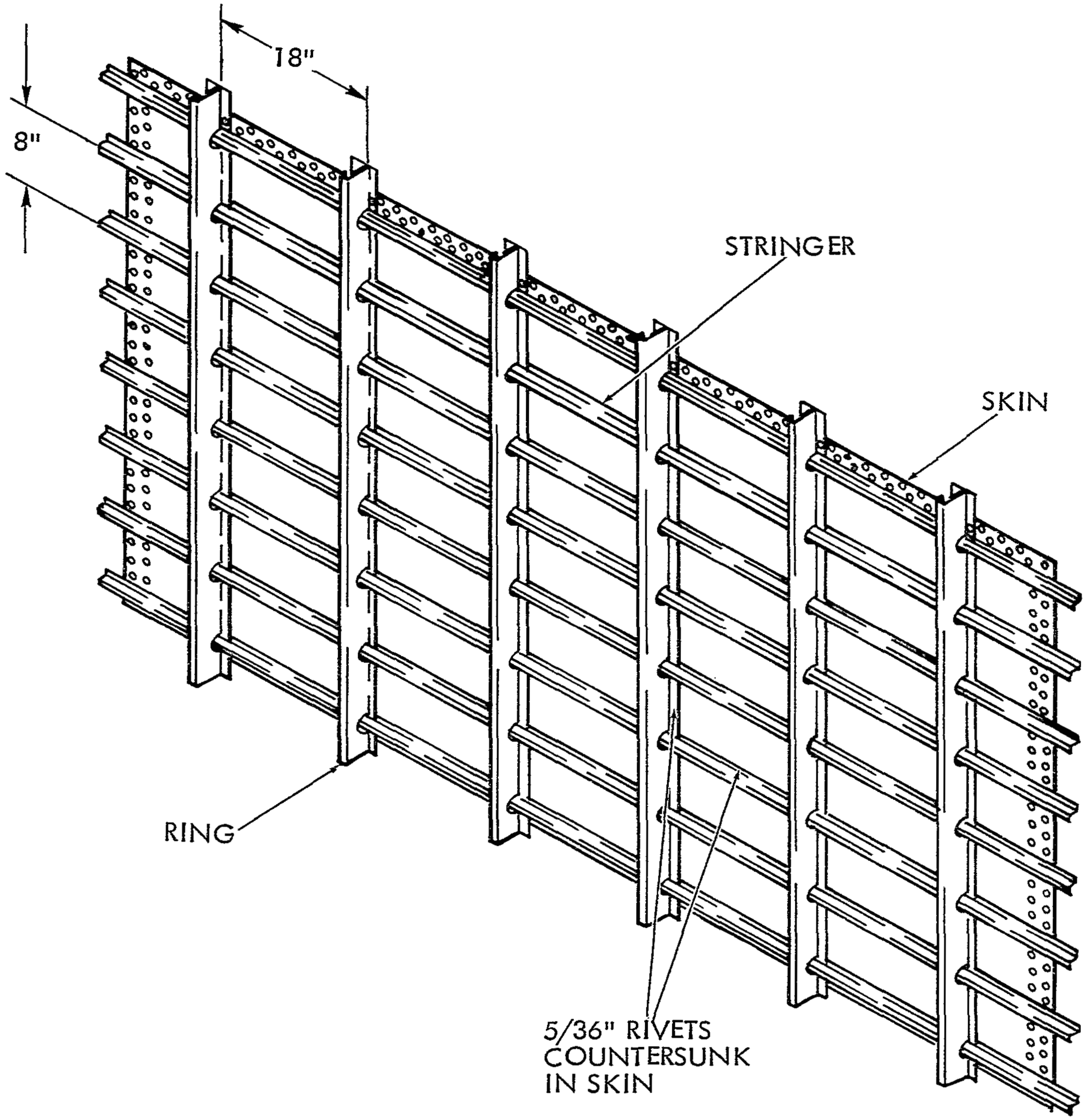

Figure 5 – Test Specimen; Forty-Nine Bay Configuration

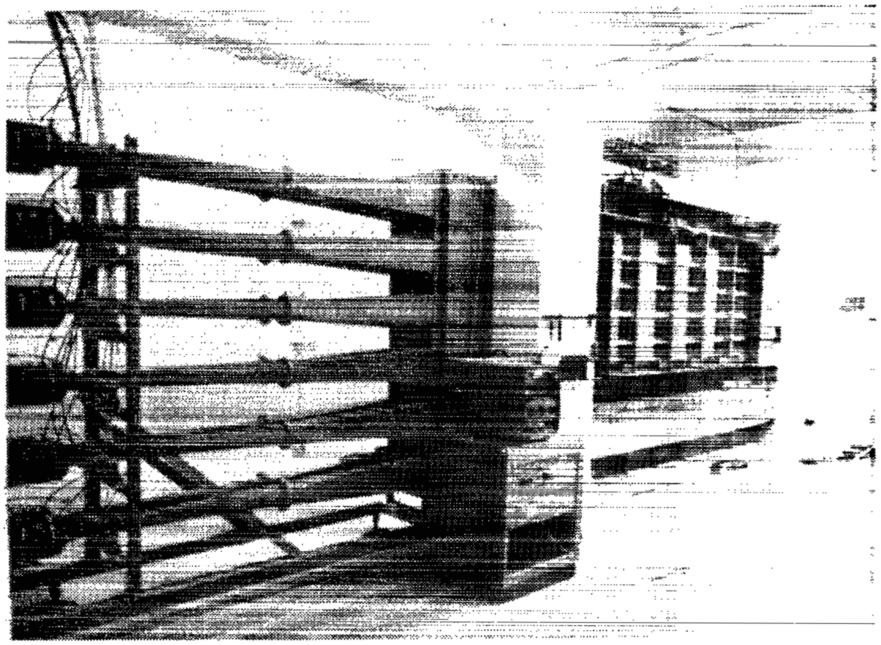

Figure 6 Progressive Wave Chamber with a Specimen Installed (far right). Sound Transducers with Expotential Horns are to the left.

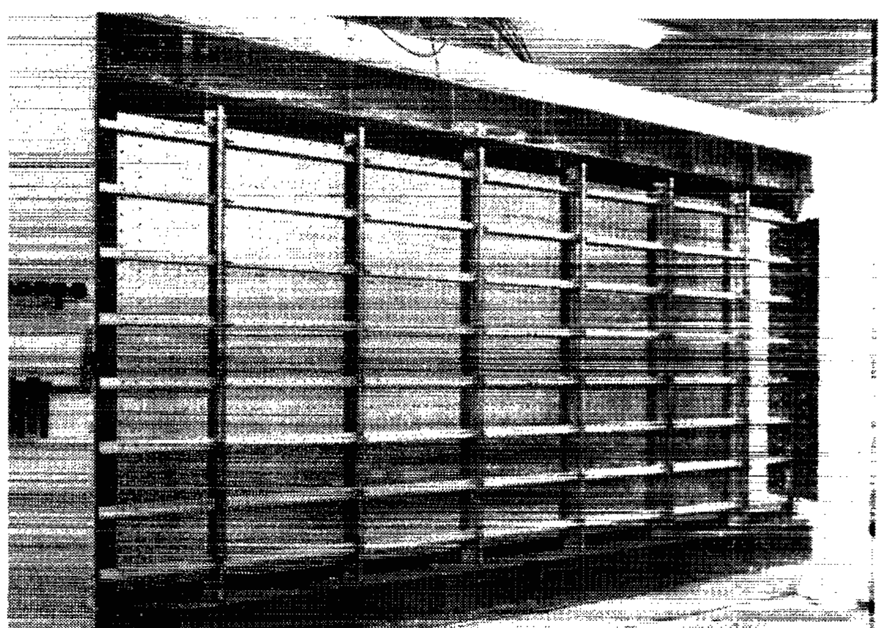

Figure 7 A Forty-Nine Bay Specimen Installed in the Test Chamber.

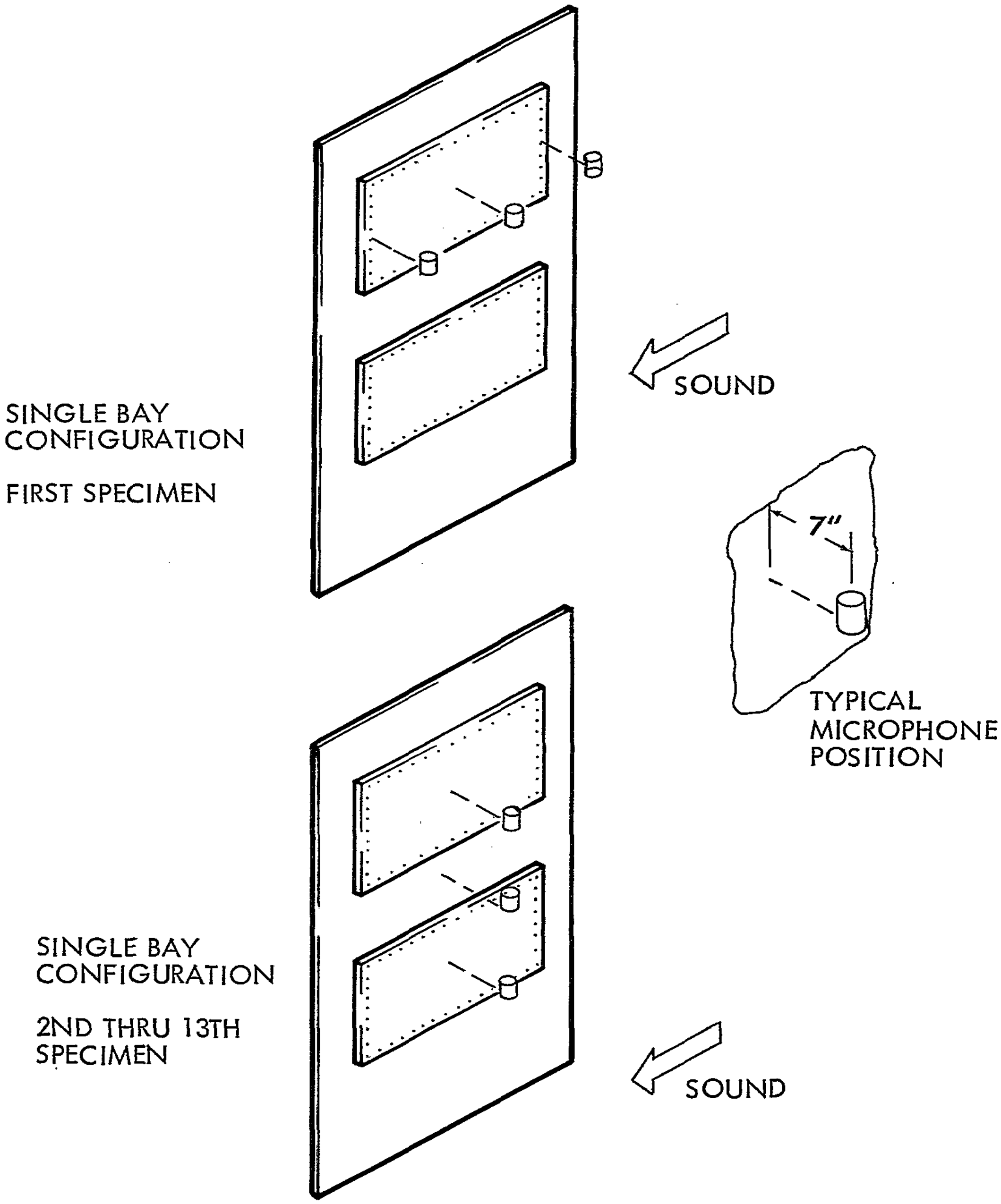

Figure 8 – Microphone Locations for All Configurations

NINE BAY, TWENTY-FIVE BAY, AND FORTY-NINE BAY CONFIGURATIONS.

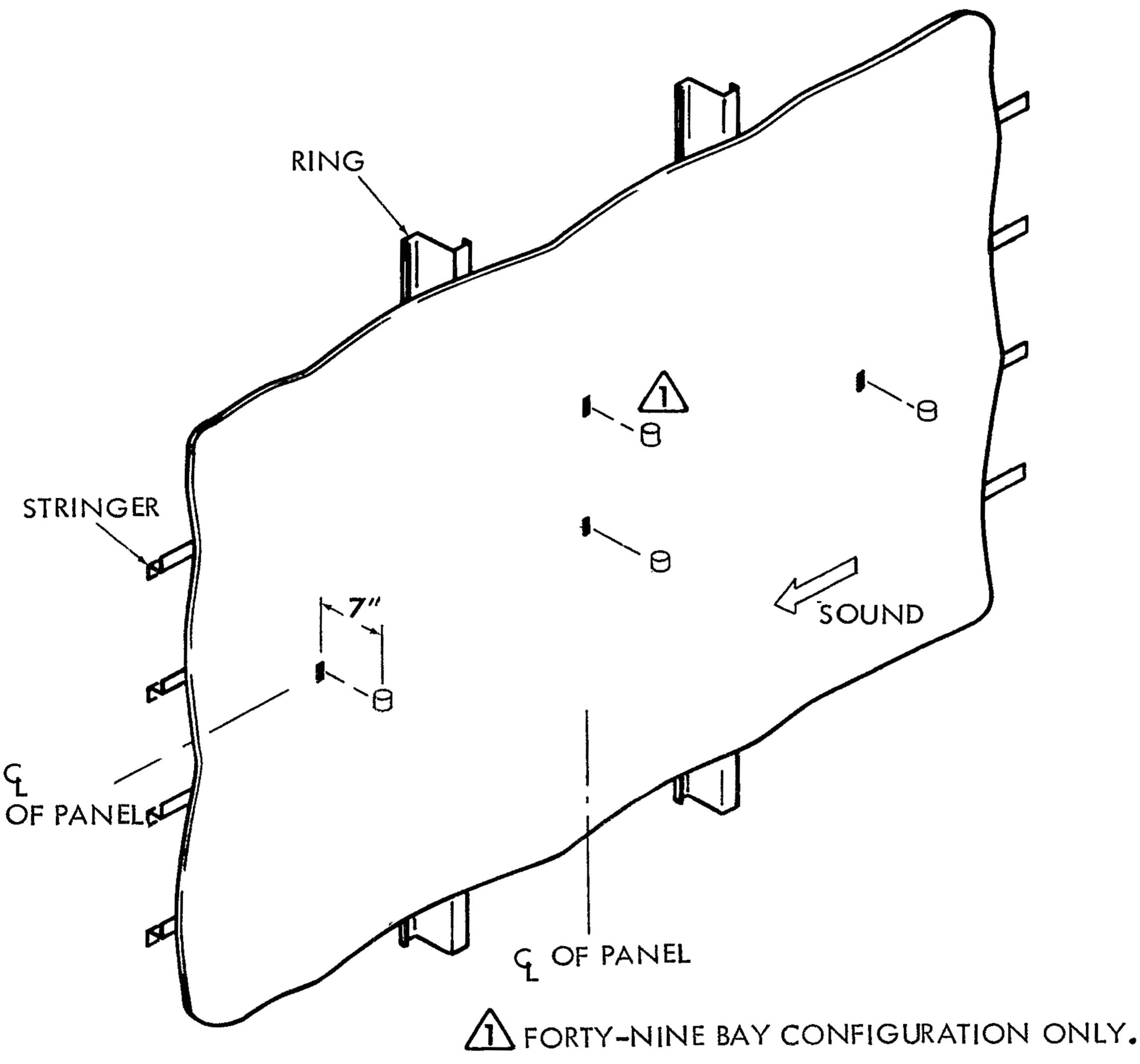

Figure 8 - Continued

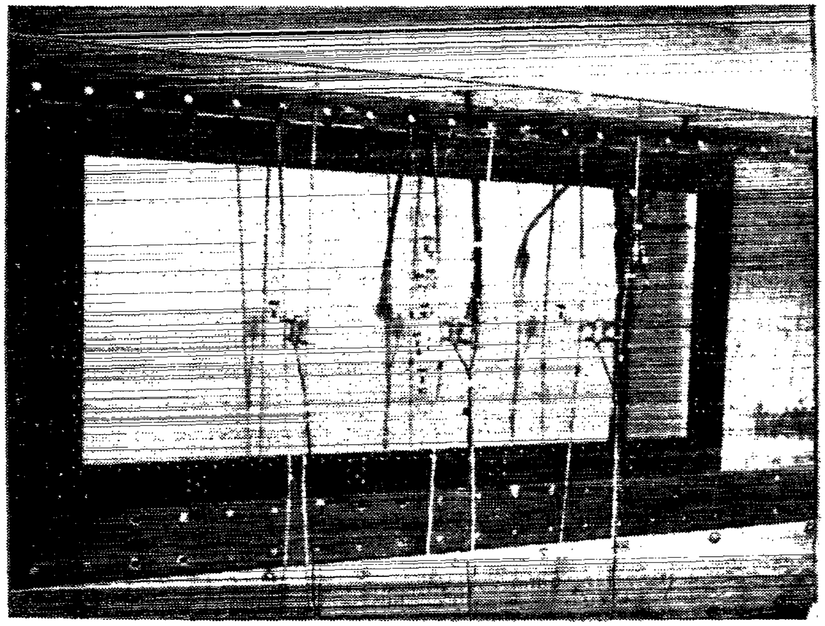

Figure 9 – The Opposing Side of the Wave Chamber has been Removed Showing a Twenty-Five Bay Specimen Surface Exposed to Sound

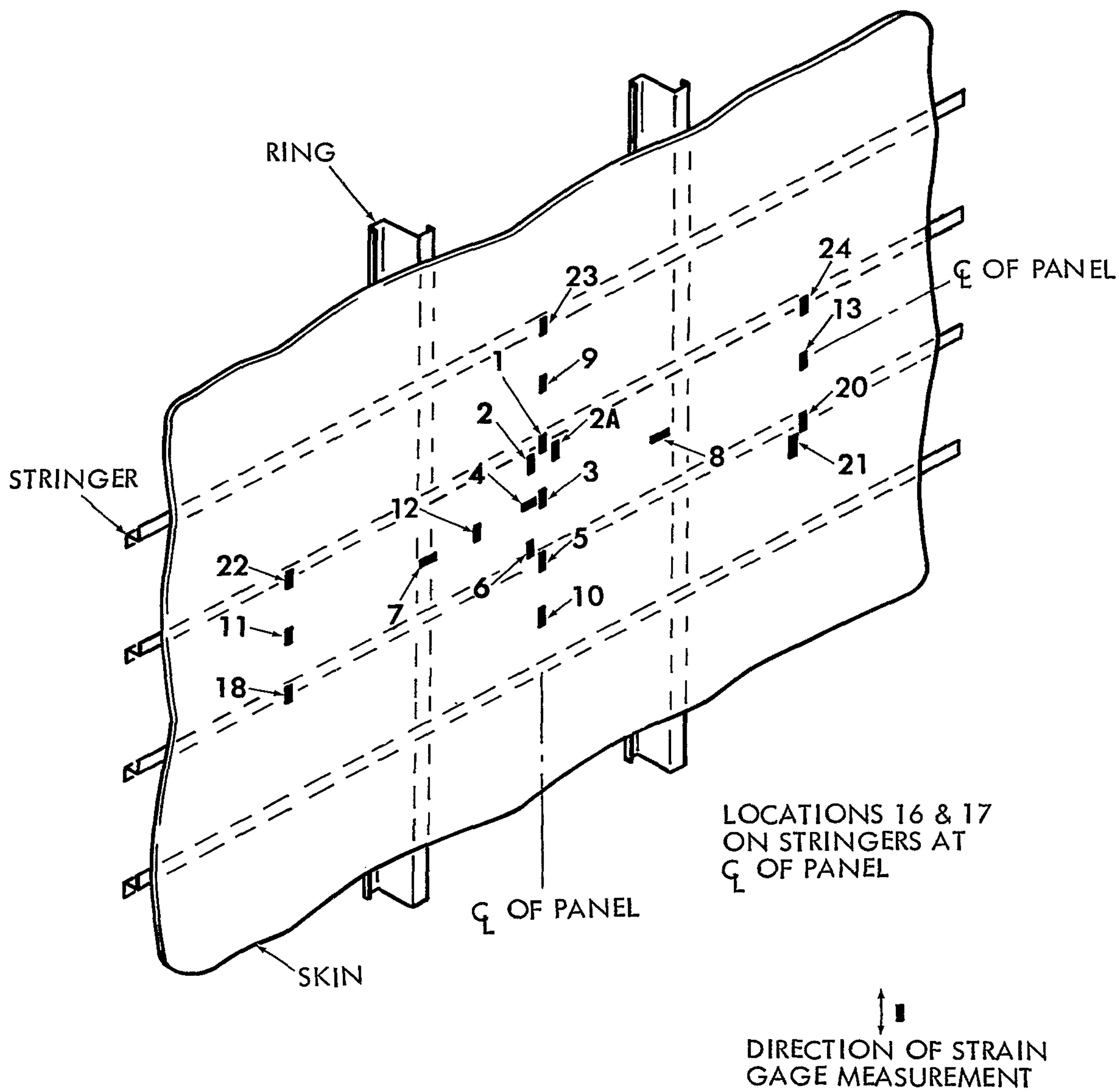

Figure 10 - Strain Gage Locations; Total Number of Different Locations Used on Any Configuration

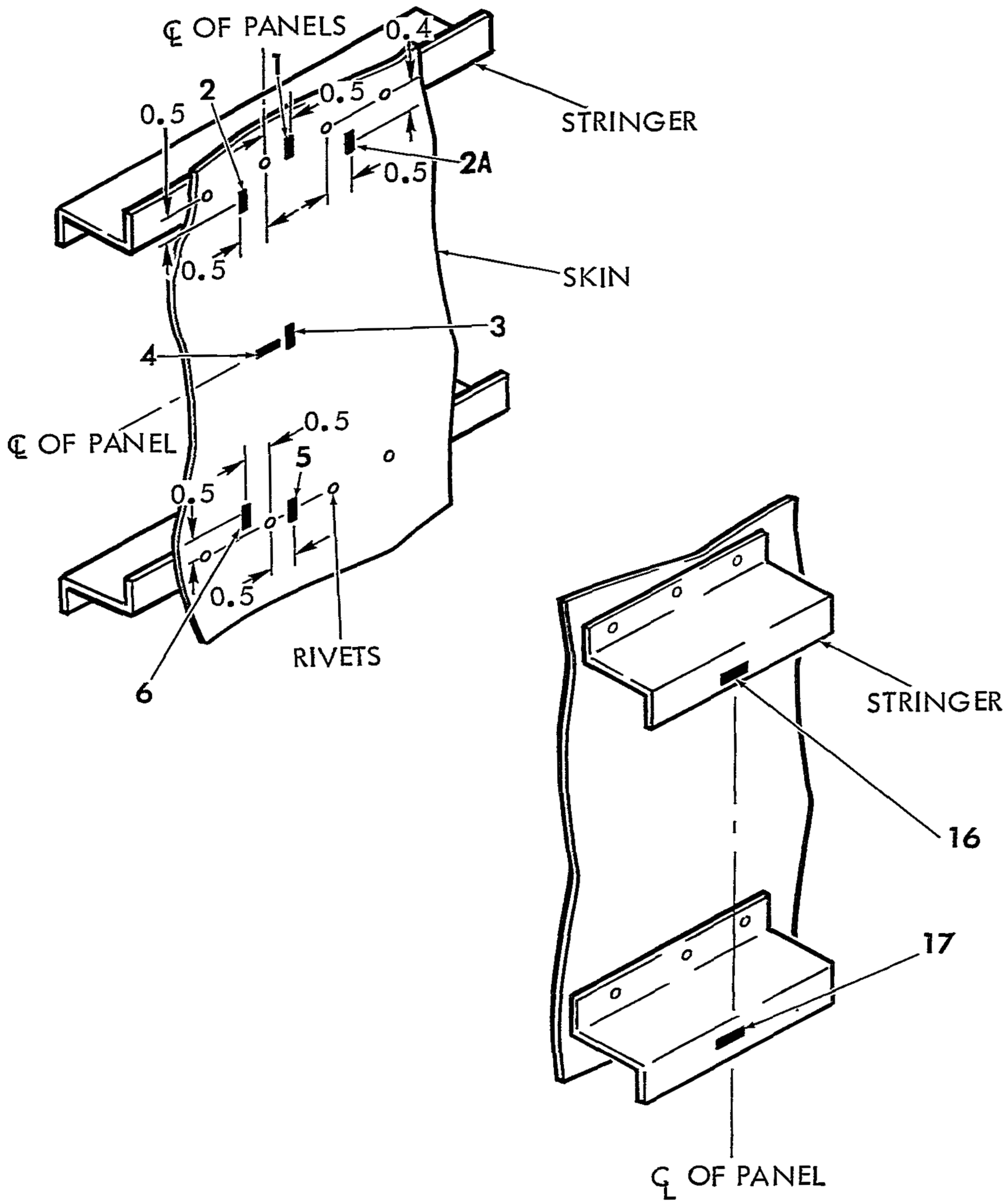

Figure 11 - Detail Locations of Primary Strain Gages

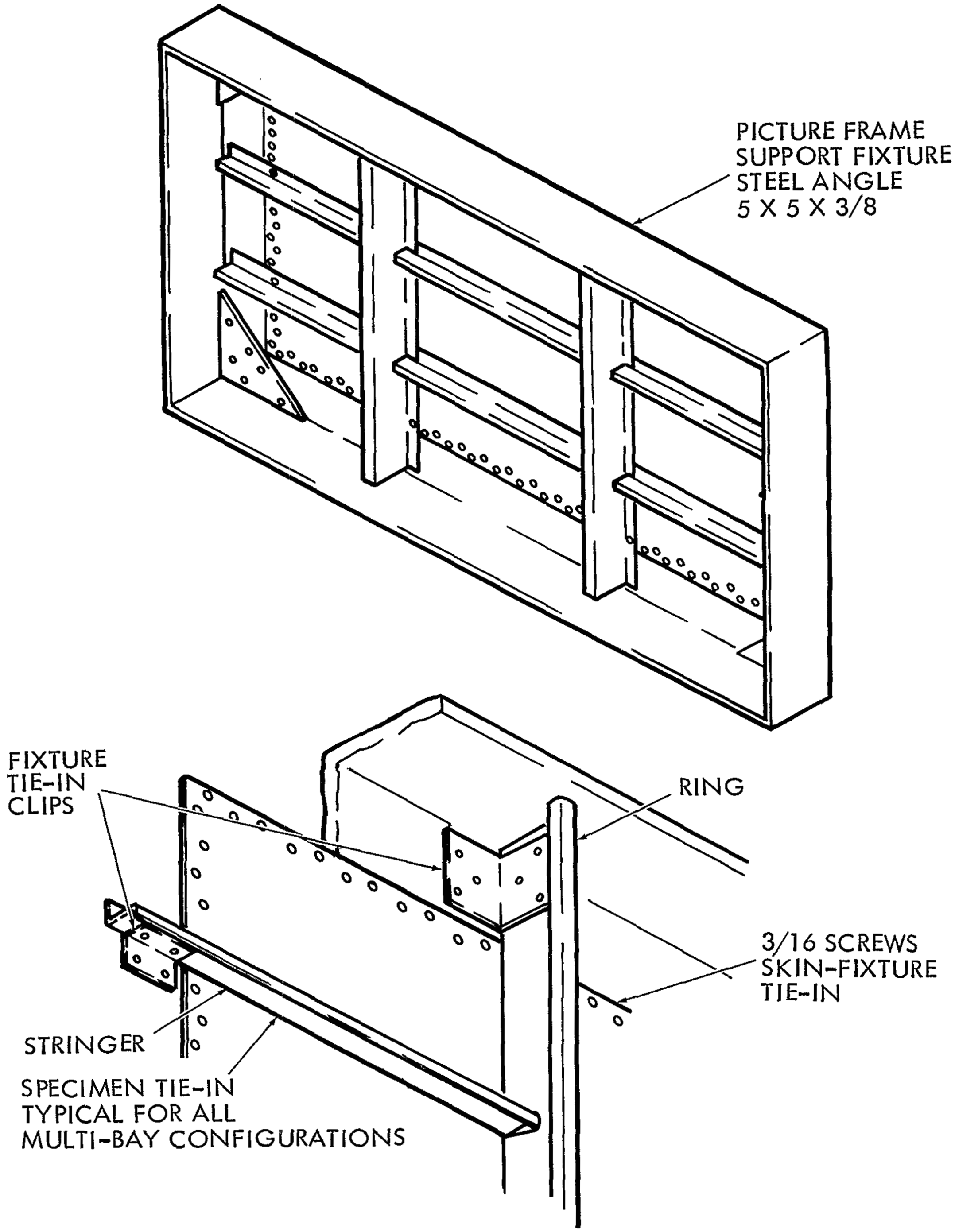

Figure 12 – Test Support Fixture for Nine Bay Configuration

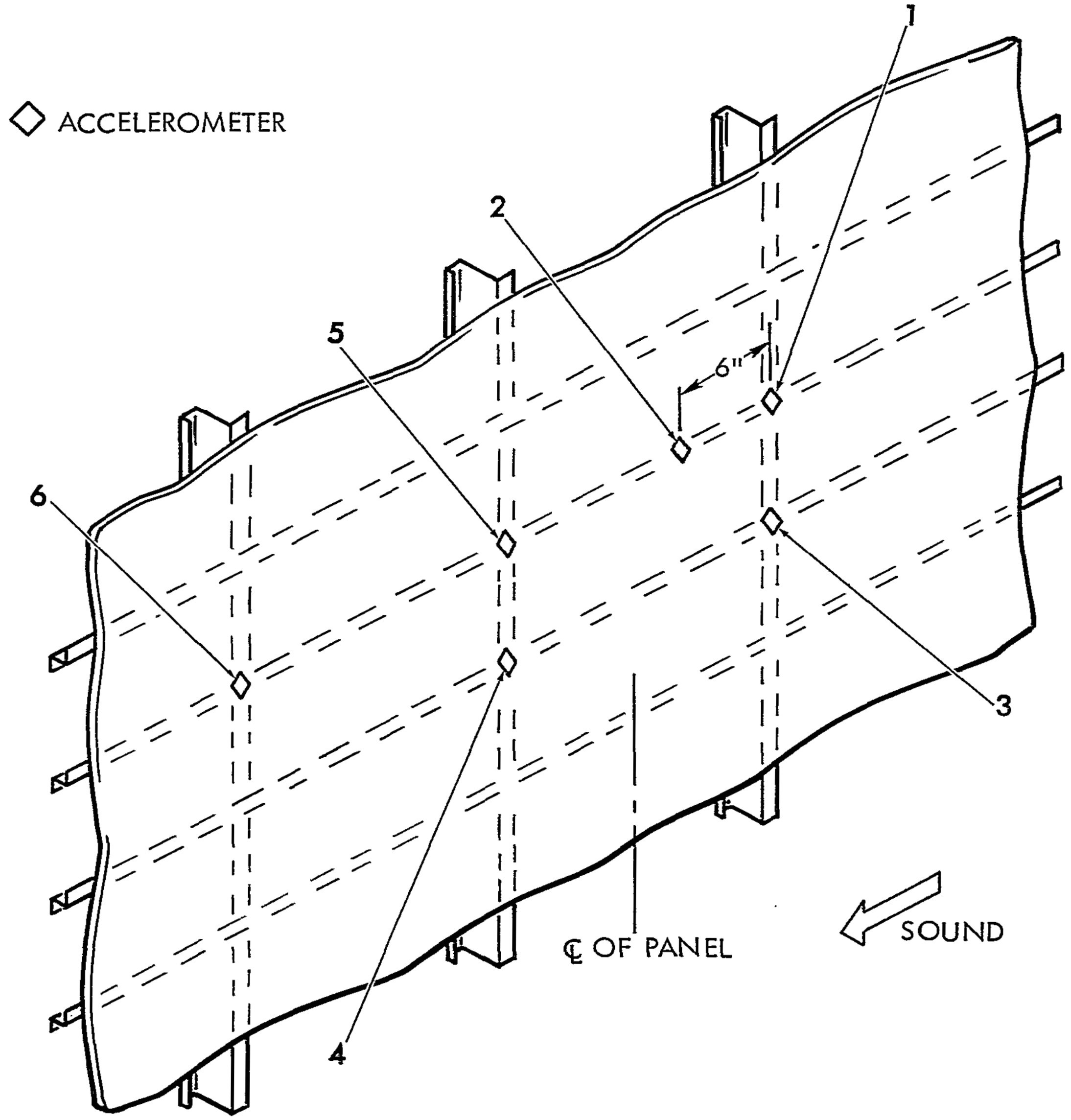

Figure 13 – Accelerometer Locations for all Configurations

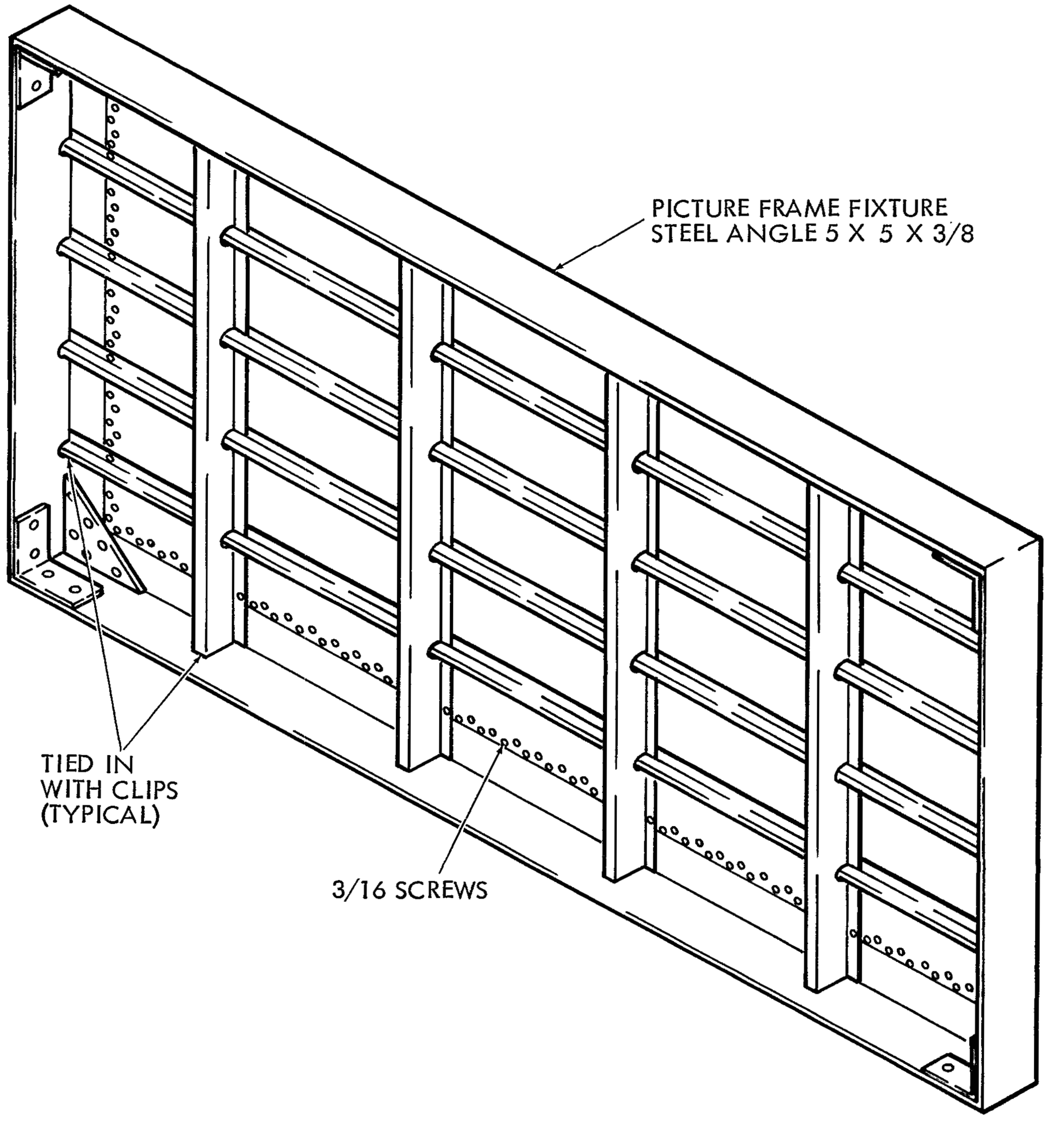

Figure 14 – Test Support Fixture for Twenty-Five Bay Configuration

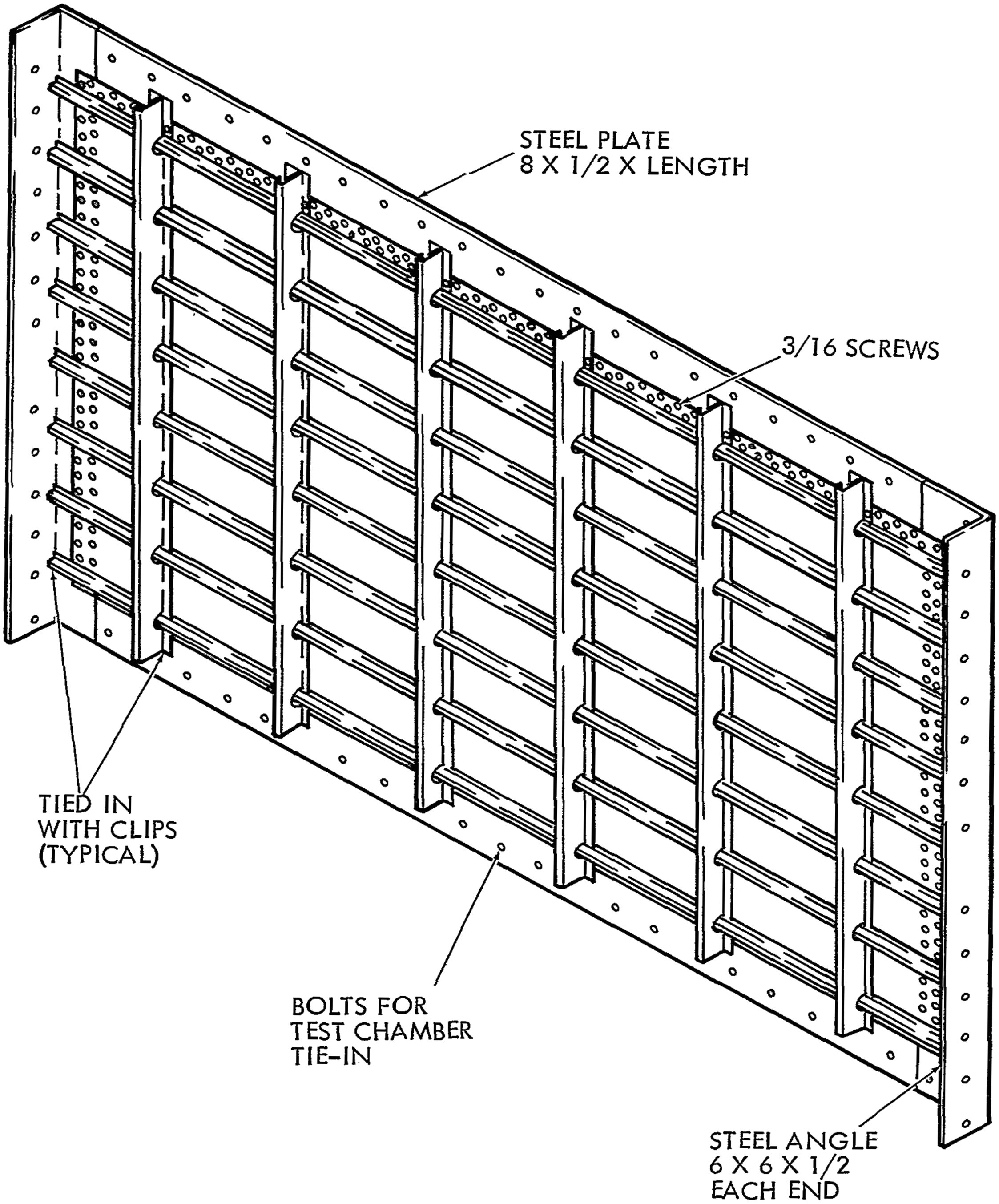

Figure 15 – Test Support Fixture for Forty-Nine Bay Configuration

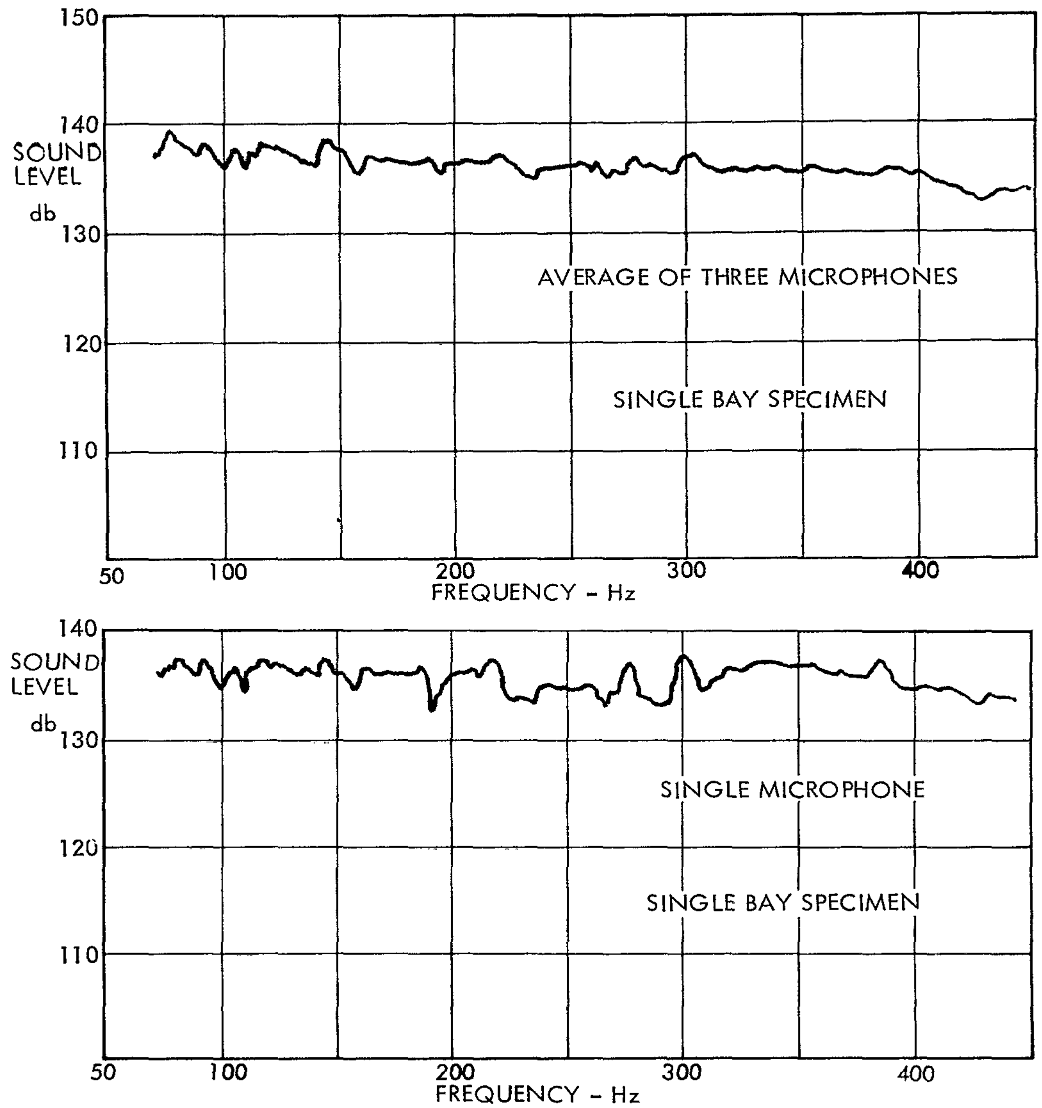

Figure 16 – Spectrum of Sound Pressure Level During a Discrete Frequency Sweep at 136 db

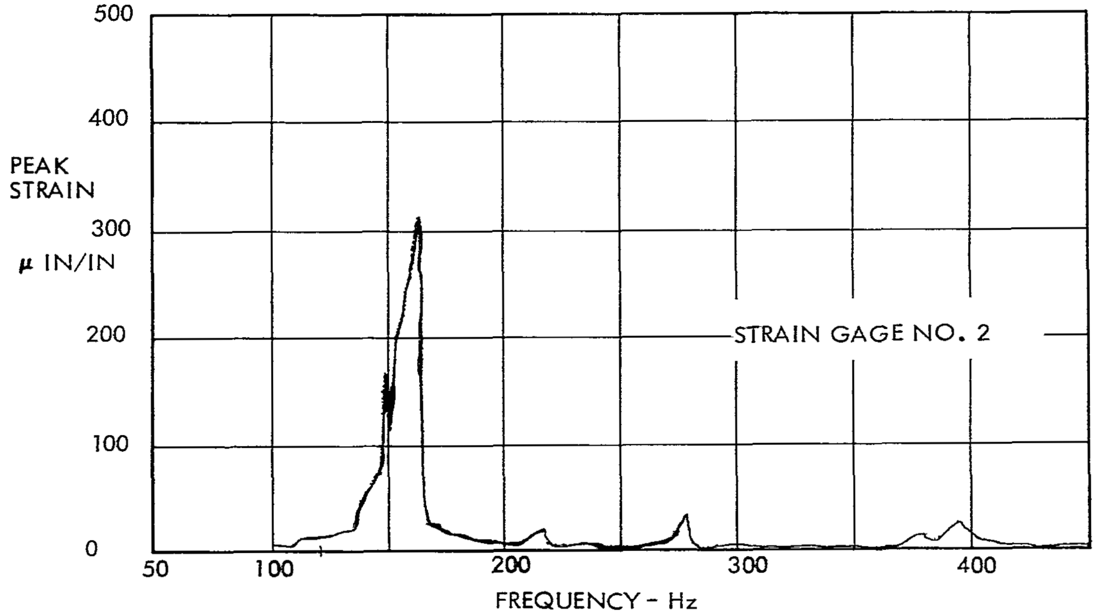

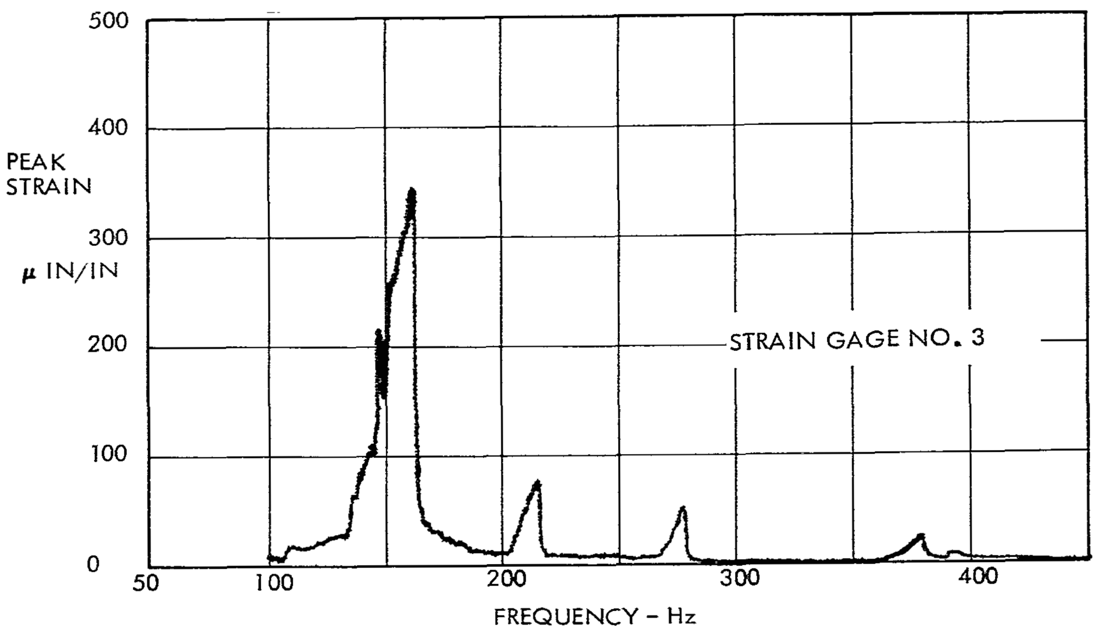

Figure 17 – Discrete Frequency Response at 130 db; Single Bay Configuration (Specimen No. 1)

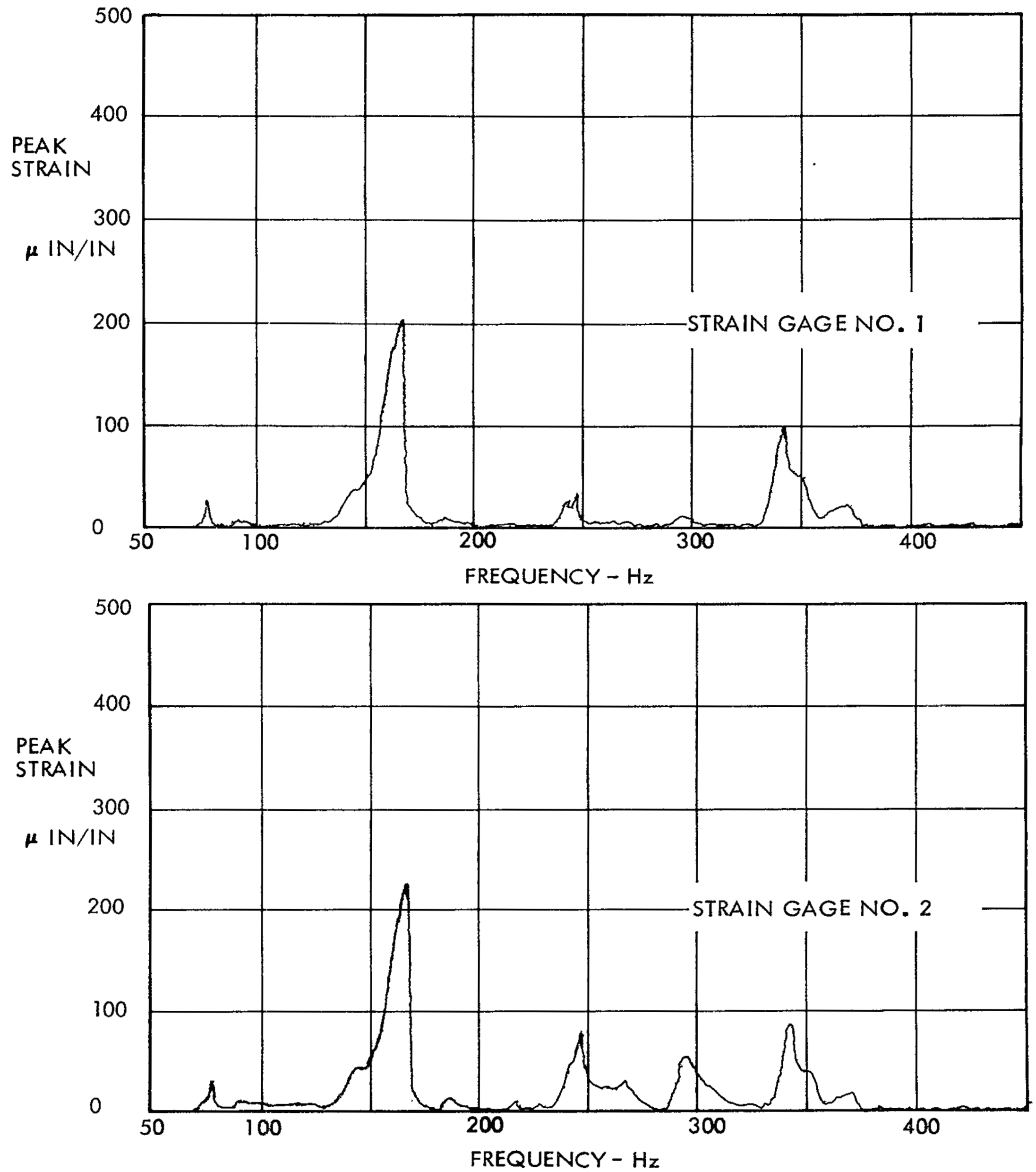

Figure 18 – Discrete Frequency Response at 136 db; Nine Bay Configuration, Specimen No. 2.

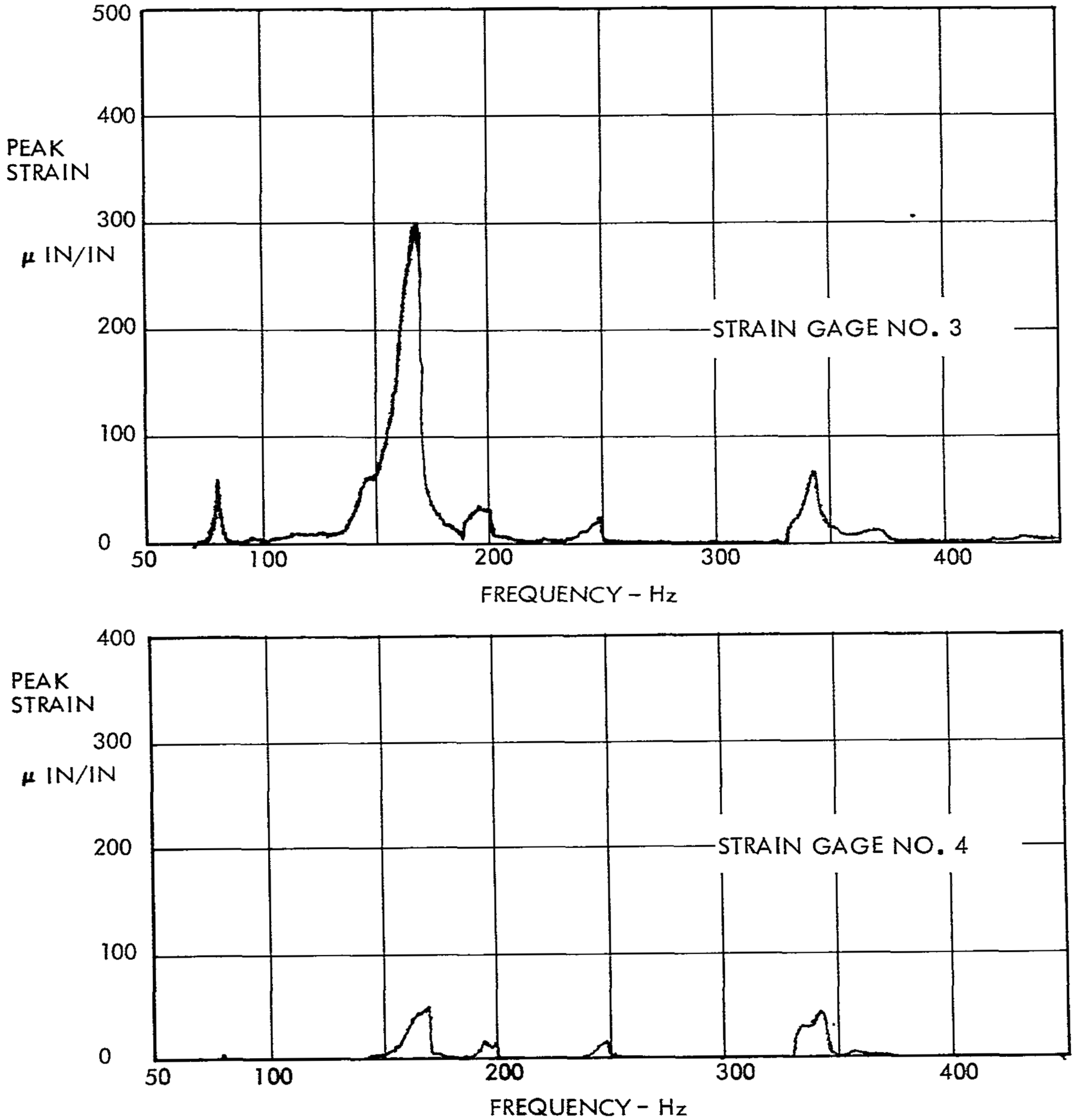

Figure 19 - Discrete Frequency Response at 136 db; Nine Bay Configuration, Specimen No. 2.

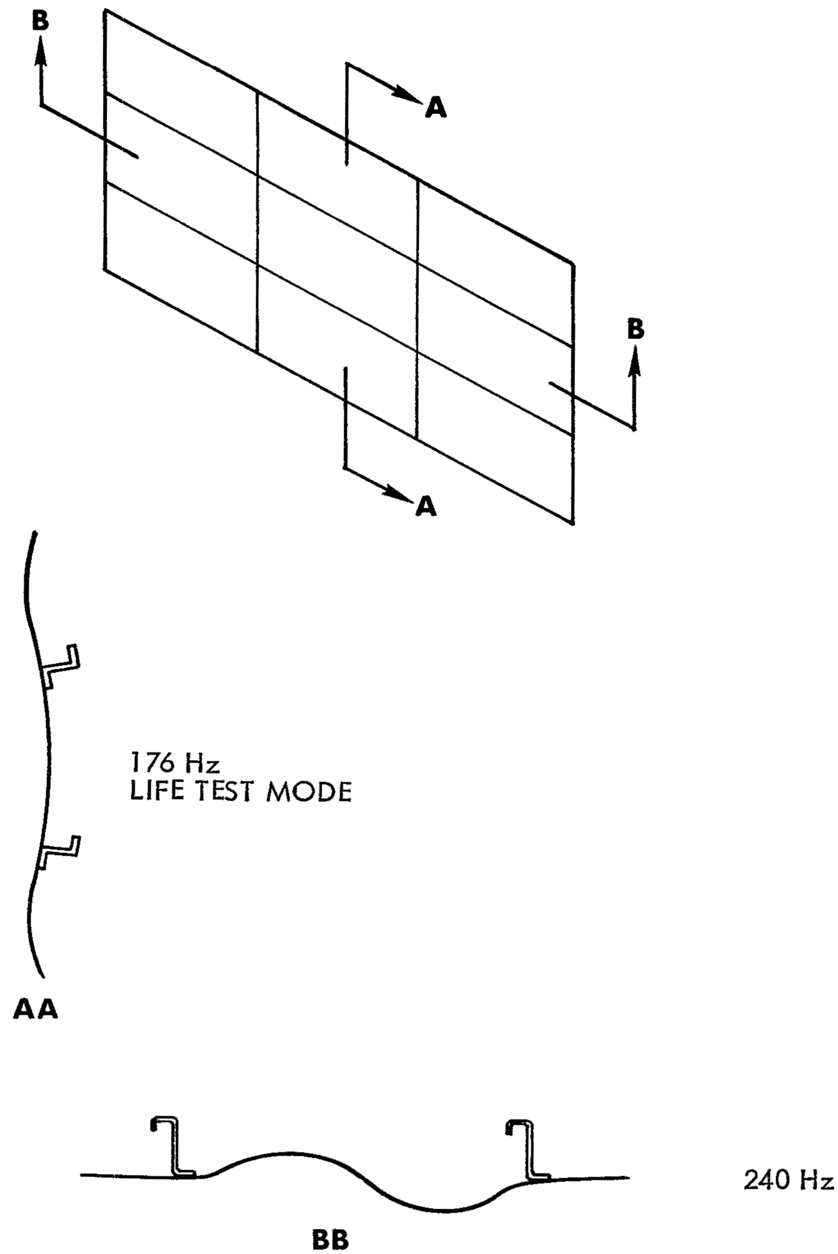

Figure 20 – Mode Shapes of a Nine Bay Configuration Specimen

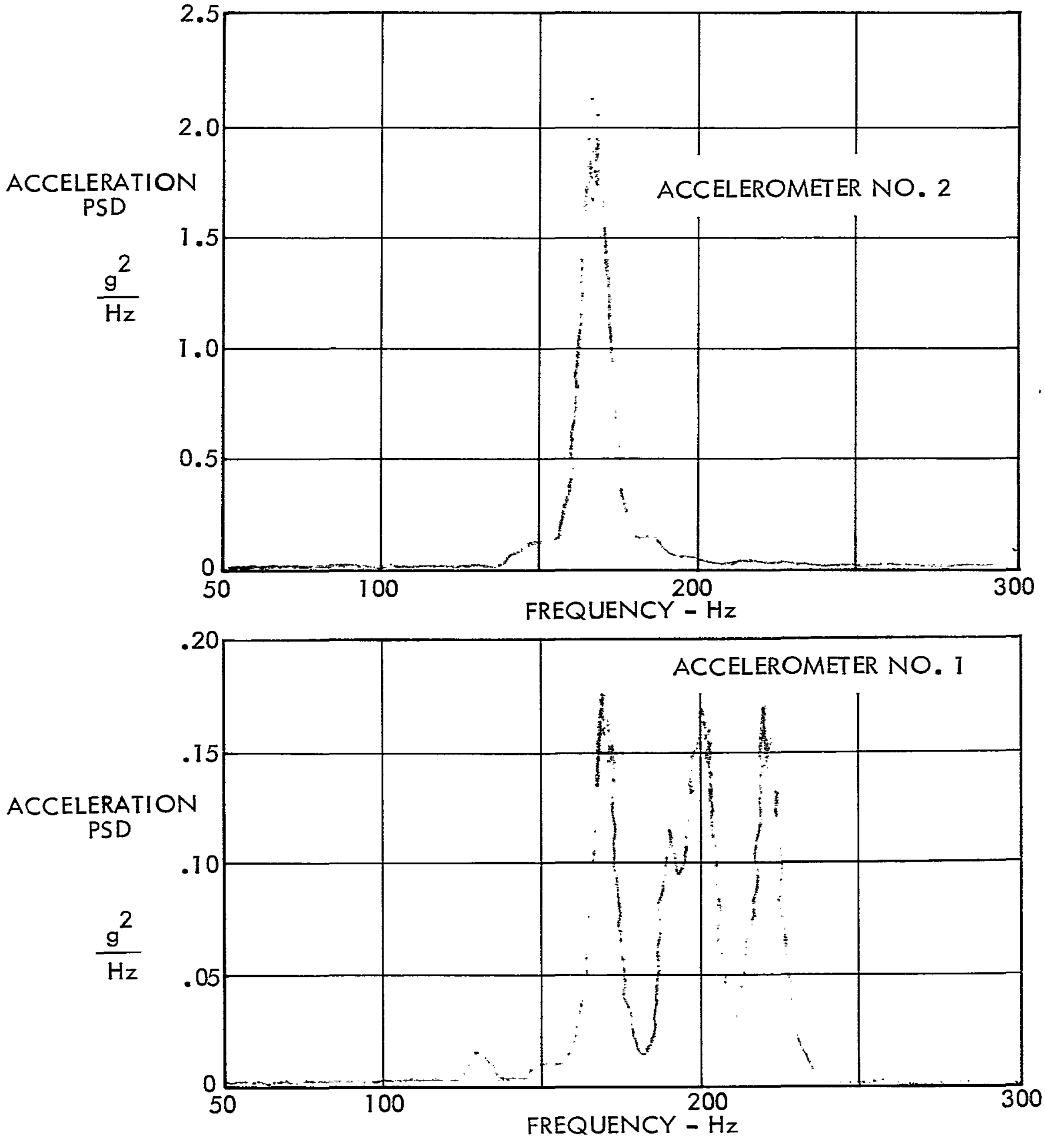

Figure 21 - Response of a Nine Bay Configuration Specimen at a Spectrum Level of 120 db. (No. 2)

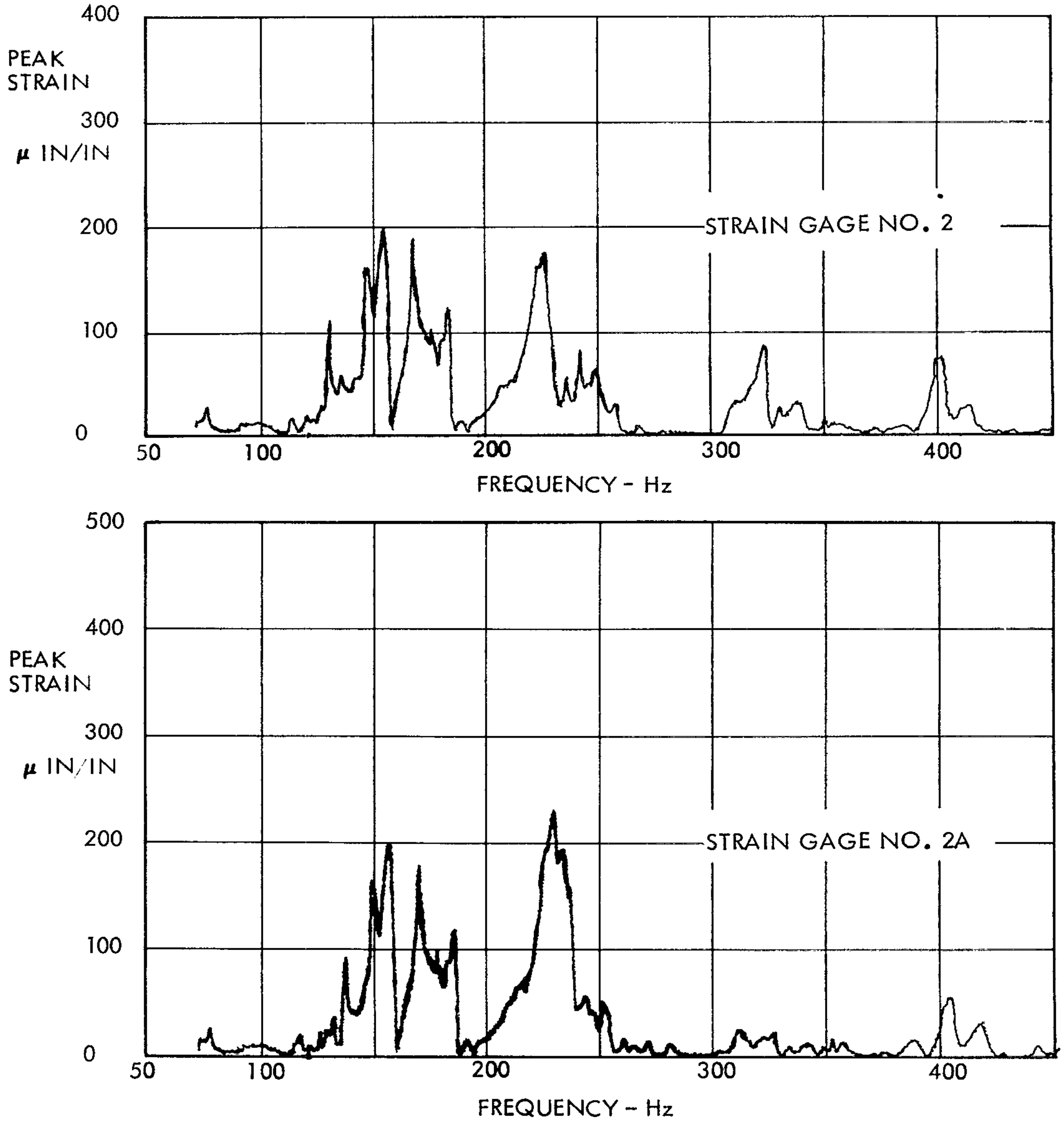

Figure 22 - Discrete Frequency Response at 136 db;
Twenty-Five Bay Configuration, Specimen No. 2.

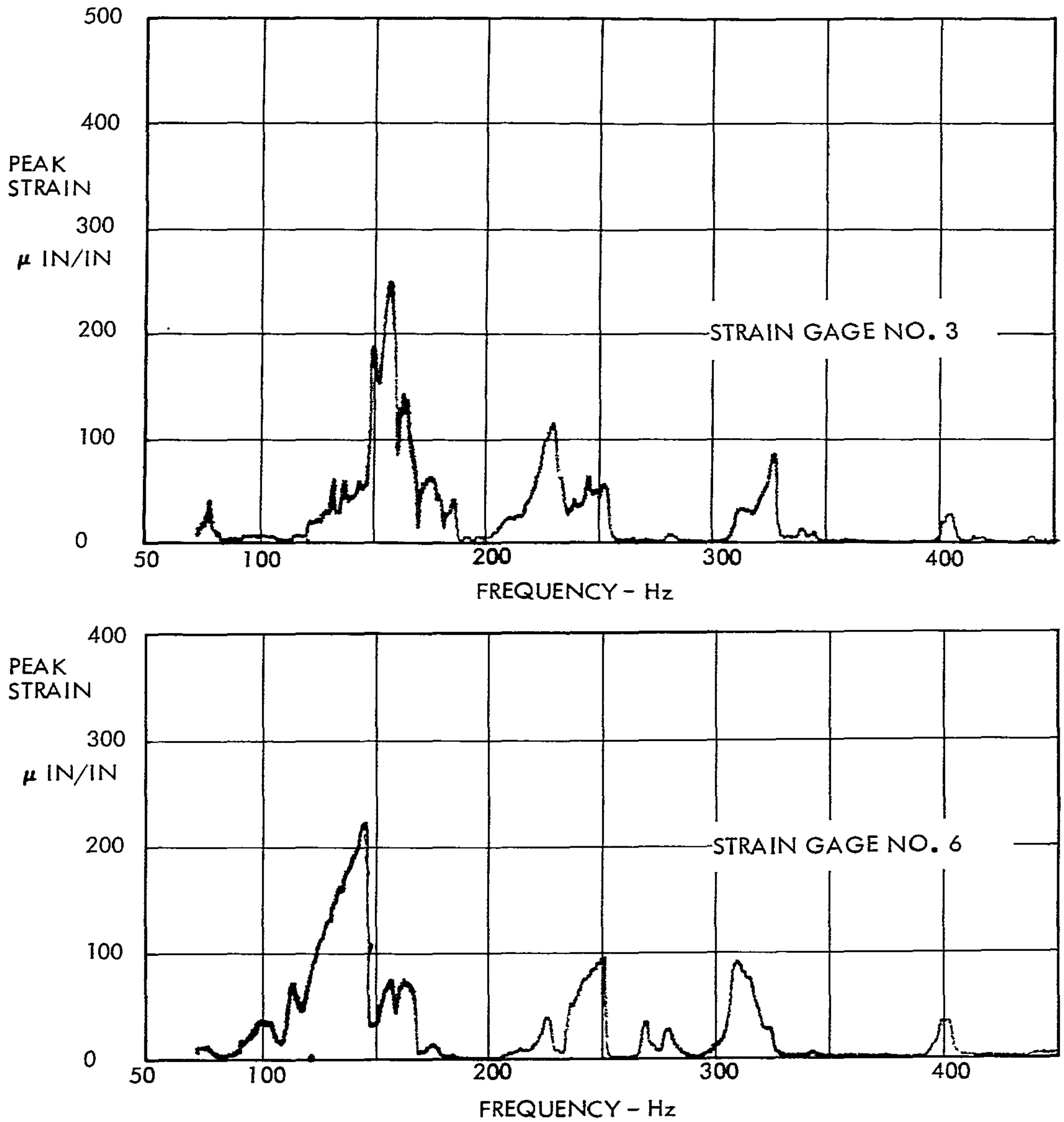

Figure 23 - Discrete Frequency Response at 136 db;
Twenty-Five Bay Configuration, Specimen 2.

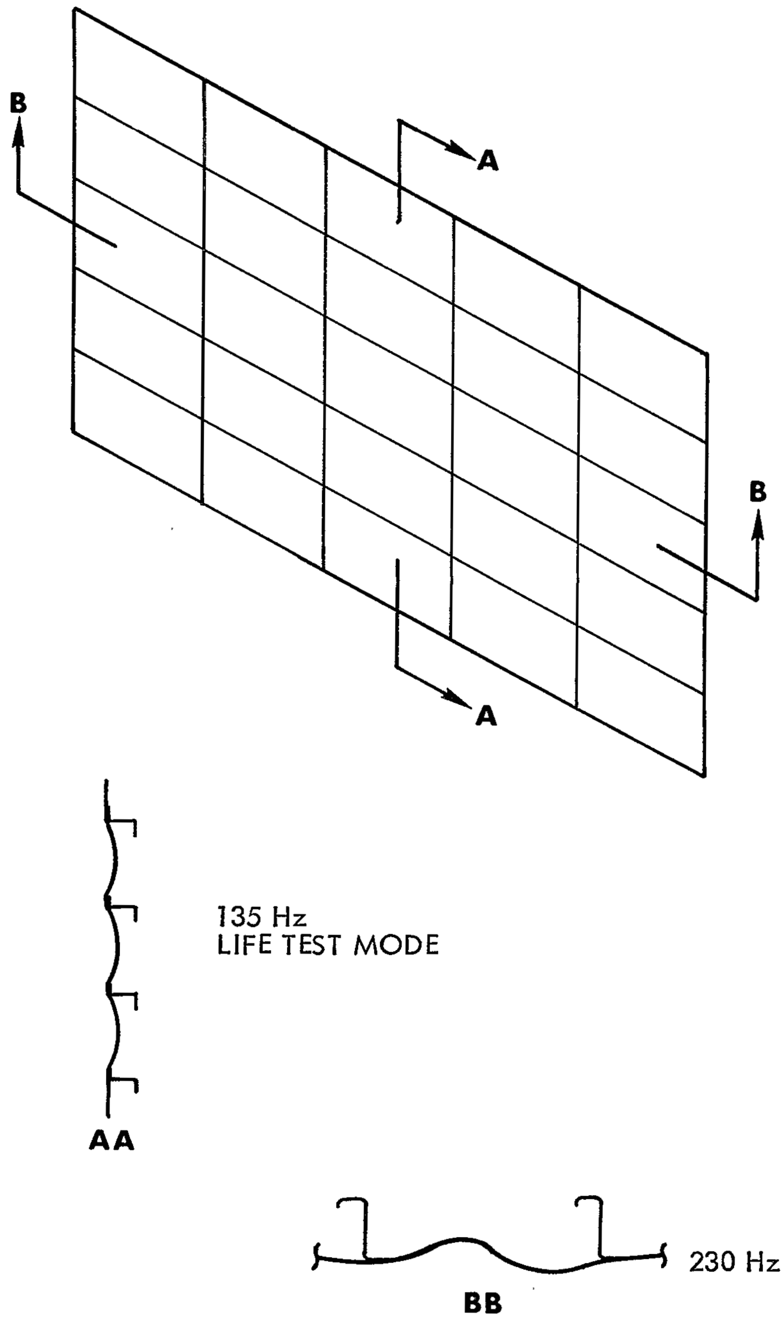

Figure 24 - Mode Shapes of a Twenty-Five Bay Configuration Specimen

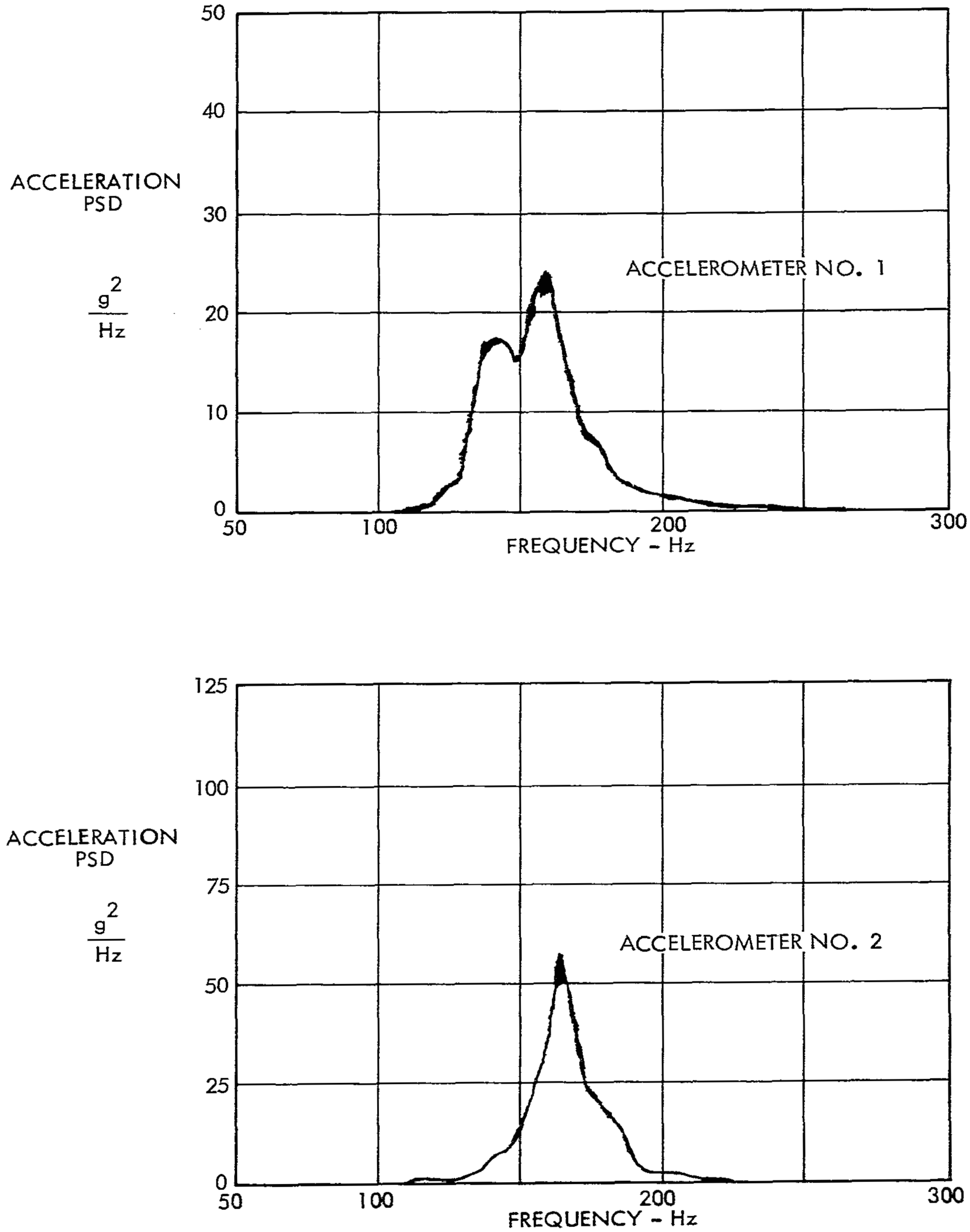

Figure 25 - Response of a Twenty-Five Bay Configuration Specimen at a Spectrum Level of 135 db. (No. 2)

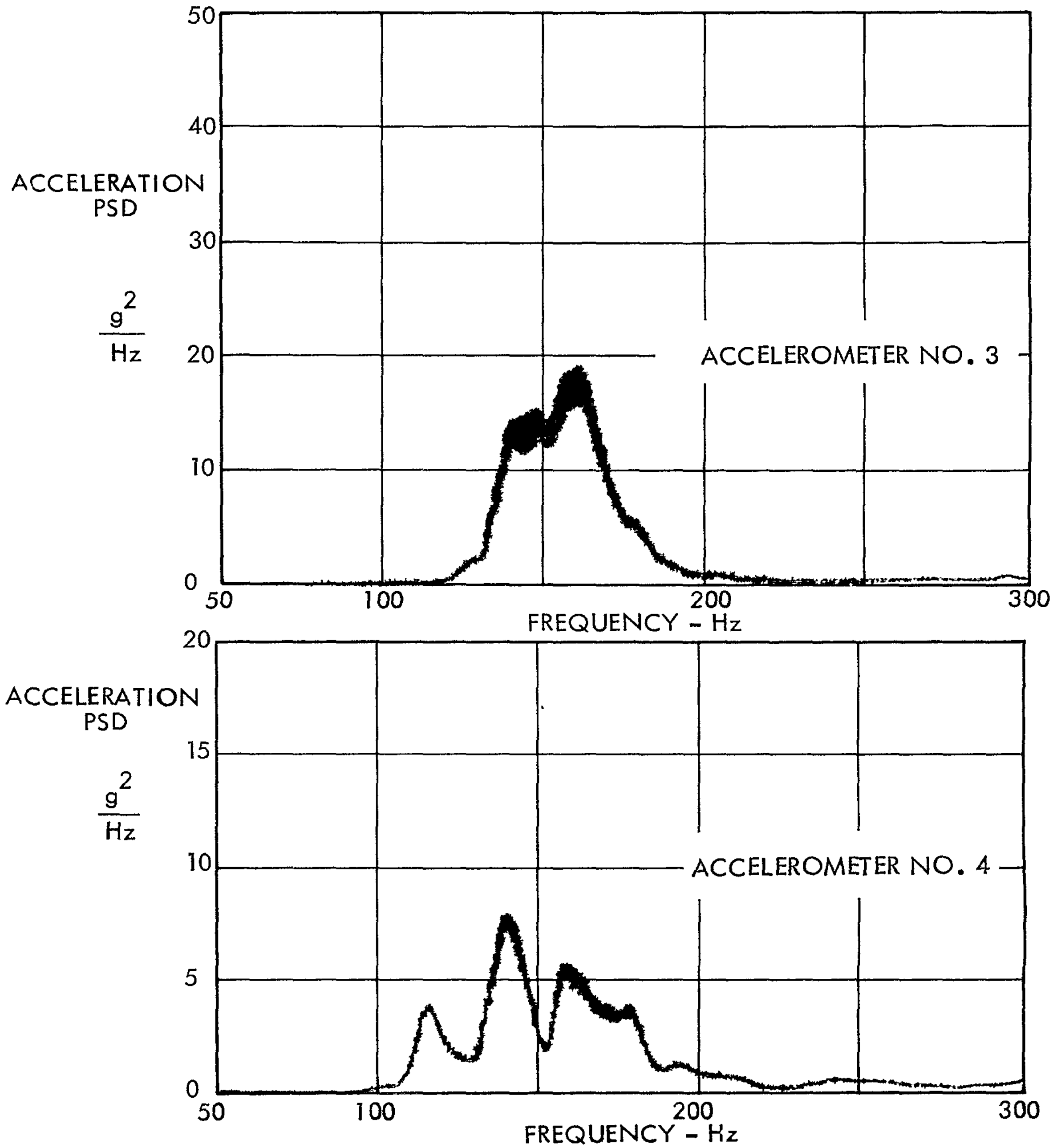

Figure 26 - Response of a Twenty-Five Bay Configuration Specimen at a Spectrum Level of 135 db. (No. 2)

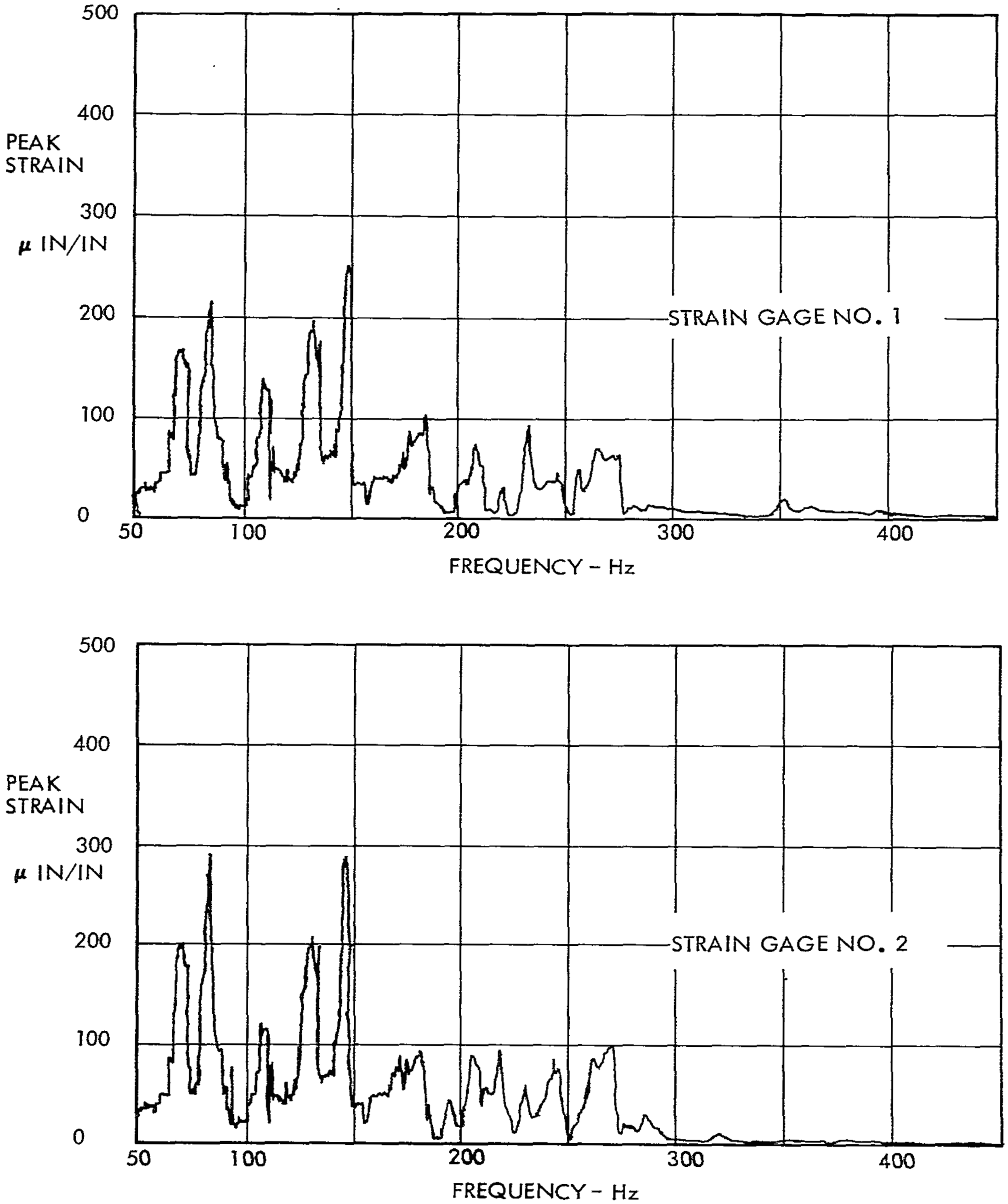

Figure 27 - Discrete Frequency Response at 136 db; Forty-Nine Bay Configuration, Specimen 3.

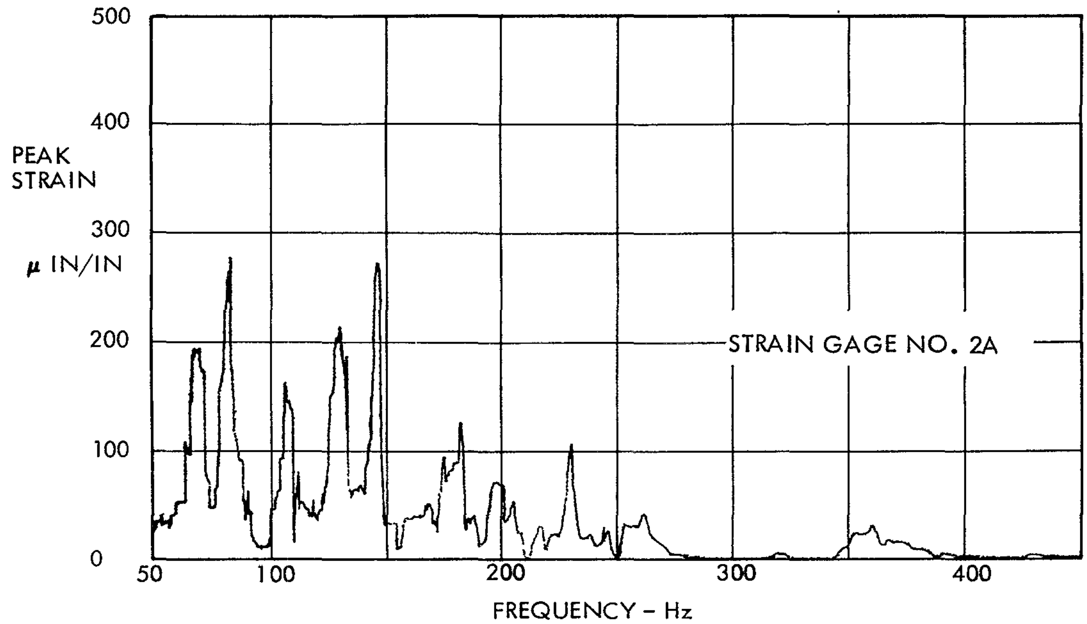

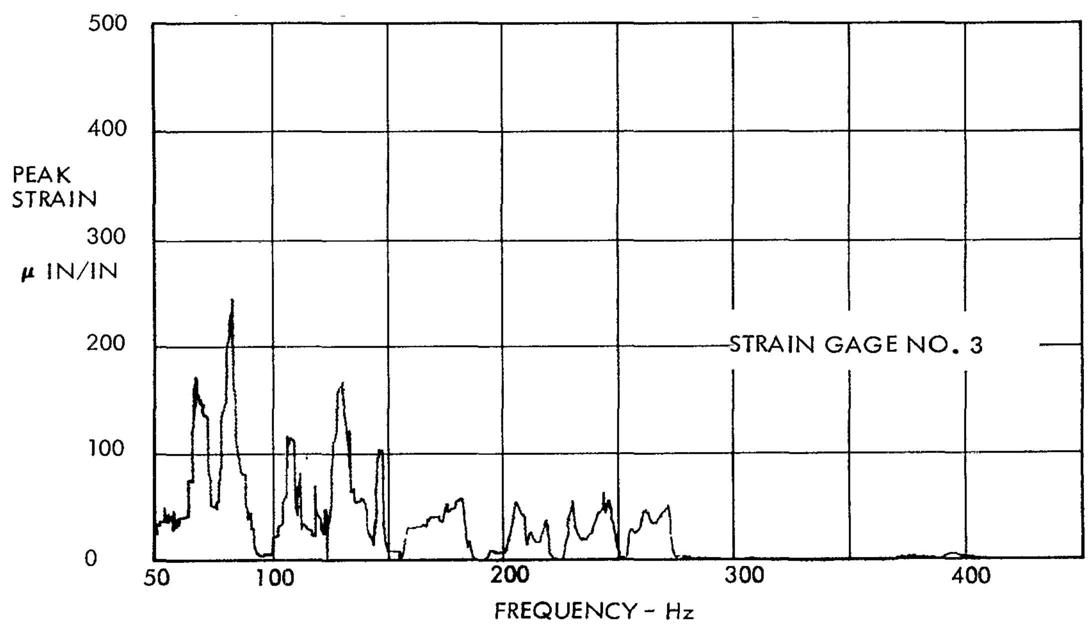

Figure 28 - Discrete Frequency Response at 136 db; Forty-Nine Bay Configuration Specimen 3.

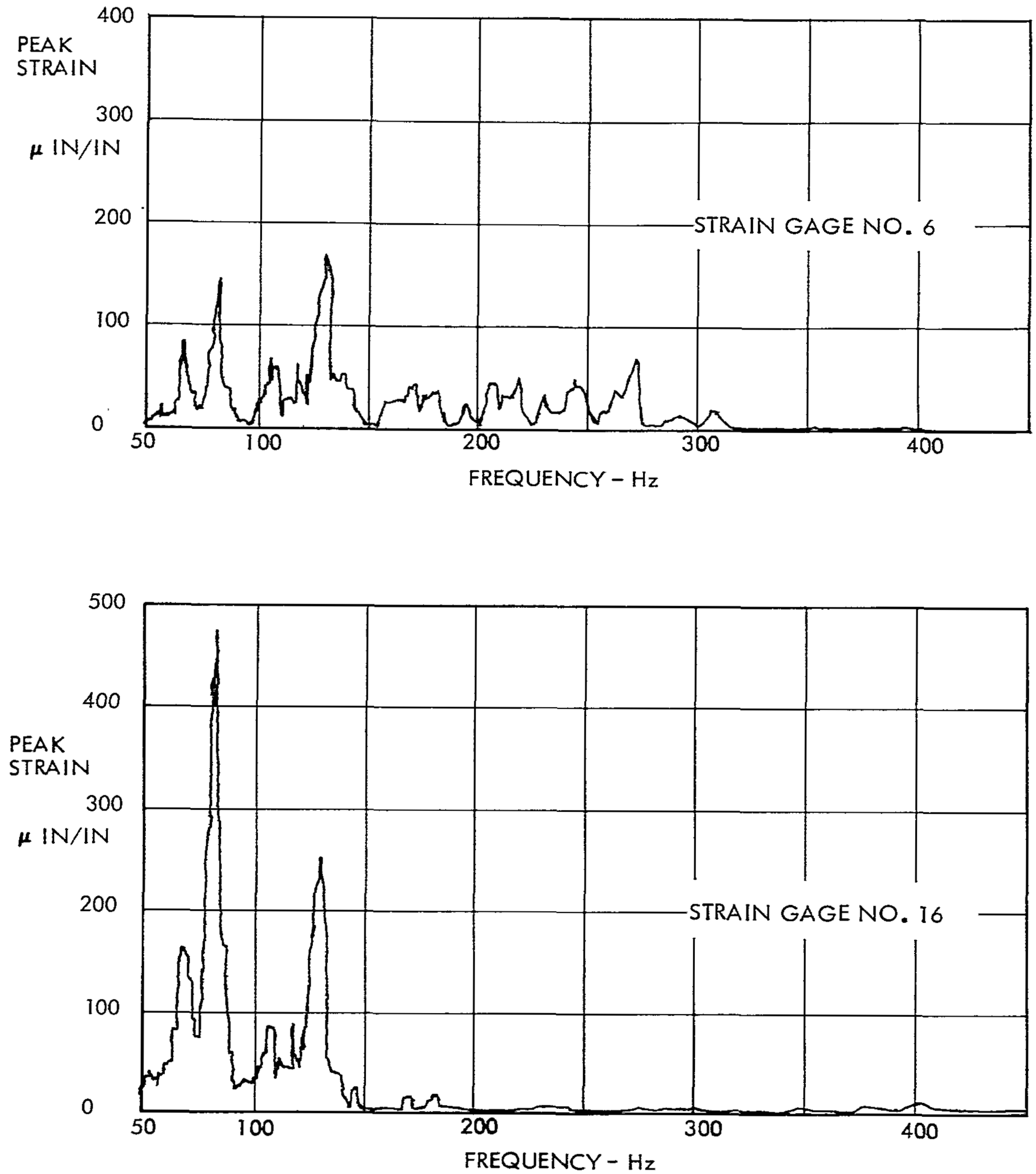

Figure 29 – Discrete Frequency Response at 136 db;
Forty-Nine Bay Configuration, Specimen 3.

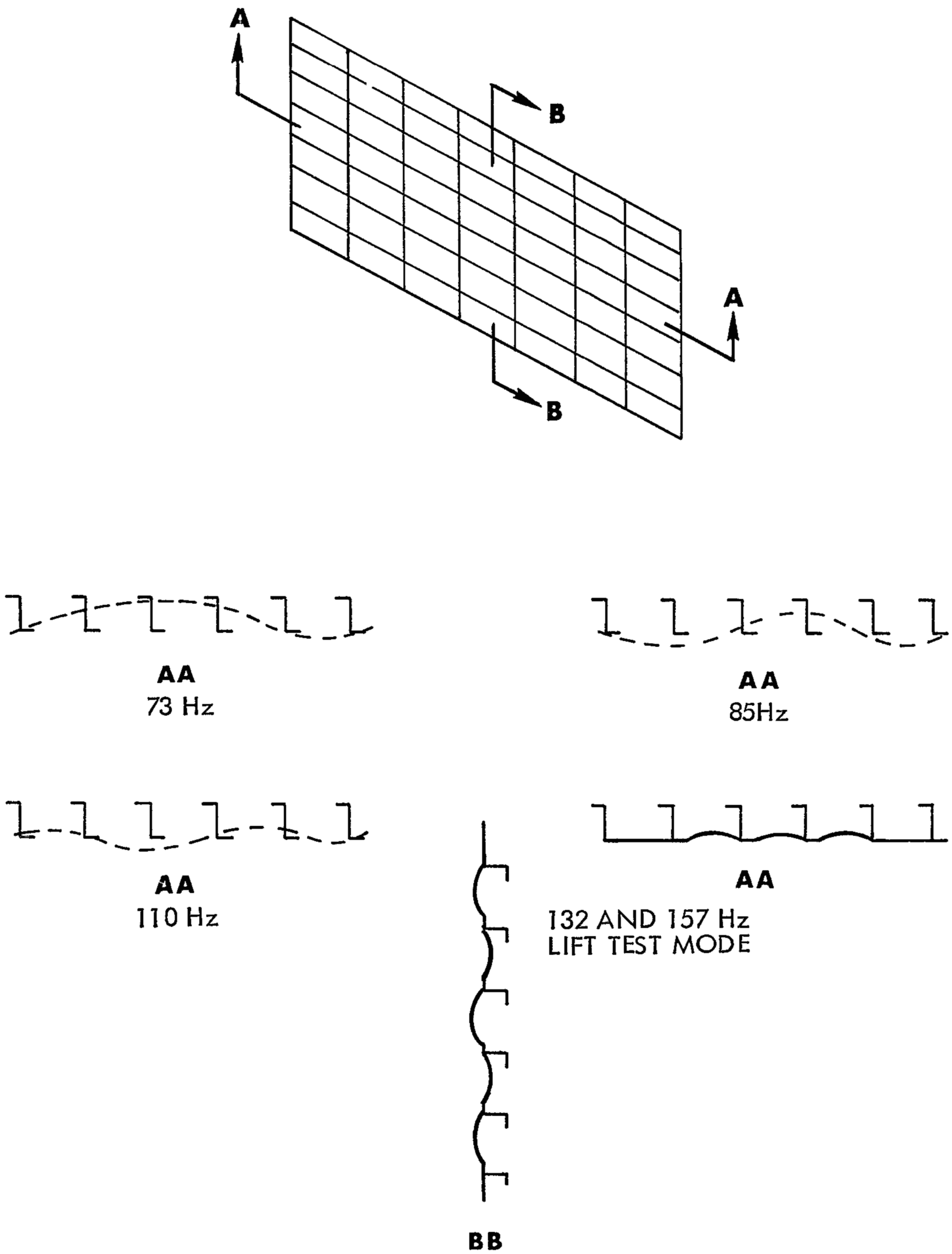

Figure 30 - Mode Shapes for a Forty-Nine Bay Configuration Specimen

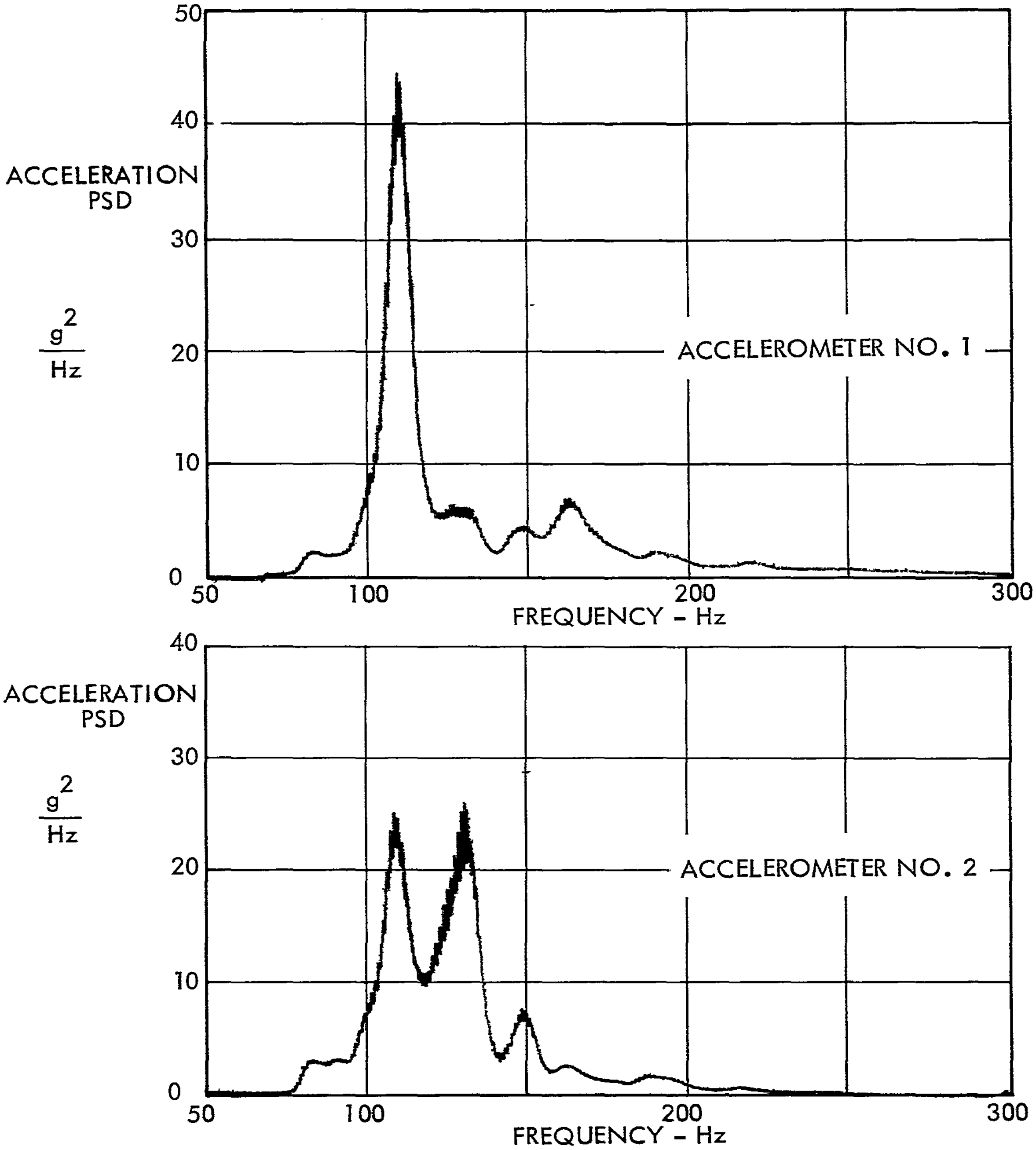

Figure 31 – Response of a Forty-Nine Bay Configuration Specimen at a Spectrum Level of 130 db. (No. 3)

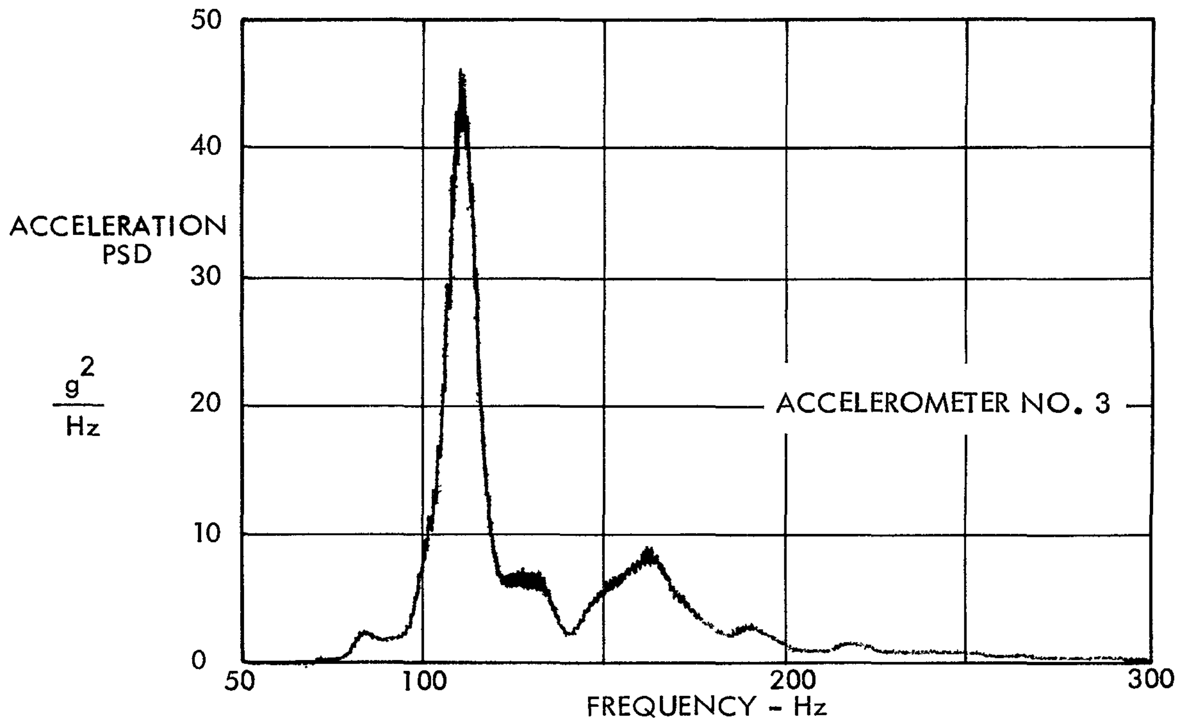

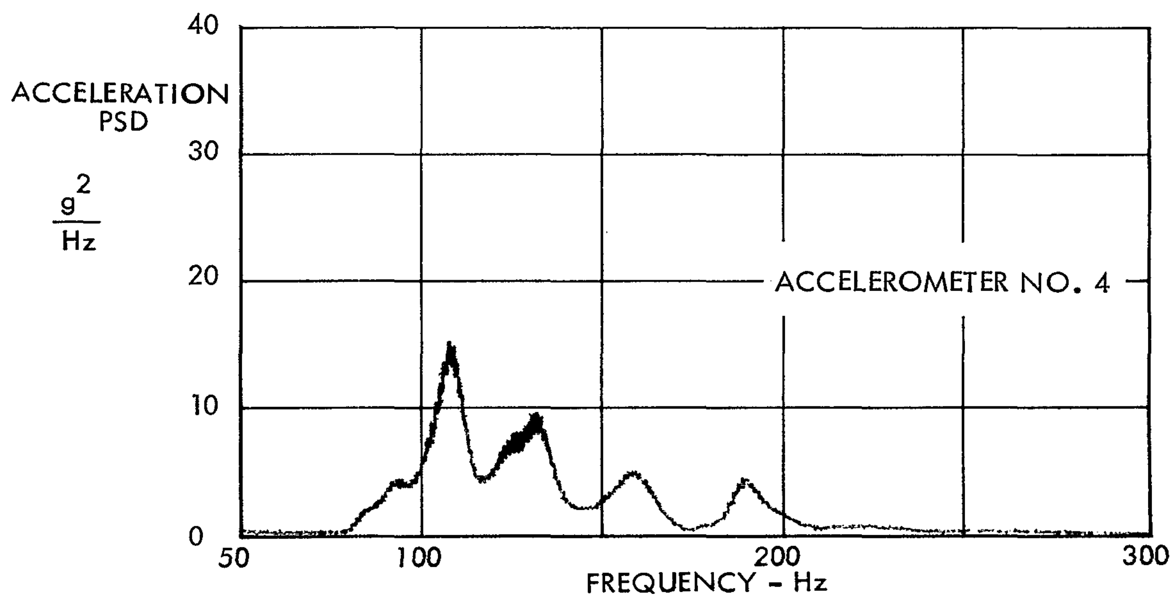

Figure 32 - Response of a Forty-Nine Bay Configuration Specimen at a Spectrum Level of 130 db. (Specimen No. 3)

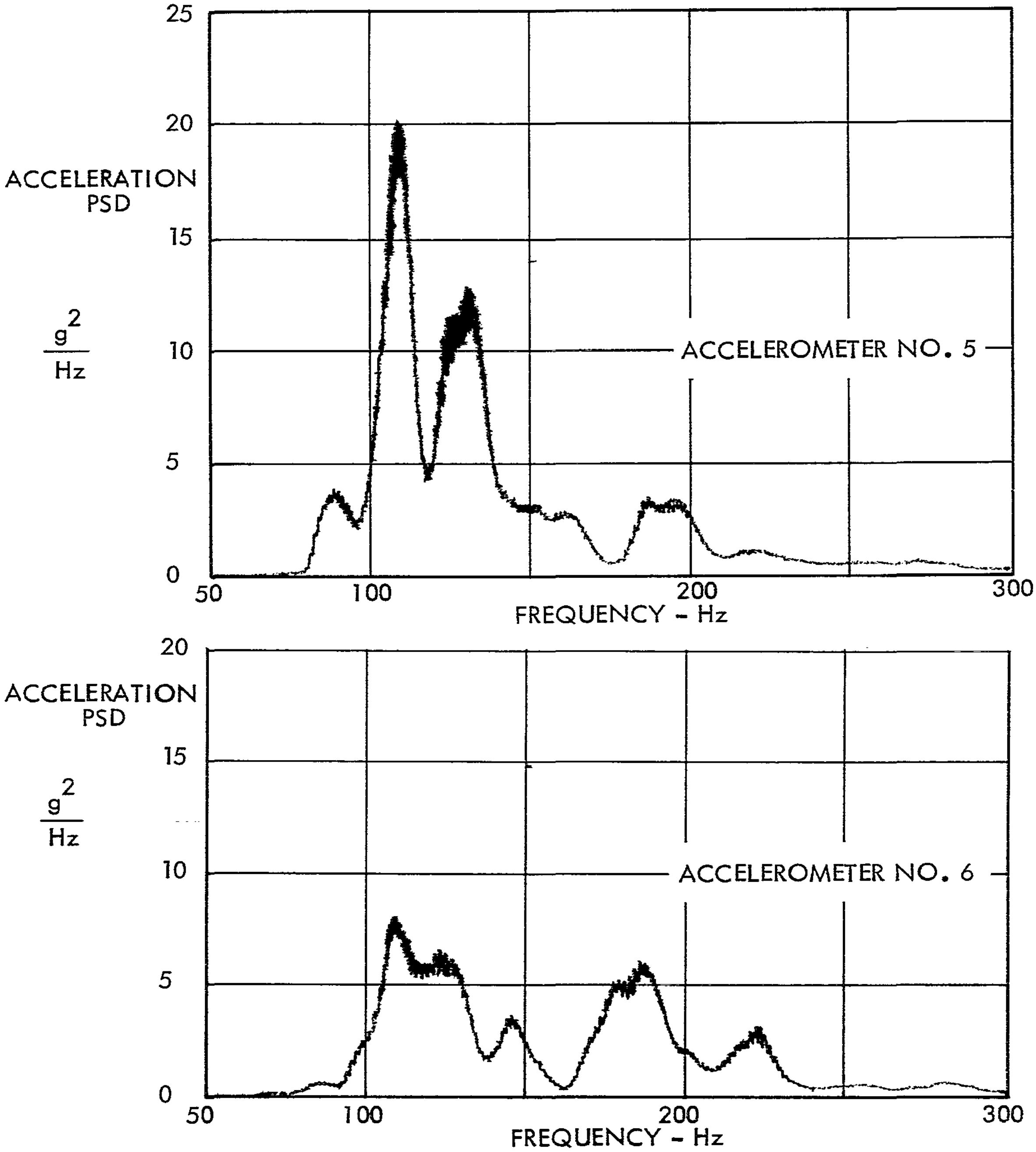

Figure 33 – Response of a Forty-Nine Bay Configuration Specimen at a Spectrum Level of 130 db. (No. 3)

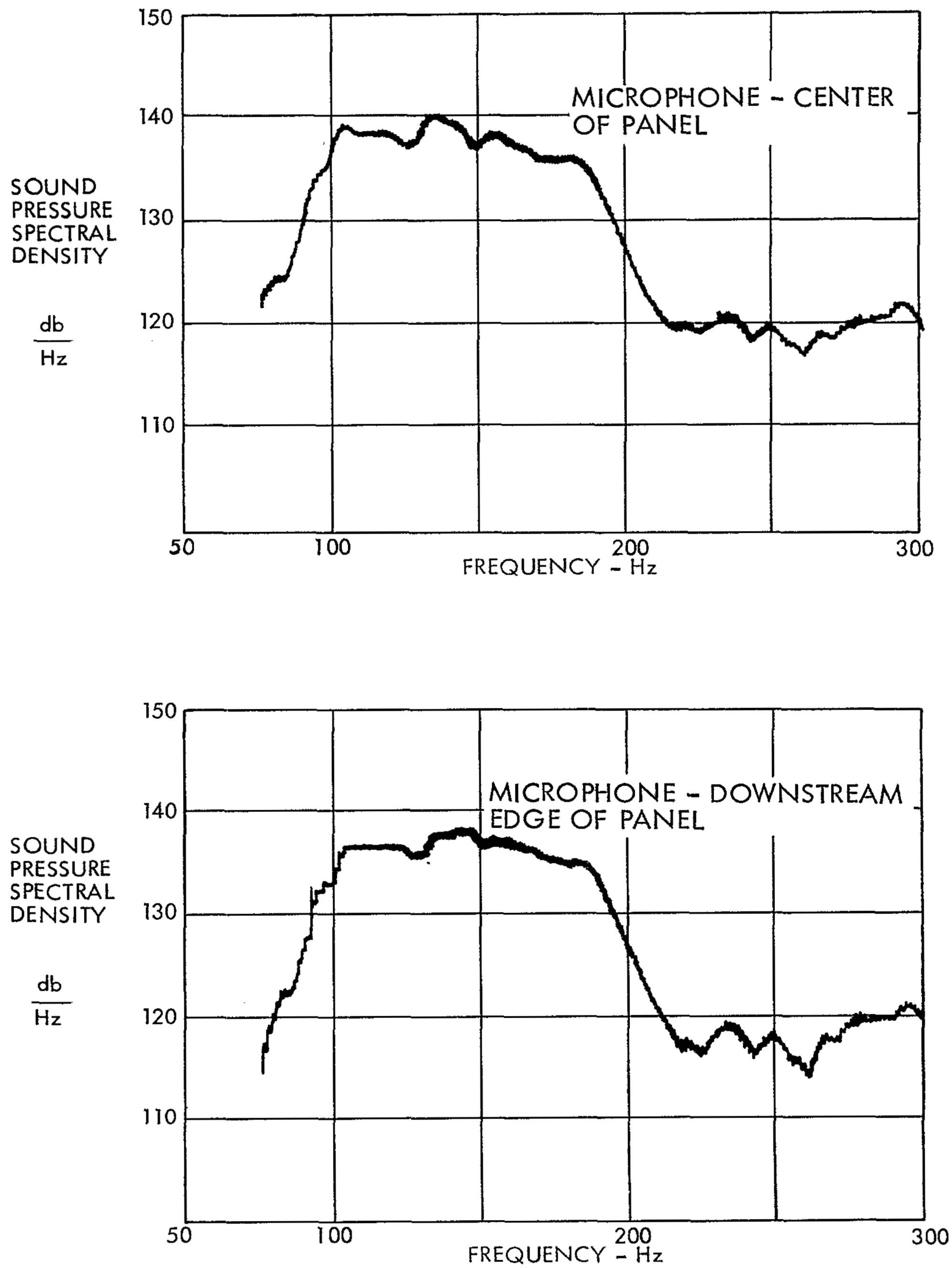

Figure 34 - Typical Shaped Acoustical Loading Spectrum for a Life Test (Single Bay Specimen)

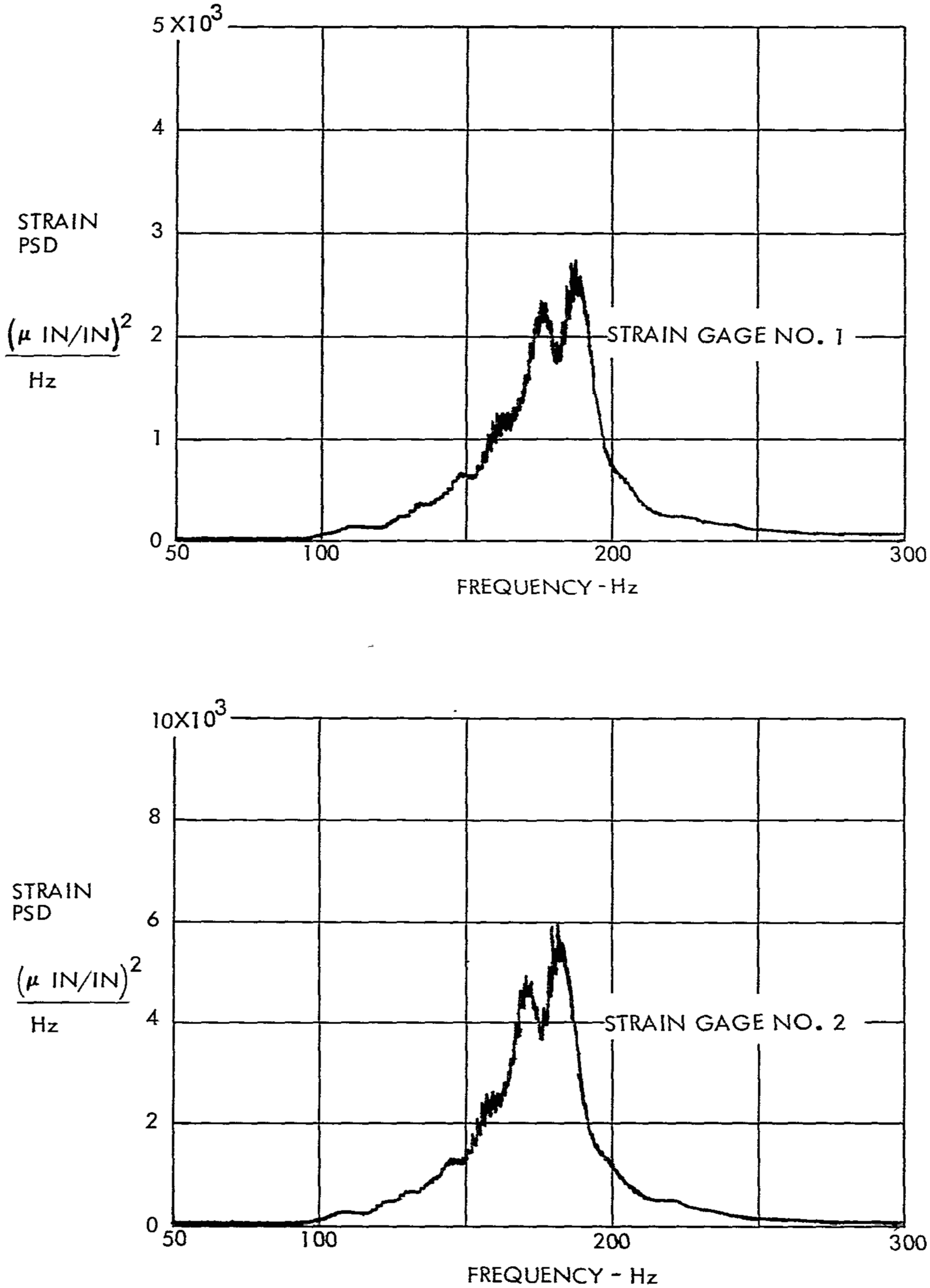

Figure 35 - Life Test Strain; Single Bay Configuration, Specimen No. 1

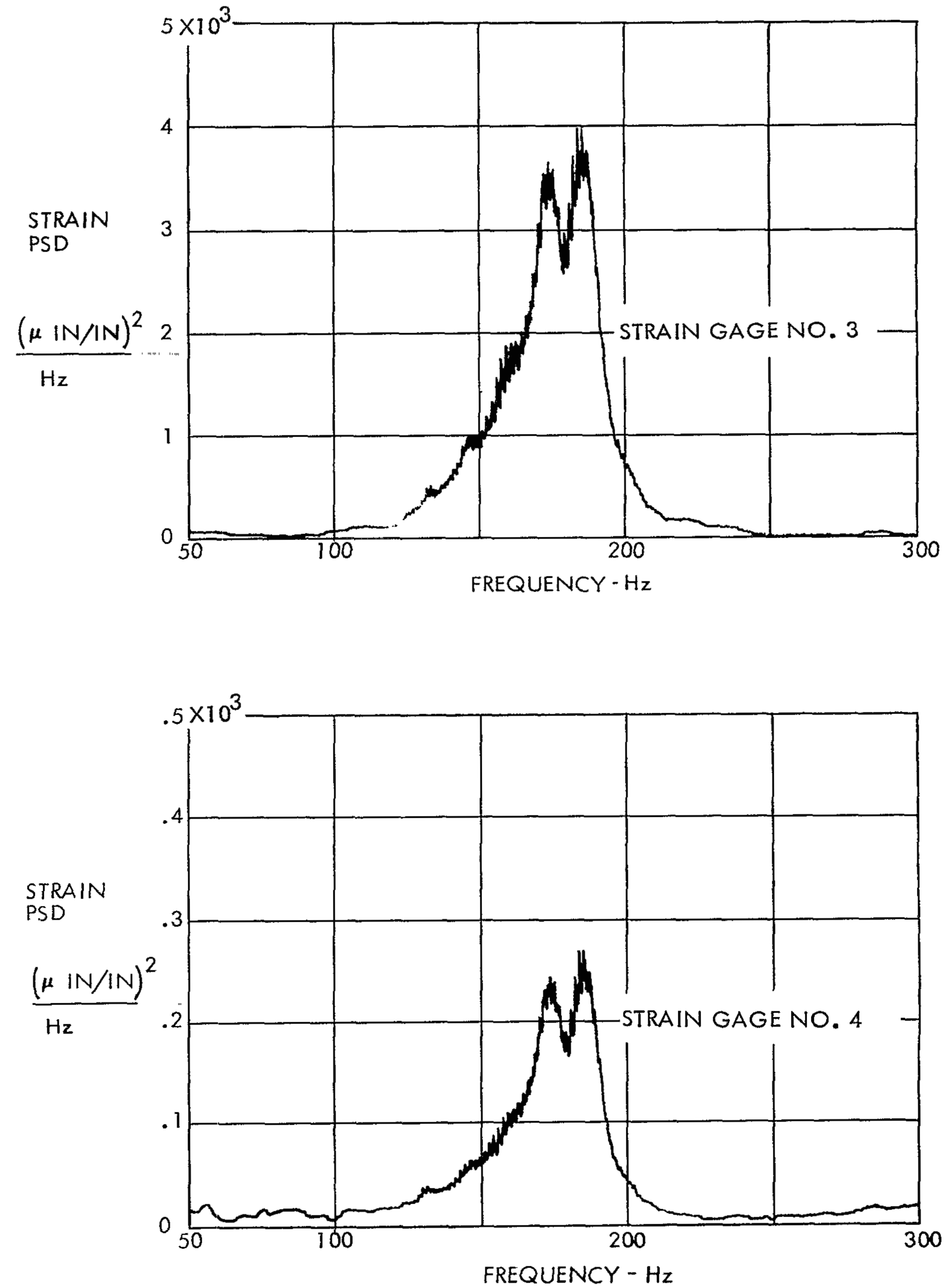

Figure 36 – Life Test Strain; Single Bay Configuration, Specimen No. 1.

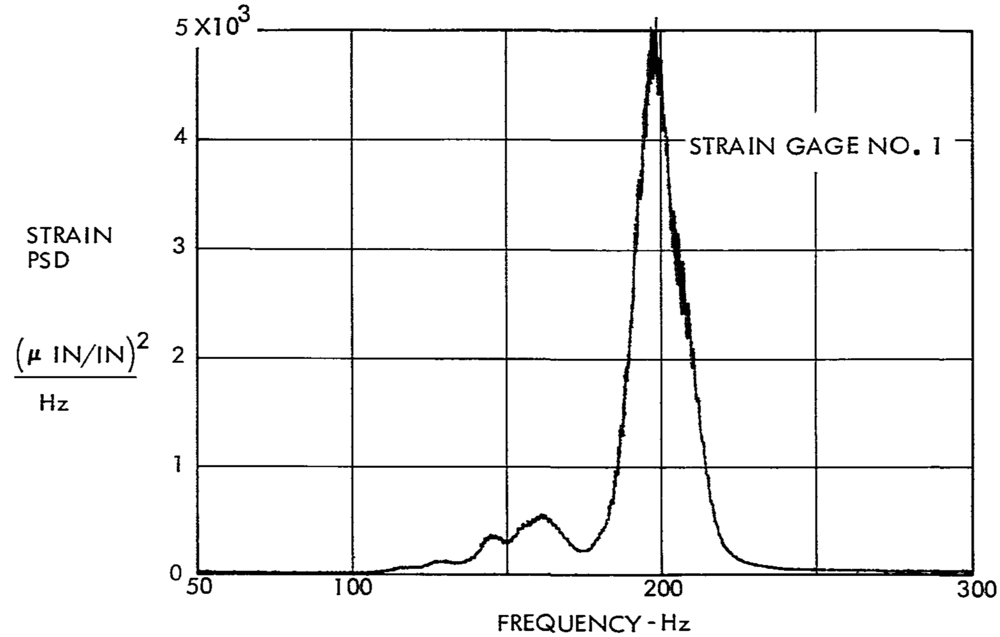

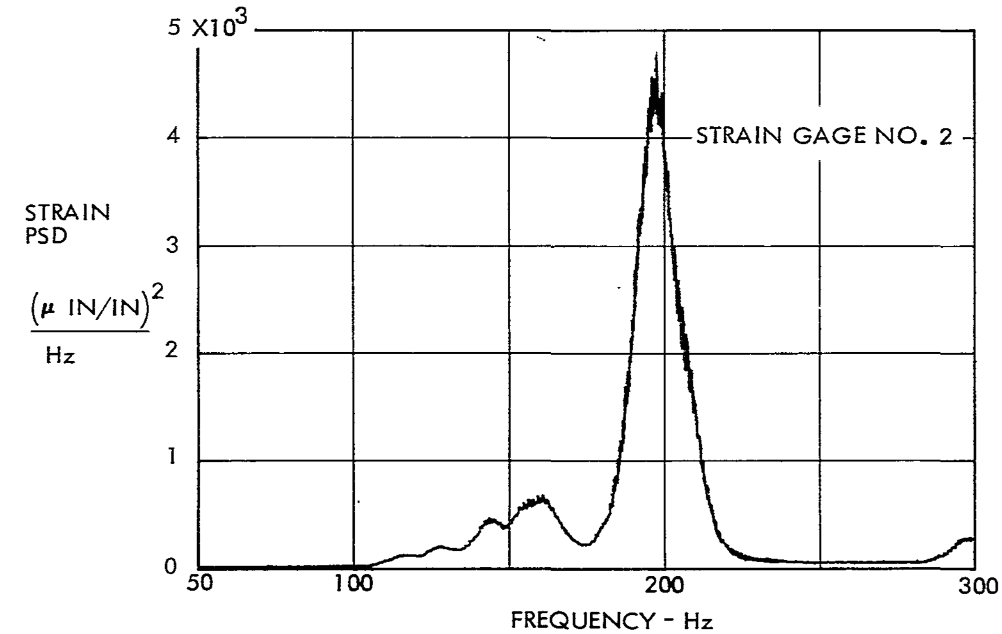

Figure 37 - Life Test Strain Nine Bay Configuration, Specimen No. 2.

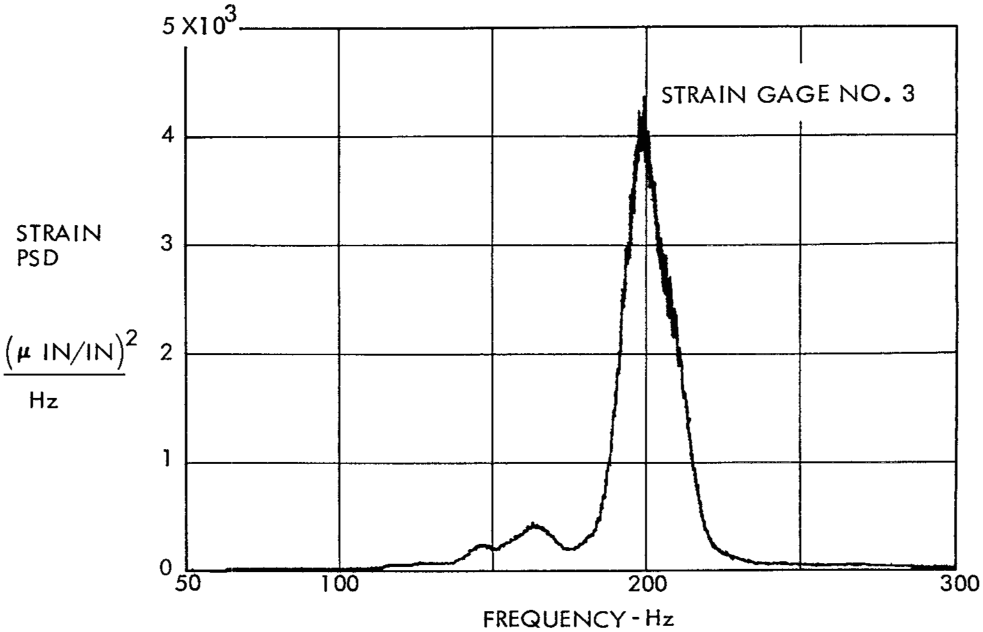

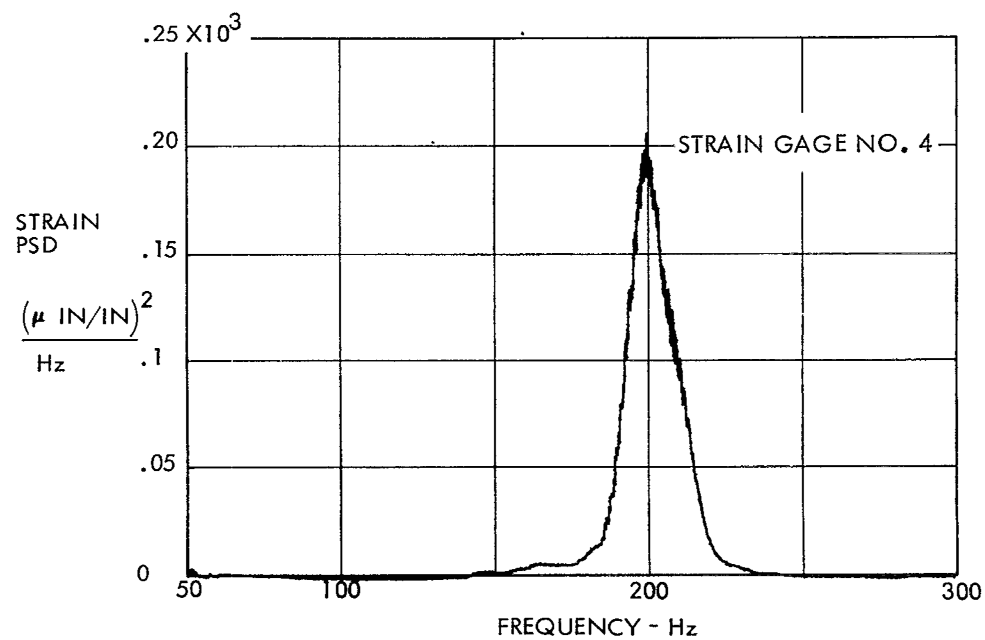

Figure 38 – Life Test Strain; Nine Bay Configuration, Specimen No. 2.

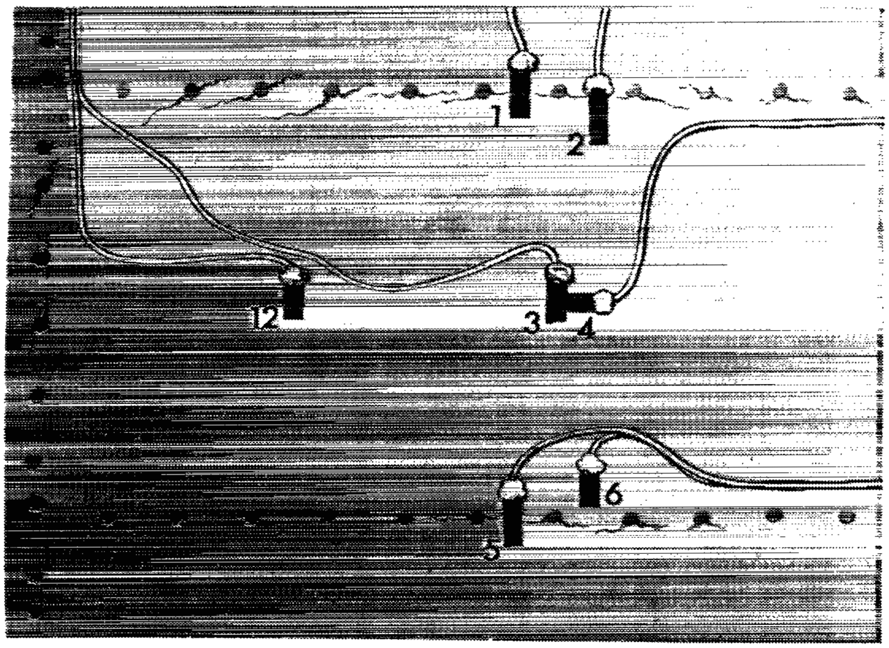

Figure 39 – Cracks Along the Rivet Lines Around the Center Skin Bay of a Nine Bay Configuration Panel

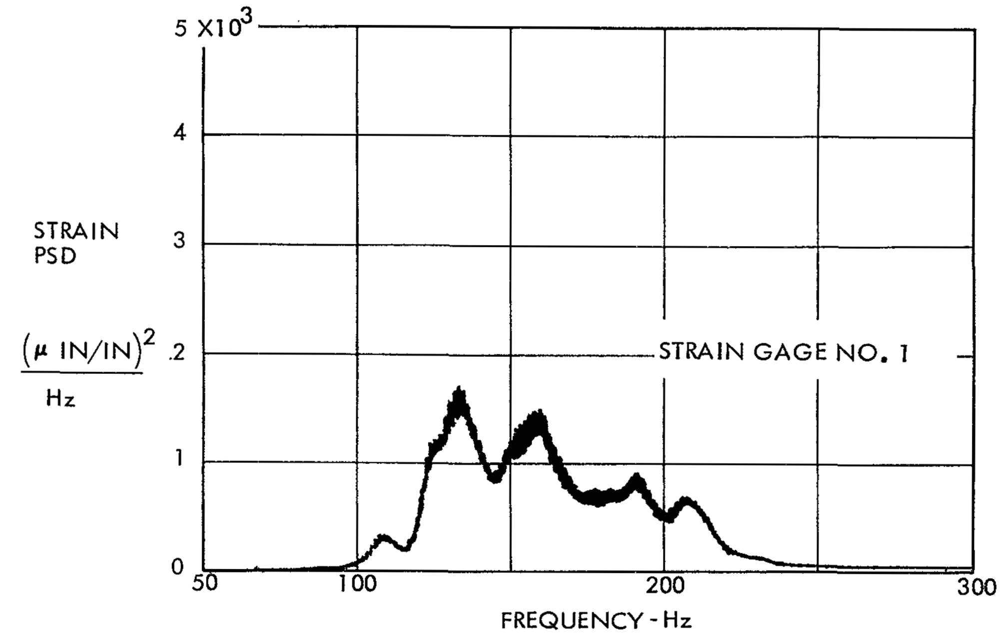

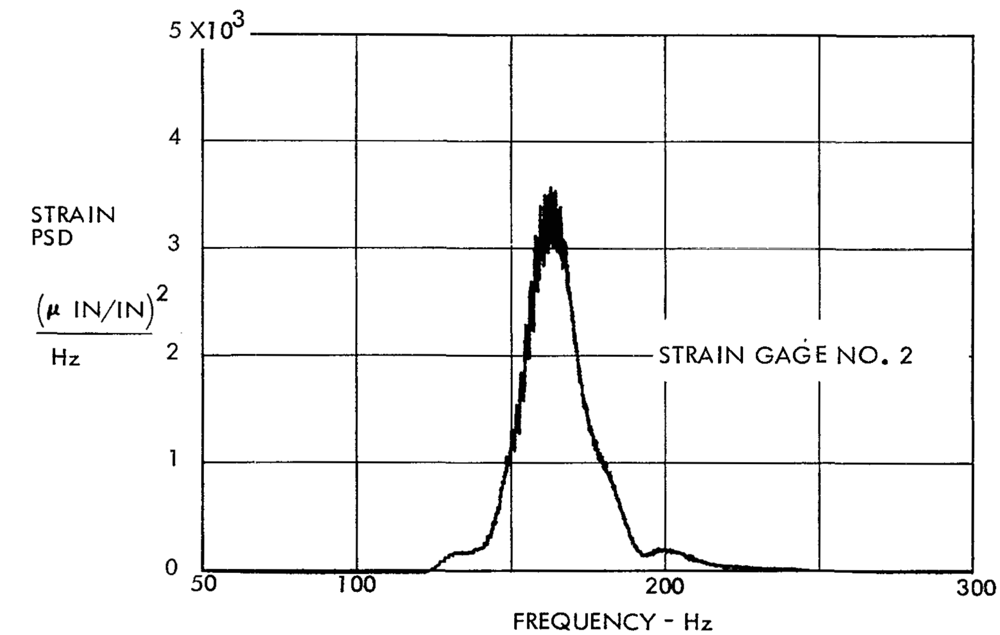

Figure 40 – Life Test Strain; Twenty-Five Bay Configuration, Specimen No. 2.

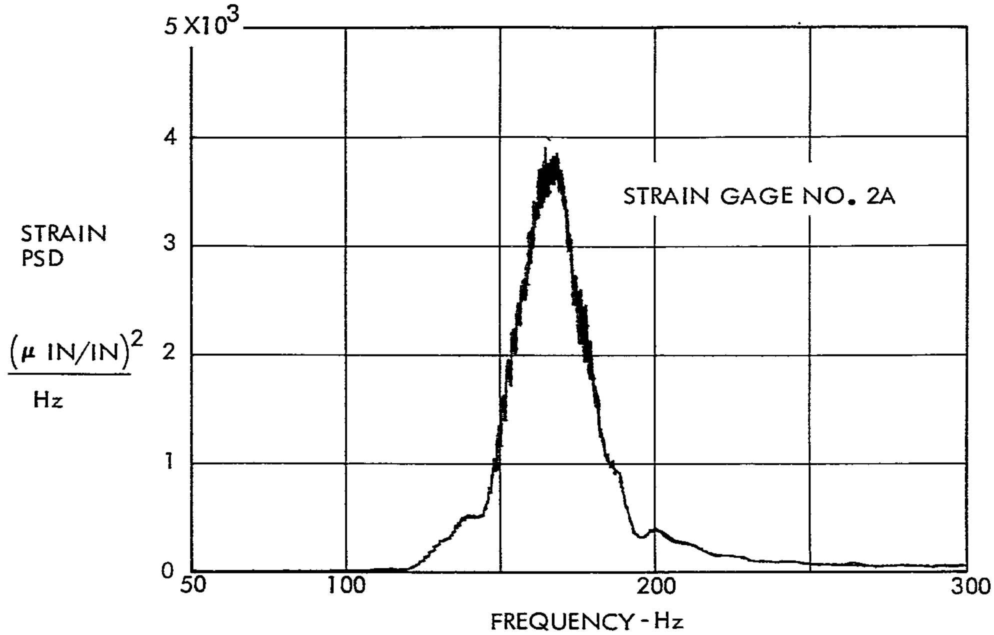

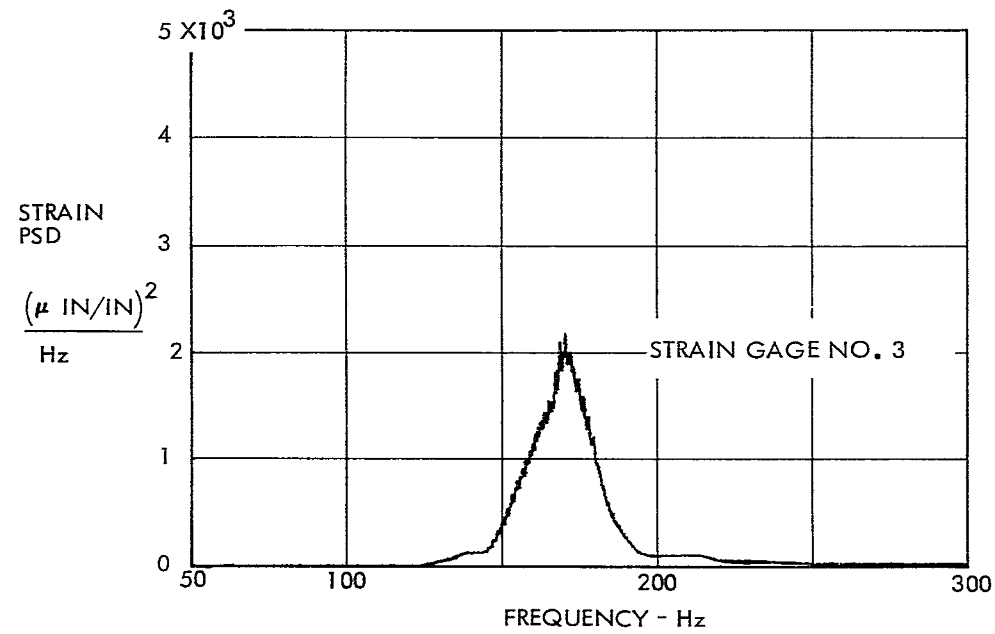

Figure 41 – Life Test Strain; Twenty-Five Bay Configuration, Specimen No. 2.

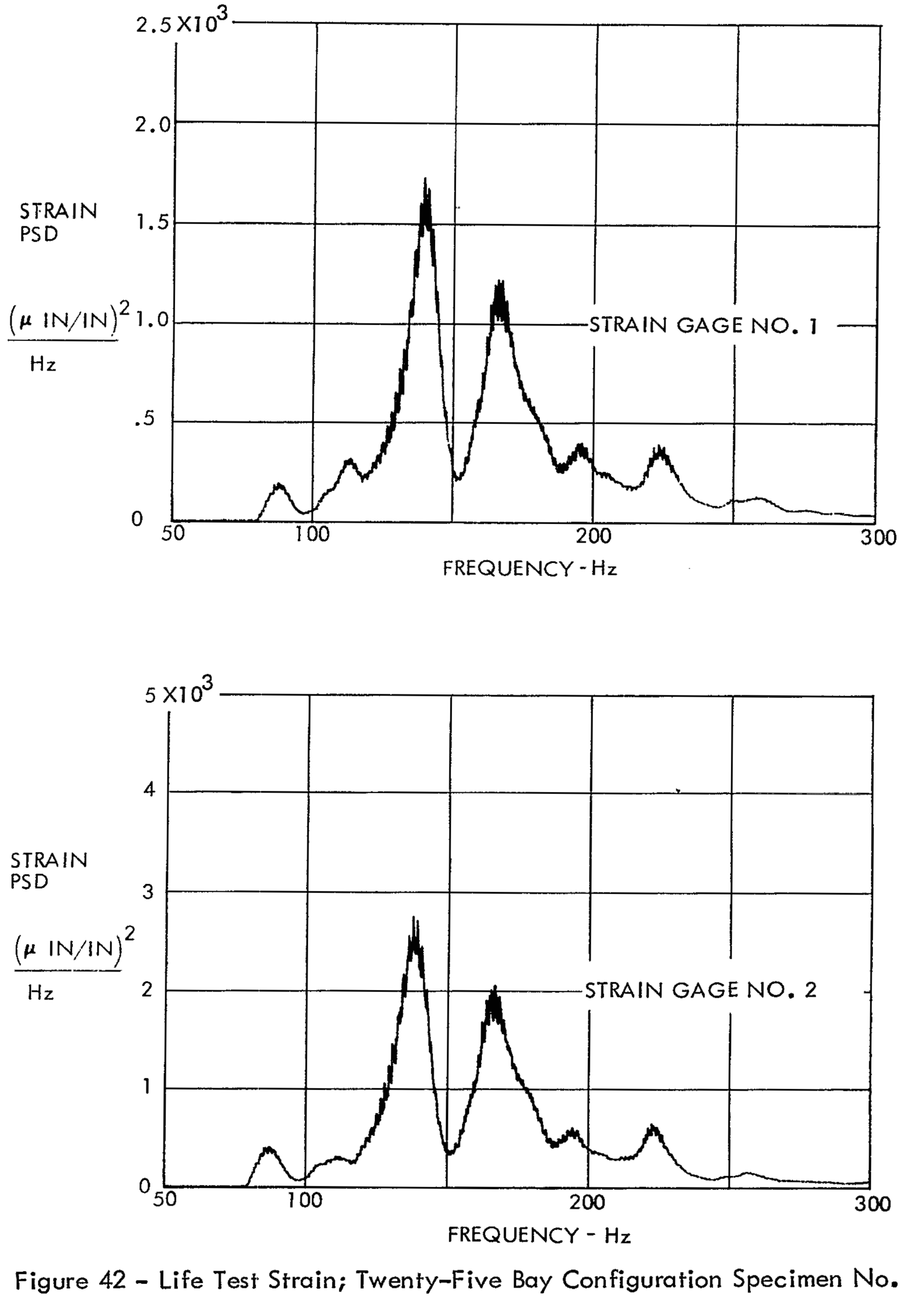

Figure 42 – Life Test Strain; Twenty-Five Bay Configuration Specimen No. 3.

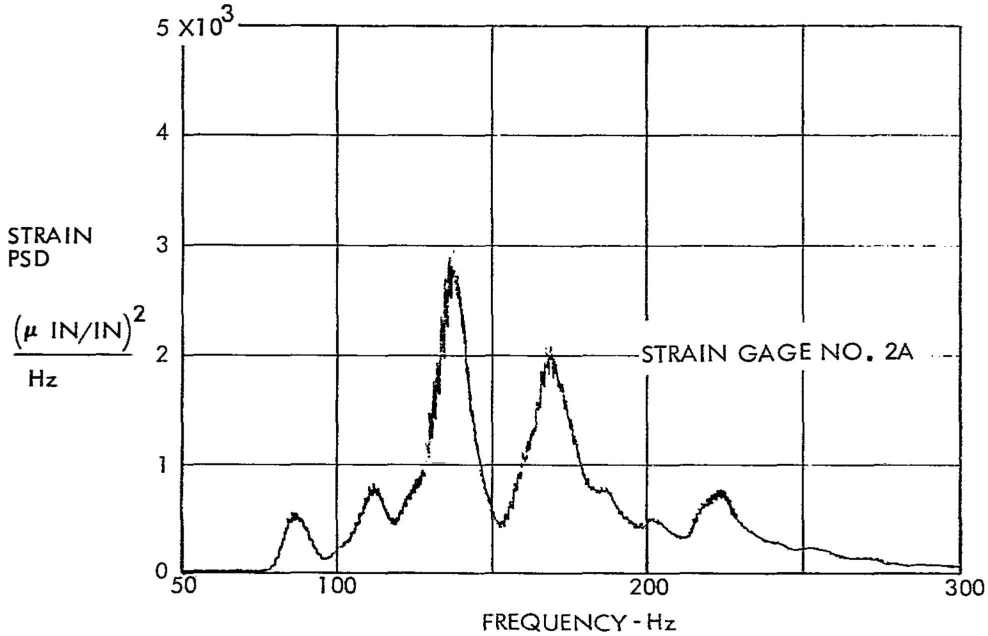

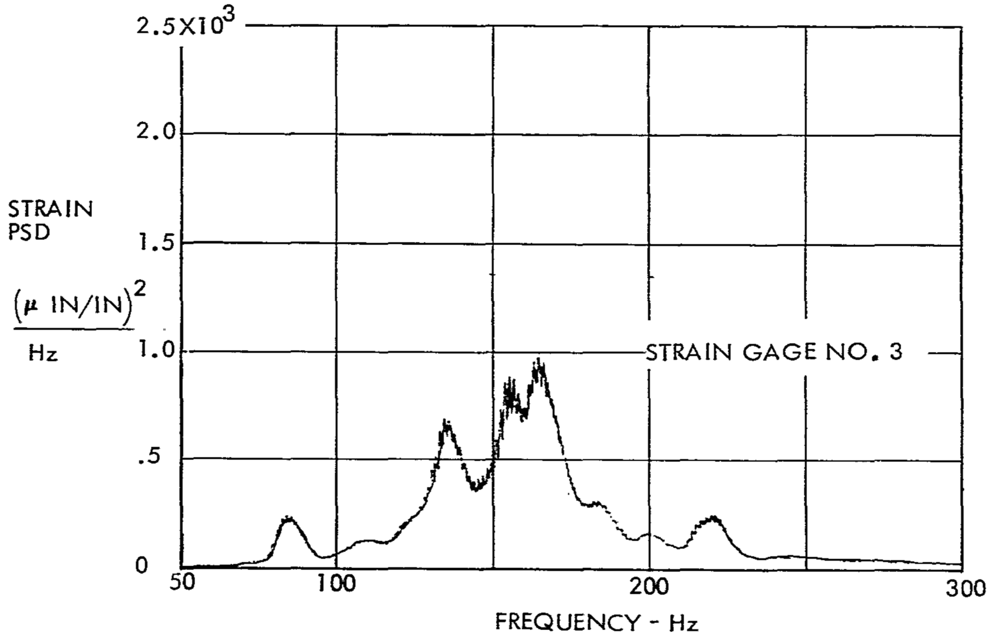

Figure 43 – Life Test Strain; Forty-Nine Bay Configuration Specimen No. 3.

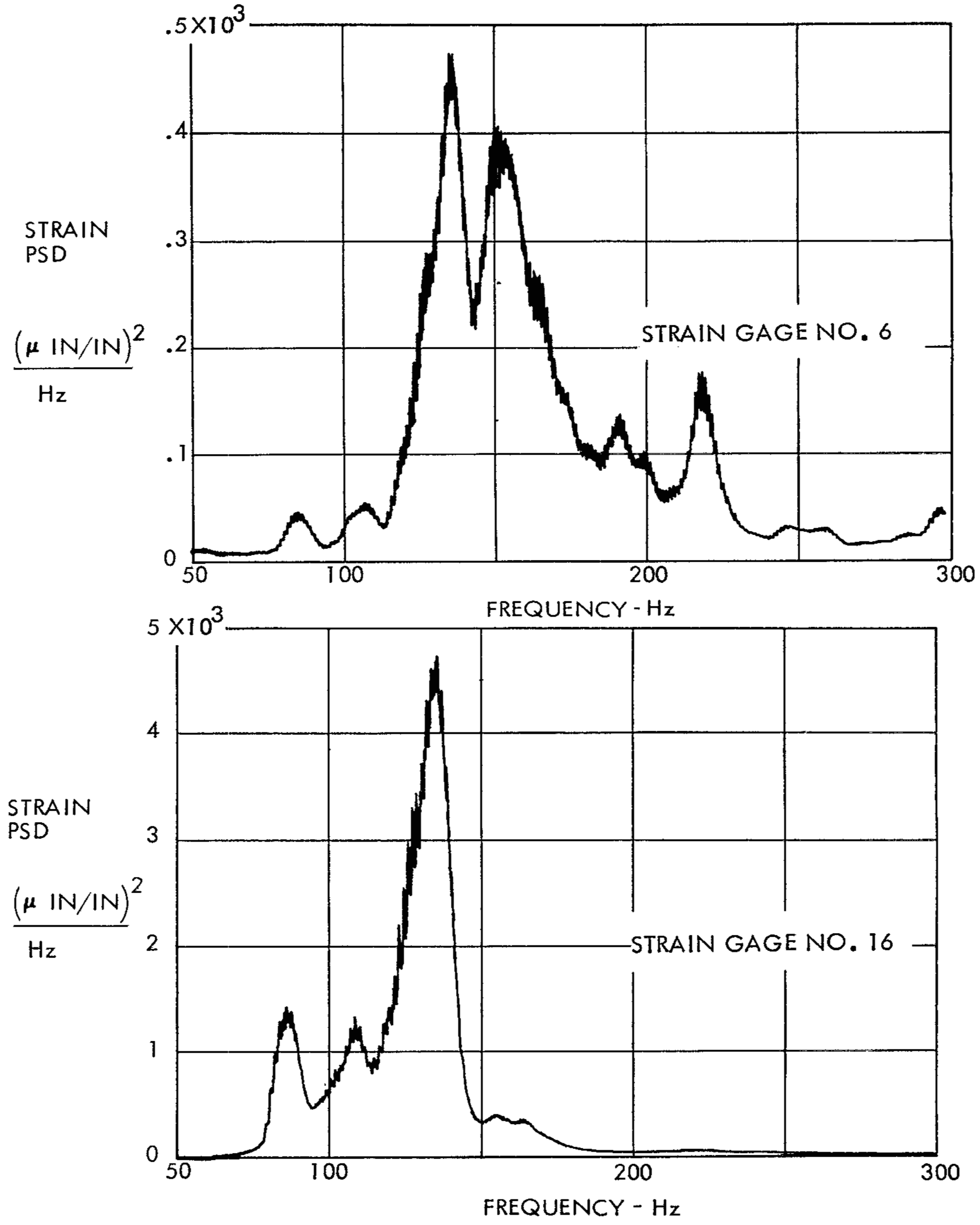

Figure 44 – Life Test Strain; Forty-Nine Bay Configuration, Specimen No. 3.

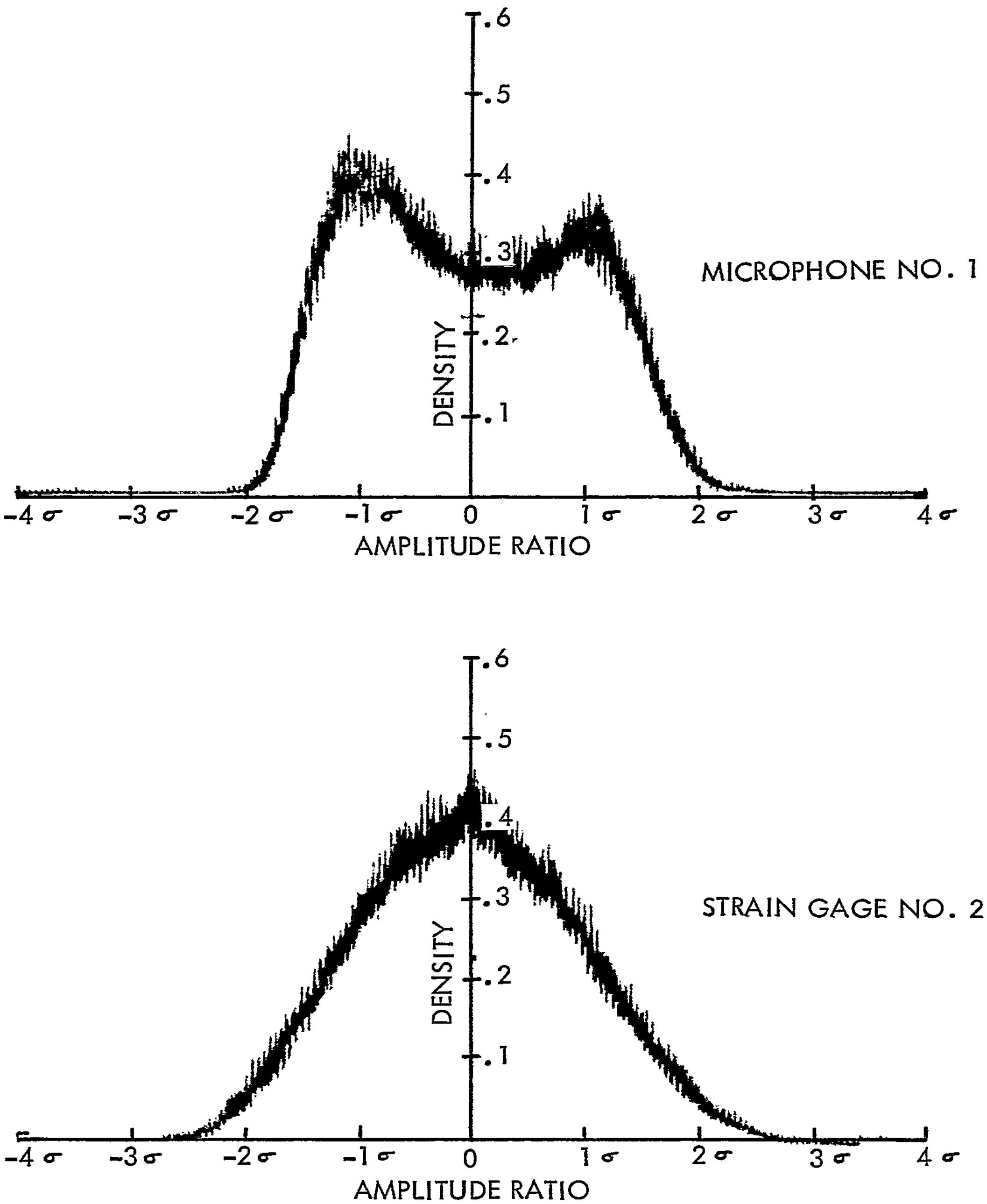

Figure 45 - Probability Density of Acoustical Loading and Strain Response on a Forty-Nine Bay Configuration Specimen

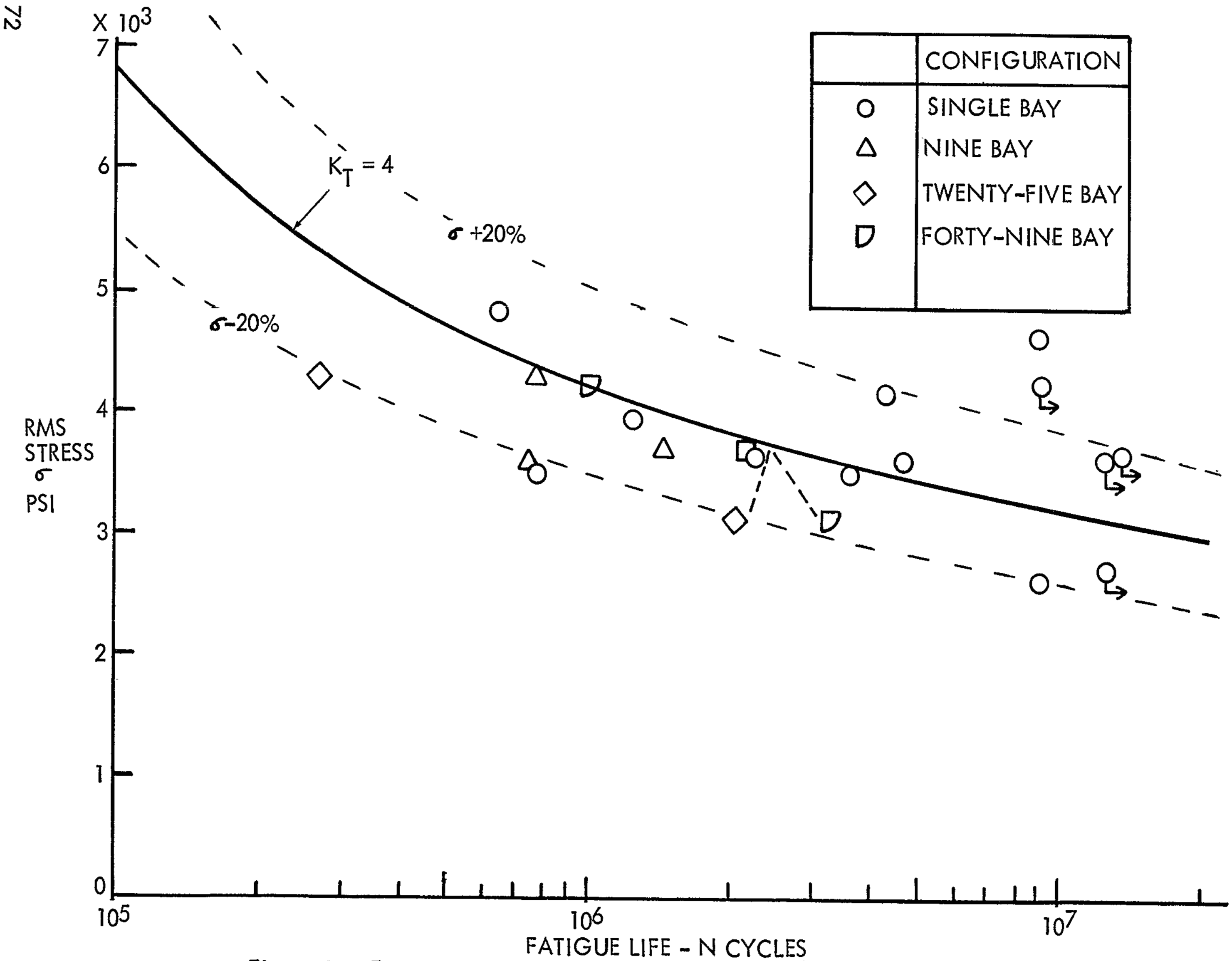

Figure 46 - Fatigue Life of Different Configurations, Based on Edge Strain Near Rivet Lines

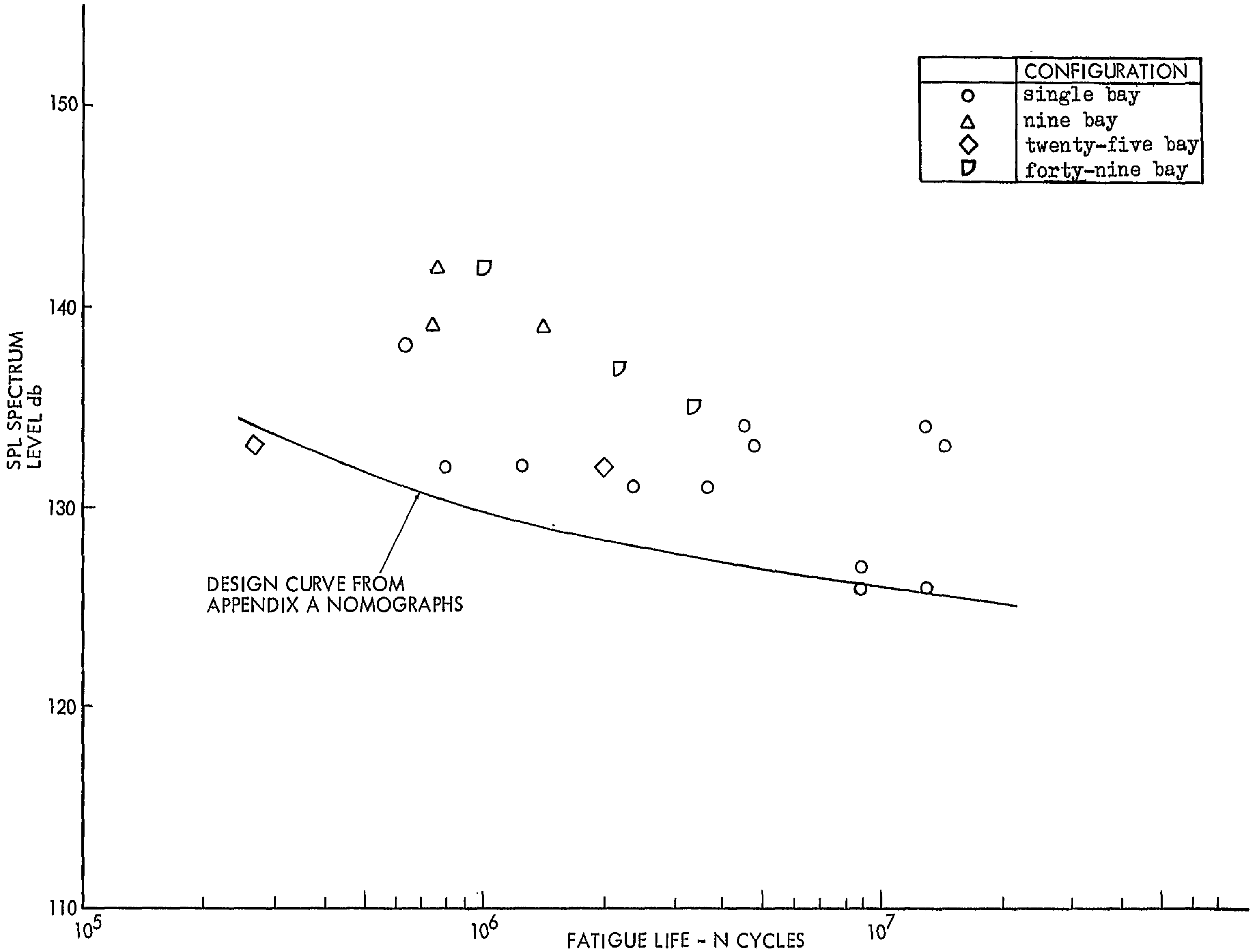

Figure 47 - Test Data as SPL vs Life

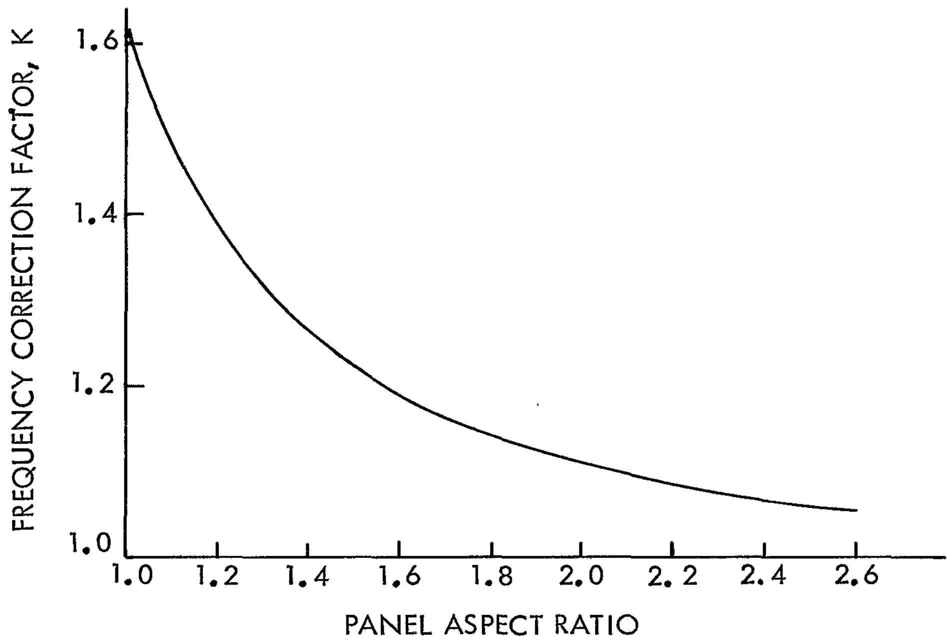

Figure 48. - Effects of Finite Aspect Ratio on Clamped Plate Frequency

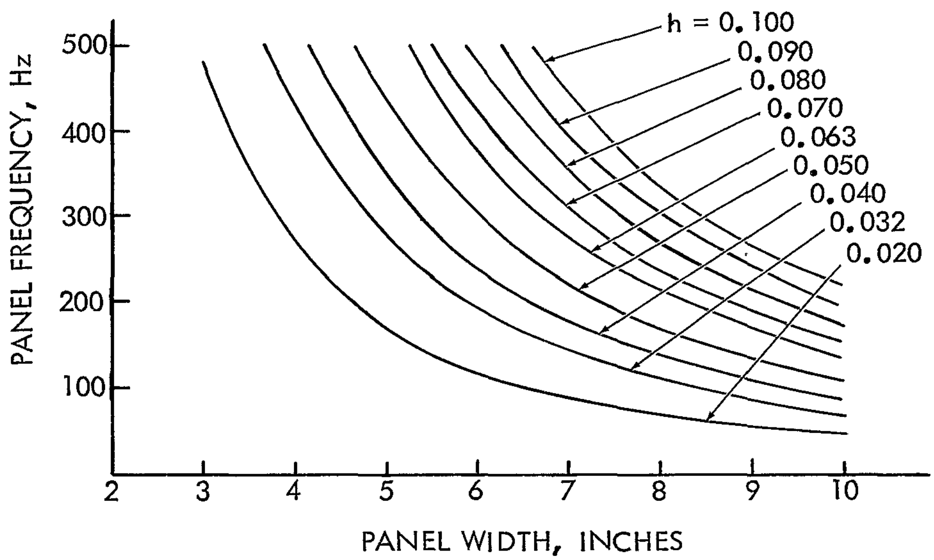

Figure 49. - Fundamental Clamped Plate Frequency, Aspect Ratio = Infinity

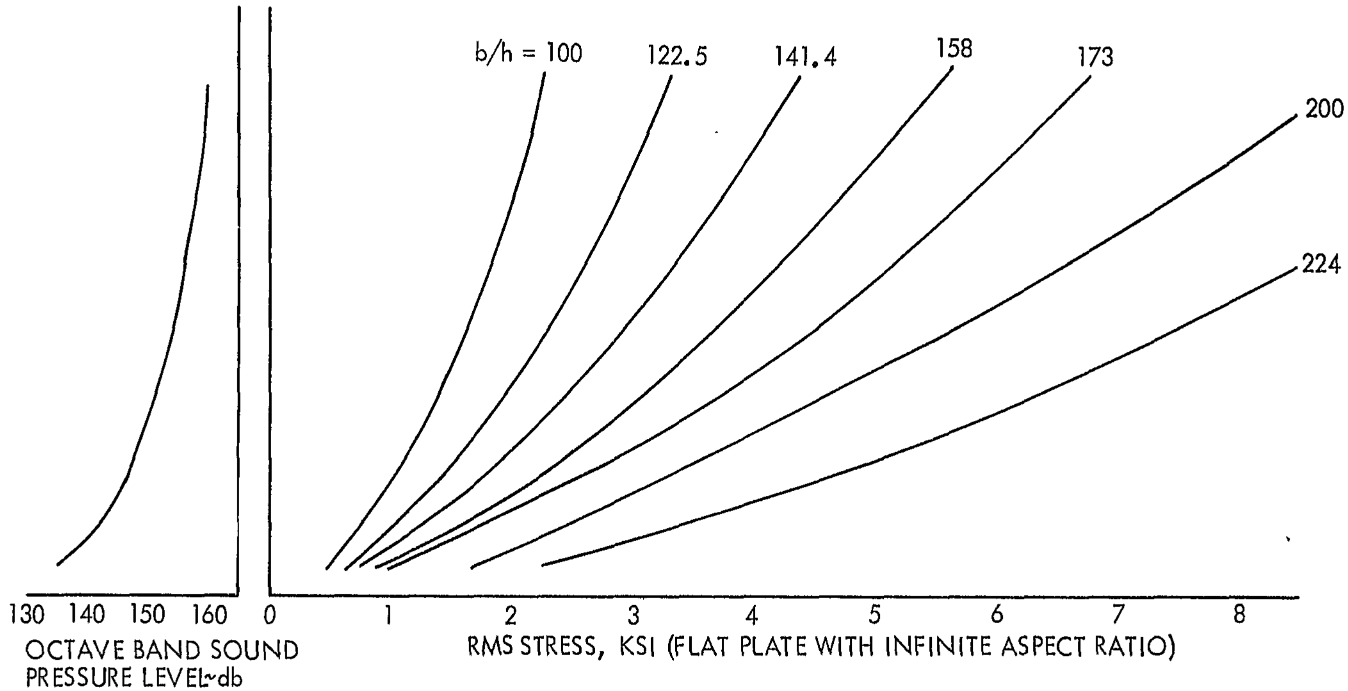

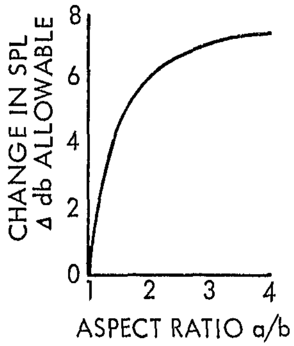

Figure 50. - Sonic Fatigure Design Monograph for Conventional Skin-Rib Construction

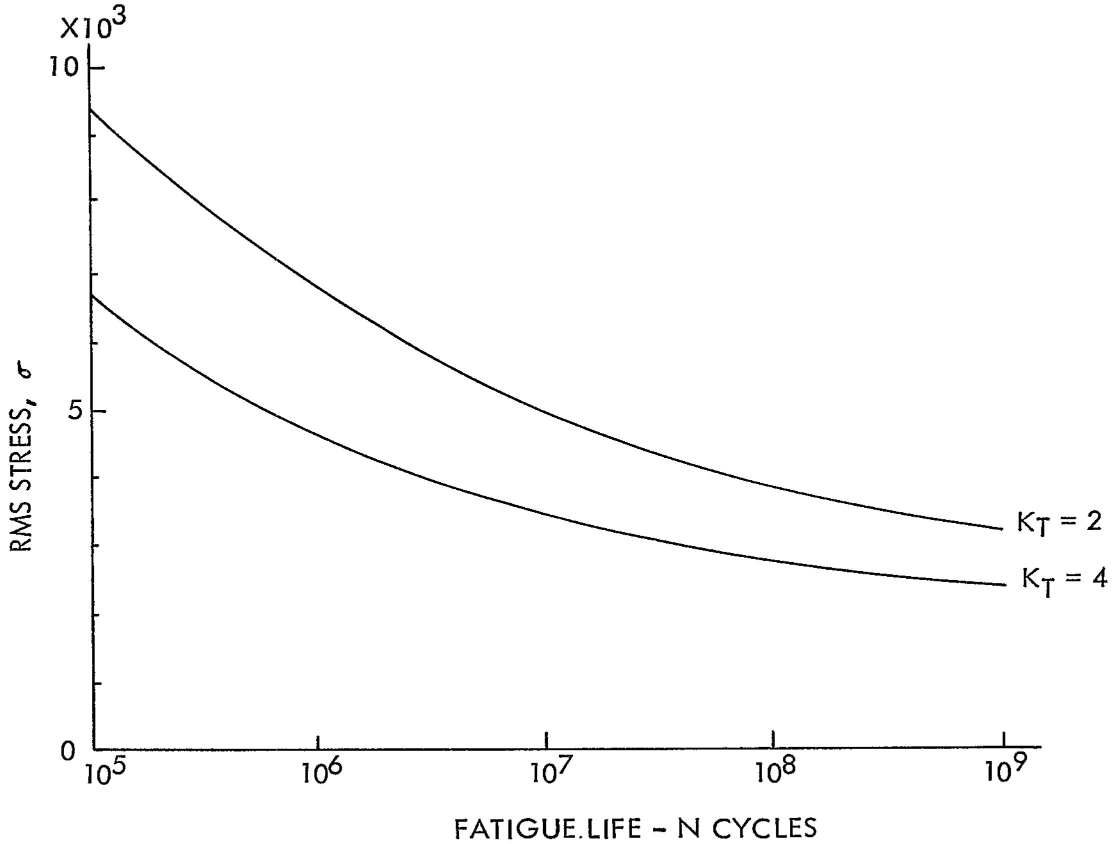

Figure 51. - Random S-N Fatigue Curves for 7075-T6 Sheet

NASA-Langley, 1970 —— 32 CR-1536